NUREG/CR-1423
Vol. I

Structural Building Response Review

Seismic Safety Margins Research Program

Prepared by J. J. Healey, S. T. Wu, M. Murga

Lawrence Livermore Laboratory

Ebasco Services Incorporated

Prepared for
U.S. Nuclear Regulatory
Commission

Available from

GPO Sales Program
Division of Technical Information and Document Control
U.S. Nuclear Regulatory Commission
Washington, D.C. 20555

and

National Technical Information Service
Springfield, Virginia 22161

NUREG/CR-1423
Vol. I
RJ, RM, RN, RO

Structural Building Response Review

Seismic Safety Margins Research Program

Manuscript Completed: February 1980
Date Published: May 1980

Prepared by
Lawrence Livermore Laboratory
Livermore, CA 94550

J. J. Healey, S. T. Wu, M. Murga
Ebasco Services Incorporated
New York, NY 10006

Prepared for
Division of Reactor Safety Research
Office of Nuclear Regulatory Research
U.S. Nuclear Regulatory Commission
Washington, D.C. 20555
NRC FIN No. A0130

ABSTRACT

The body of this report is organized in six chapters: Chapter 2 treats the subject of structural modeling including methods of discretization, basic modeling approaches, decoupling and other important modeling topics; Chapter 3 covers the various methods of linear and nonlinear structural dynamic analysis, numerical methods, damping, etc.; Chapter 4 contains a discussion of the nonlinearity as it relates to nuclear plant structures and presents a discussion of basic analytical considerations and computational algorithms for treating nonlinearity; Chapter 5 treats the subject of combining seismic and nonseismic load effects with particular reference to the state-of-the-art in this area as related to the probabilistic methodology. This materi .l was not fully elaborated on in this report since the SSMRP has a special project to address this topic; Chapter 6 presents a summary of the various sources of uncertainty in seismic dynamic analysis together with a discussion of the sources of data available to quantitatively define these uncertainties; Chapter 7 provides a summary of the principal observations and recommendations of the study.

TABLE OF CONTENTS

Page

LIST OF TABLES

LIST OF FIGURES

LIST OF FIGURES (CONT"D)

LIST OF FIGURES (CONT'D)

PREFACE

This study was performed by Ebasco Services Incorporated under subcontract to the University of California, Lawrence Livermore Laboratory. The comments and cooperation of the LLL Project personnel, Drs. J. J. Johnson and Ting-Yu Lo are gratefully acknowledged. The principal investigators would also like to express their appreciation to Mr. J. J. Gilmore for his interest and support, and to Messrs. E. Odar and K. D. Chiu for their assistance, review and cooperation. Finally, special thanks to Dr. C. Gong for his valuable technical input and to Mr. S. P. Plate for his substantial assistance in the production of the final report.

Chapter 1

Introduction

As part of the Phase I effort of the Seismic Safety Margins Research Program (SSMRP) being performed by the University of California Lawrence Livermore Laboratory for the U.S. Nuclear Regulatory Commission, the basic objective of Subtask IV.1 (Structural Building Response Review) is to review and summarize current methods and data pertaining to seismic response calculations particularly as they relate to the objectives of the SSMRP. This material forms one component in the development of the overall computational methodology involving state of the art computations including explicit consideration of uncertainty and aimed at ultimately deriving estimates of the probability of radioactive releases due to seismic effects on nuclear power plant facilities.

The scope of this study, as originally formulated, consisted of thirteen different items. The following list of items provides then an overview of the basic objectives of the study subject to some redefinitions of scope which were made in the course of project performance:

Task	Description
1	Describe available methods and the methods under development to analyze structural building response and in addition, discuss the advantages and disadvantages of each method;
2	Describe and discuss the methods used to handle the interactions between structural building response and soil-structure interaction response and between structural response and subsystem response (piping, mechanical and electrical equipment);
3	Describe the various structural and component idealization methods and mathematical models and discuss advantages and disadvantages of each method and model;

Task (Cont'd)	Description (Cont'd)
4	Discuss advantages and disadvantages of finite element idealization versus a beam element model for various buildings and heavy equipment for a four-loop PWR/1 system;
5	Describe the various structural analysis computer codes and discuss advantages and disadvantages of each code;
6	Describe the various material properties used in the mathematical models and discuss the approach of modifying material properties to simulate the structures nonlinear behavior and further discuss how the concrete cracking phenomena is considered and handled in structural building response calculations;
7	Describe the methods used to evaluate nonseismic response and discuss the approach to combine various responses;
8	Describe and provide information on the experience for structural building nonlinear analysis and structural damping evaluation;
9	Identify sources of random variables (parameters) in the structural building response calculation and quantify the contribution of each parameter to the final structural response result;
10	Describe the various numerical methods used for solving structural building dynamic response and discuss the advantages and disadvantages of each numerical method;
11	Recommend the most appropriate methods to be used in the SSMRP Phase I effort on structural building response and discuss the approach to be used for developing the required transfer functions with a minimum number of random variables;
12	Recommend the most appropriate method and model to be used for the limited effort on structural damping and nonlinear structural building analyses for the SSMRP Phase I effort;
13	Identify sources of systematic uncertainty in the structural building response calculation and quantify the systematic uncertainty.

The body of this report is organized in six chapters: Chapter 2 treats the subject of structural modeling including methods of discretization, basic modeling approaches, decoupling and other important modeling topics; Chapter 3 covers the various methods of linear and nonlinear structural dynamic analysis, numerical methods, damping, etc; Chapter 4 contains a discussion of the nonlinearity as it relates to nuclear plant structures and presents a discussion of basic analytical considerations and computational algorithms for treating nonlinearity; Chapter 5 treats the subject of combining seismic and nonseismic load effects with particular reference to the state of the art in this area as related to the probabilistic methodology. This material was not fully elaborated on in this report since the SSMRP has a special project to address this topic; Chapter 6 presents a summary of the various sources of uncertainty in seismic dynamic analysis together with a discussion of the sources of data available to quantitatively define these uncertainties; Chapter 7 provides a summary of the principal observations and recommendations of the study. It is hoped that this material will help the SSMRP to define the analytical developments and data acquisition required for the detailed development of the probability-based methodologies in subsequent phases of this overall program.

Chapter 2

Structural Modeling

2.1 General

The essential dynamic characteristics of a system are mass distribution, initial stiffness and material behavior. To perform an accurate analysis, it is necessary to model these basic characteristics properly taking into account the geometrical configuration of the structure, the significant degrees of freedom, the characteristics of the forcing functions, anticipated level of response, material characteristics, the mathematical requirements of the available analytical tools, the objectives of the particular analysis, output quantities, etc. This task includes consideration of: (a) The methods of discretization; (b) The basic approaches for finding the masses and the stiffnesses; (c) The engineering decisions involved in coupling a subsystem with the main system; and (d) The isolation of the structural system from the adjacent medium, etc. The discussions in this chapter address these important topics.

2.2 Methods of Discretization

The major methods of discretization of a building structural system are the lumped-mass cantilever beam approach and the 2-dimensional or 3-dimensional finite element approach.

The lumped-mass cantilever beam model is adequate for a system where the mass can be considered as concentrated in a series of points, and where the overall building stiffness, or a significant part, can be associated with that of a simple cantilever beam. This modeling step entails the simplifying assumptions that plane sections remain plane after deformation and that no shape distortion occurs because of the diaphragm action of the floor slabs.

The 2-dimensional or 3-dimensional finite element approach does not require such simplifying assumptions in regard to the overall building behavior, as the method permits the use of various types of elements such as shell elements, plate elements, etc (Refs 2.9-2.16) to describe the overall stiffness. In addition, representation of local behavior of a structural system can be incorporated with ease.

In engineering practice, the lumped-mass beam approach is being widely used. The beam is selected such that the significant stiffnesses are properly represented. The approach is quite convenient and straightforward, as its properties can be chosen so that its natural frequencies match those of a more refined 3-dimensional finite element modal. For a specific structure, the accuracy with the lumped-mass beam approach is dictated by the total number of masses chosen. As an example (Ref 2.2), a cylindrical containment structure has been studied with two different methods, ie, the constant mass method and the constant member length method (Figure 2.1). For each method, the total number of lumped masses, N, was plotted against the ratios of the computed frequencies, ω_j, and the theoretical frequency values $(\omega_j)_T$, for each mode j. It was found, as a rule of thumb, that the maximum error in frequency associated with using the lumped-mass beam model is always within 10 percent so long as N is at least twice the mode number j. The results are reprinted in Figure 2.2. In Reference 2.3, a thin shell containment vessel was investigated. For the lumped-mass representation as shown in Figure 2.3(a), the linear stress results for the beam model and for the axial symmetric model in both the meridional and the circumferential directions are within 10 percent of each other for most of the regions (Figures 2.3(b) and 2.3(c)). Ebasco has performed a similar study with the axial symmetric shell as shown in Figure 2.4 for a beam model versus a shell model. The eigenvector for the first corresponding mode are shown in Table 2.1. The final difference in acceleration responses for seismic analysis are within 7 percent for all the points along the elevations (Table 2.2). The input seismic spectra is shown in Figure 2.5. The program utilized was STARDYNE (Ref 2.4). These examples demonstrate that a beam model is satisfactory for representing a containment structure where the lower modes (especially the first mode) dominate the behavior of the structure.

2.3 Basic Mathematical Modeling Approaches

The purpose of mathematical modeling is to find an idealized computational model to represent the system. The goal is to have the frequencies and the mode shapes of the model match with those of the real structure. The degree of sophistication in the modeling depends on the required degree of accuracy in the solution. Naturally, the capability of the computer codes available (Table 2.3) is a significant concern. As discussed in the previous section, an equivalent single or multiple-beam model is usually satisfactory for seismic analysis of typical power plant structures which are usually uniform and regular in structural arrangement. To correctly reflect the actual system section properties, certain procedures are established. Typical procedures for finding the section properties are: (a) Selection of the type of the equivalent members that can properly represent the dynamic characteristics of the structural system; (b) Definition of the stiffness(es) of the original system by static analysis; (c) Solution of the equations that correlate the stiffnesses found in (b) with the section properties of the equivalent beam. As an illustration, the section properties I and A, of an equivalent beam for horizontal analysis along a principal direction are written in terms of the rotational and translation stiffness of the original structure:

$$\frac{K_2 L^3}{12} + K_2 \frac{EIL}{GA_s} = EI \tag{2-1a}$$

$$K_1 L \left(1 + \frac{12EI}{GA_s L^2}\right) = \left(4 + \frac{12EI}{GA_s L^2}\right) EI \tag{2-1b}$$

where, E = Young's modulus

G = shear modulus

L = bent height

A_s = effective shear area

I = moment of inertia

K_1, K_2 = rotational, translational stiffness obtained through a FEM model subjected to unit loads

For vertical seismic analysis, the most important characteristic of a structural system is the axial stiffness of the walls and columns. Therefore, the selected gross area of the equivalent member should properly reflect the axial stiffness of the original vertical members. In engineering practice, floor slabs housing important equipment are usually considered in the model. The simplest method is to place pseudo-beams at the floor elevations with their frequencies corresponding to those of the floor slabs.

The traditional method for finding the geometric properties of the beam model is to calculate the sectional properties of the structural system by assuming plane sections behavior. For box-type wall-frame structures, the results are quite close to those obtained by solving the above equations and by assuming no local distortion of the section. There are cases, however, where the errors introducted in modeling may be large, eg, (a) Frame-type systems where the columns provide a substantial contribution to the lateral load resistance; (b) Shearwalls with large openings between floor levels; (c) Floor slabs which do not extend over the entire floor area.

In cases where an equivalent beam model is employed and the geometric layout of a structure is 3-dimensional in nature, the mathematical model should include overall torsion as a degree of freedom. The cantilever models may possess mass points offset with respect to the centerlines of the idealized beams elements. The location of the resistance centerlines may also vary along the building height.

2.4 Decoupling of Equipment or Subsystems for Structural Analysis

The dynamic characteristics of subsystems are such that they can display behavior independent from that of the main supporting structure to which they are attached. The subsystem dynamic behavior, when performing a joint analysis together with the building model, may be modified by the latter or may even cause a modification of the dynamic behavior of the building itself.

Several references (2.17, 2.33, 2.34) shed light on whether to attach rigidly the mass of the subsystem, neglecting any dynamic interaction, or whether to include the subsystem with its own dynamic behavior. In both cases, the analysis of the subsystem may proceed at a later stage as decoupled, that is, an analysis where the subsystem model is subjected to the seismic environment prevalent at its anchor point.

The following criteria are currently employed in engineering practice:

(1) For $R_m < 0.01$, decoupling can be done for any R_f.

(2) For $0.01 \leq R_m \leq 0.1$, decoupling can be done if $R_f \leq 0.8$, or $R_f \geq 1.25$.

(3) For $R_m > 0.1$, an approximate model of the subsystem should be included in the primary system model.

where,

R_m is the ratio of the total mass of the supported subsystem, to the modal mass of the building model for the dominant frequency(ies), and,

R_f is the ratio of the fundamental frequency of the supported subsystem, to the dominant frequency(ies) of the building model.

If it is judged that a local mode might govern the response (eg, equipment resting on a floor slab subjected to vertical excitation), the above ratios should be based, of course, on the local building mode.

With regard to the definition of R_f, it is noted that since the building seismic response results in filtering of the base seismic motion, the frequency of the motions experienced throughout the building tend to coincide with the predominant building natural frequencies. This observation leads to the more manageable definition, shown above, for R_f as opposed to that in Reference 2.17.

A reduction of response in the main structure may result from a coupled analysis. As can be seen on Figure 2.6(a), a reduction in building response might prove to be very sensitive to minor changes in the subsystem model. This figure represents the response of a two degree-of-freedom system excited at its base by a white noise motion. The mass m_2 attaches with its stiffness K_2 to the top of mass m_1, which is subjected to the base motion. Similarly, the response of mass point m_2, representing the subsystem, is shown on Figure 2.6(b) as a fraction of its frequency and mass ratio with respect to the single degree of freedom (m_1) representing the building.

For a PWR system, a study was made by combining the 4 loop-plant system with the ice condenser (Ref 2.6). Ebasco has also performed studies to evaluate the coupling effects between the internal structures and the main Nuclear Steam Supply System (NSSS) equipment. Figure 2.7 shows the overall building model including soil-structure interaction, while Figure 2.8 represents a more detailed model of the NSSS equipment to be analyzed by subjecting it to the mat time-histories obtained with the global model (uncoupled analysis). Figure 2.9 depicts the response of the top of the internal structures for both models, while Figure 2.10 describes the response for a lower elevation. The global analysis was performed utilizing the EBASCO 2037 computer program, and the decoupled analysis, with the STARDYNE program. Both responses are very close, in spite of the fact that EBASCO 2037 uses a "mass" modal damping approach, and STARDYNE, a "stiffness" modal damping approach.

In Reference 2.30, a dynamic analysis has been performed to compare the solutions by coupling or decoupling the subsystems, (ie, the interior building and the reactor coolant system). Both 3-dimensional and 2-dimensional cases were considered. In 2-dimensional analysis, all the reactions are within 5 percent of each other. In 3-dimensional analysis, all the reaction forces are within 10 percent while the reaction moments are slightly more. In general, the solutions show good agreement between the coupled and uncoupled models, in spite of the added complexity of multi-support excitation.

2.5 Structural Analyses Decoupled from Soil

There are situations in which structural analysis must be performed on structural models decoupled from the soil, eg, to find the local dynamic behavior of a location which had not been included in the soil-structure interaction analysis (SSIA) model for reasons of computational economy.

Power plant structures are, in general, very rigid at the mat level. Responses obtained from a SSIA can be reproduced approximately with a decoupled superstructure model. An investigation was made by performing a SSIA with the FLUSH program (Ref 2.7) for a 2-mass beam (Figure 2.11). The response acceleration time histories at the mat were saved for both the rocking and horizontal translational cases. By inputing these time histories to the superstructure at the mat level, an analysis was performed with EBASCO 2037 (Ref 2.8) with a stick beam model decoupled from the soil. As shown in Figure 2.12, a response spectra similar to the one obtained directly from the SSIA was obtained. Even though the solutions are not exactly the same, due perhaps to numerical round-off errors and to the different damping formulation in the time and frequency domains, the results may be considered as acceptable for structural design.

2.6 Dynamic Modeling for Fluid Effects

Hydrodynamic effects developed during an earthquake cannot be ignored in the design of power plant structures in cases where the quantity of water is large. The mathematical formulation for determining the seismically-induced fluid pressures to the structure is very complex. An engineering approach was developed first by Housner (Ref 2.18) in the investigation of dynamic pressures developed on accelerated liquid containers. The containers were flat-bottomed and of arbitrary constant cross section. Housner considered an incompressible liquid undergoing small displacements, and developed simplified expressions to approximate the pressures caused by the portion of the liquid accelerating with the tank (impulsive pressures) and the portion of the liquid sloshing in the tank (convective pressures). The results of previous analytical investigations (Refs 2.19-2.22) and experiments (Refs 2.23, 2.24) were used by Housner in verifying his results. In Reference 2.25, various cases for water contained in the tank were considered. The model is reprinted in Figure 2.13.

When a tank containing fluid of weight W is accelerated in a horizontal direction, a certain portion of the fluid acts like a solid mass of weight W_0 in rigid contact with the walls. Assuming that the tank moves as a rigid body, the mass will exert a maximum horizontal force directly proportional to the maximum acceleration of the tank bottom. The force is expressed as an impulsive force, P_0 in Figure 2.13. The acceleration also induces oscillations of the fluid, contributing additional dynamic pressures on the walls and bottom, in which a certain portion of the fluid, of weight W_1, responds as if it were a solid oscillating mass flexibly connected to the walls. The forces related are defined as a convective force, P_1, induced by the weight W_1 and the pseudo-springs as shown in Figure 2.13. Semi-empirical formulas to characterize these quantities for rectangular and cylindrical tanks are given in Reference 2.25. Along the same approach, there are still further developments in modifying those formulas (eg, Ref 2.26). The results of a recent experimental study of the seismic response behavior of cylindrical tanks are described in Reference 2.32. For structures with shapes different from the tanks or for cases where the hydrodynamic effects are 3-dimensional in nature, various approaches have been attempted, eg, References 2.27, 2.28, and 2.29. The approaches are either (a) To find the added mass by either a discrete approach such as finite element method (eg, Ref 2.27), or (b) To find the responses by including hydrodynamic effects directly from analytical solutions (eg, Refs 2.28 and 2.29). Reference 2.31 presents the results of a literature and industry survey of methods currently in use and under development for the analysis of submerged structures. Due to the complicated nature of this problem as described earlier, there is no single universally accepted code that can be utilized for computing hydrodynamic effects for generalized conditions.

References (Chapter 2)

2.1 Lazan, B J, Damping of Materials and Members in Structural Mechanics, Pergamon Press, 1965.

2.2 Bechtel Power Corporation, BC - Top. 4, Seismic Analysis of Structures and Equipment for Nuclear Power Plants.

2.3 Hagstorm, J, "The Design of a Thin Shell Nuclear Containment Vessel for Seismic Loading," ASME Transactions, Paper No. 71-WA.

2.4 Control Data Corporation, Stardyne Manual.

2.5 Crandall, S H and Mark, W D, Random Vibration in Mechanical Systems, Academic Press, 1963.

2.6 Chen, C, "Seismic Resistant Analysis of Heavy Equipment of PWR Plants," 2nd International Conference on Structural Mechanics in Reactor Technology, Berlin, 1973.

2.7 Lysmer, J, et al, FLUSH Manual, EERC 75-30, University of California, 1975.

2.8 EBASCO, Program 2037, User's Manual prepared by K D Chiu and N S Huang, July 1977.

2.9 Zienkiewicz, O C, The Finite Element Method in Engineering Science, McGraw-Hill, 1971.

2.10 Washizu, K, Variational Methods in Elasticity and Plasticity, Pergamon Press, 1968.

2.11 Courant, R, "Variational Methods for the Solution of Problems of Equilibrium and Vibration," Bulletin of the American Mathematical Society, 49, 1-23, 1943.

2.12 Clough, R W, "The Finite Element in Plane Stress Analysis," Proceedings 2nd ASCE Conference on Electronic Computation, Pittsburg, PA, September 1960.

2.13 Oden, J T, "A General Theory of Finite Elements," International Journal of Numerical Methods in Engineering, 1, 1969.

2.14 Fox, R L and Stanton, E L, "Developments in Structural Analysis in Direct Energy Minimization," Journal of the American Institute of Aeronautics and Astronautics, AIAA, 6, 1036-44, 1968.

2.15 Pain, T H H and Tong, P, "Basis of Finite Element Methods for Solid Continua," International Journal of Numerical Methods in Engineering, 1, 3-28, 1969.

2.16 Belytschko, T, "A Survey of Numerical Methods and Computer Programs for Dynamic Analysis," Nuclear Engineering and Design, 73, 1976.

2.17 USNRC, Standard Review Plan, Section 3.7.2, 1976.

2.18 Housner, G W, "Dynamic Pressures on Accelerated Fluid Containers," Bulletin of the Seismological Society of America, Vol 47, No. 1, January 1957, pp 15-35.

2.19 Graham, E W and Rodriguez, A M, "Characteristics of Fuel Motion Which Affect Airplane Dynamics," Journal of Applied Mechanics, Vol 19, No. 3, September 1952, pp 381-388.

2.20 Jacobsen, L S, "Impulsive Hydrodynamics of Fluid Inside a Cylindrical Tank and of Fluid Surrounding a Cylindrical Pier," Bulletin of the Seismological Society of America, Vol 39, No. 3, July 1949, pp 189-204.

2.21 Werner, P W and Sundquist, K J, "On Hydrodynamic Earthquake Effects," Transactions of the American Geophysical Union, Vol 30, No. 5, October 1949, pp 636-657.

2.22 Westergaard, H M, "Water Pressures on Dams During Earthquakes," Transactions, ASCE, Vol 98, 1933, pp 418-472.

2.23 Hoskins, L M and Jacobsen, L S, "Water Pressure in a Tank Caused by a Simulated Earthquake," Bulletin of the Seismological Society of America, Vol 24, 1934, pp 1-32.

2.24 Jacobsen, L S and Ayre, R, "Hydrodynamic Experiments with Rigid Cylindrical Tanks Subjected to Transient Motions," Bulletin of the Seismological Society of America, Vol 41, No. 4, October 1951, pp 313-346.

2.25 "Nuclear Reactors and Earthquakes," TID 7024, prepared by Lockheed Aircraft Corp and Holmes and Narver, Inc, for the U.S. Atomic Energy Commission, August 1963, pp 183-209 and 367-390.

2.26 Epstein, H I, "Seismic Design of Liquid-Storage Tanks," Journal of the Structural Division, ASCE, Vol 102, No. ST9, September 1976.

2.27 Shabban, Samia H, Users Manual for Admass Computer Code for Fluid-Structure Interaction Using the FEM Technique, Ebasco Services Inc, June 1979.

2.28 Au-Yang, N K, "Free Vibration of Fluid Coupled Coaxial Cylindrical Shell of Different Lengths," Journal of Applied Mechanics, Vol 68, No. 3, September 1976.

2.29 Chen, S S, Wambsganess, M W, and Jendrzejczyk, J A, "Added Mass and Damping of a Vibrating Rod in Confined Viscous Fluids," Journal of Applied Mechanics, Vol 98, No. 2, June 1976.

2.30 Gerdes, L D, "Dynamic Structural Analysis of Uncoupled Subsystems," Transactions of the 4th International Conference on Structural Mechanics in Reactor Technology, San Francisco, 1977, Vol K(b), Paper 6/18.

2.31 Dong, R G, "Effective Mass and Damping of Submerged Structures," Lawrence Livermore Laboratory, UCRL-52342, April 1978.

2.32 Clough, R W, Niwa, A and Clough, D P, "Experimental Seismic Study of Cylindrical Tanks," Journal of the Structural Division, ASCE, Vol 105, No. ST12, December 1979, pp 2565-2590.

2.33 Pickel, T W, Jr, "Evaluation of Nuclear System Requirements for Accommodating Seismic Effects," Nuclear Engineering and Design, 20, 1972, pp 323-337.

2.34 Hadjian, A H, "Some Problems with the Calculation of Seismic Forces on Equipment," ASCE Specialty Conference on Structural Design of Nuclear Plant Facilities, December 1973, Vol II.

TABLE 2.1
EIGENVECTORS FOR MODELS SHOWN IN FIGURE 2.4

COMPARISON OF CORRESPONDING NATURAL MODE			
ITEM		CANTILEVER MODEL	SHELL MODEL
MODE NUMBER		1	1
FREQUENCY		4.687 CPS	4.511 CPS
MODE SHAPE	1	1.000000	1.000000
	2	0.992148	0.991537
	3	0.954755	0.953623
	4	0.864885	0.867952
	5	0.707787	0.715413
	6	0.561195	0.561231
	7	0.404235	0.407782
	8	0.249167	0.257641
	9	0.109712	0.119578

NOTE: MODE SHAPE OF SHELL MODEL ARE AVERAGE VALUES OF THE SAME ELEVATION NODE POINTS IN Y COMPONENT

TABLE 2.2

COMPARISONS BETWEEN SHELL AND LUMPED MUDELS AS SHOWN IN FIGURE 2.4

CANTILEVER MASS PT. NO.	RESPONSE DIFFERENCE IN %	ACCELERATION RESPONSE OF CANTILEVER MODEL	CORRESPONDING AVERAGE RESPONSE OF SHELL MODEL IN THE SAME LEVEL
1	+0.4%	0.69816	0.69534
2	+0.49%	0.69173	0.68839
3	+0.25%	0.65865	0.65701
4	-1.5%	0.57933	0.58825
5	-1.87%	0.46083	0.46962
6	-0.45%	0.37381	0.37553
7	-2.03%	0.29452	0.30062
8	-5.75%	0.21214	0.22507
9	-6.11%	0.11730	0.12494

NOTE: 1. UNIT IS IN 'G'
2. RESPONSE DIFFERENCES ARE CALCULATED FROM CANTILEVERS AGAINST SHELL MODELS
3. SHELL MODEL RESPONSE ARE CALCULATED BY CONSIDERING 30 MODES

TABLE 2.3

A BRIEF SUMMARY OF THE AVAILABLE COMMERCIAL PROGRAMS (REF. 2.16)

PROGRAMS	LINEAR NONLINEAR	DAMPING	INTEGRATION (SCHEME)	SYSTEMS	PROGRAM SOURCES
ANSYS	NL, L	V, S	———	I, C, U	SWANSON
NASTRAN	L[1]	V, S	MODAL SUP NEWMARK INT	I, C, U	COSMIC
STARDYNE	L	V	———	C	CDC
MARC	NL, L	V, S	MODAL SUP NEWMARK INT	I, C, U	CDC
STRUDL	L	V	MODAL SUP	I, U	ICES
ADINA SAP IV (NON-SAP)	NL, L	V	NEWMARK INT MODAL SUP WILSON INT	C, (I, U)	MIT UC (BERK)
EBASCO 2077	L	V	MODAL	B	EBASCO

NOTATION: NL NONLINEAR　　I IBM
L LINEAR　　C CDC
V VISCOUS　　U UNIVAC
S STRUCTURAL　　B BURROUGHS

[1] WITH SPECIFIC NONLINEAR FEATURES

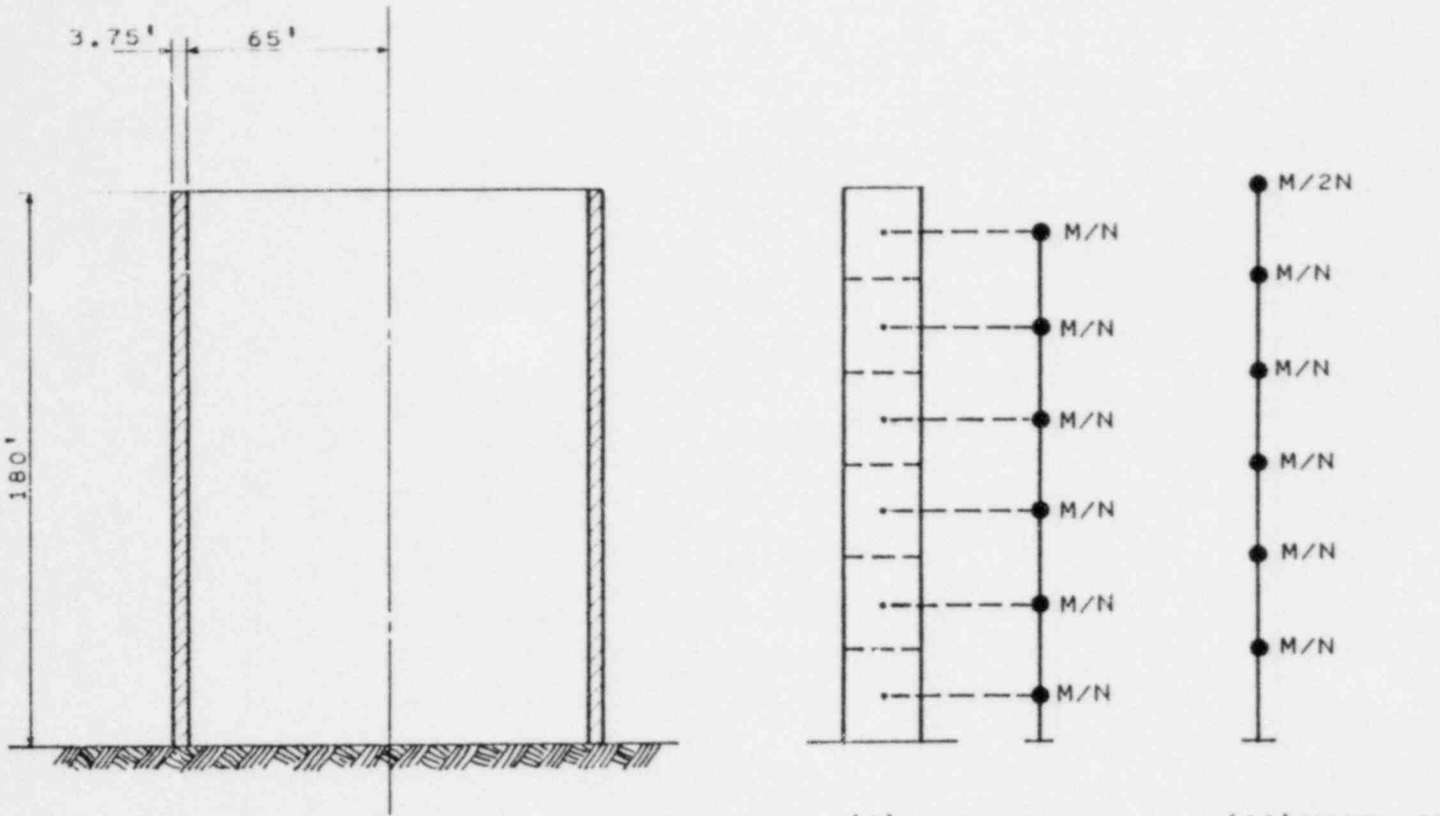

(i) MODEL I (ii) MODEL II

(a) THE EXAMPLE CYLINDRICAL CONTAINMENT STRUCTURE

(b) THE TWO COMMON METHODS OF CONSTRUCTING AN N-MASS LUMPED MODEL: (i) CONSTANT MASS, AND (ii) CONSTANT MEMBER LENGTH

FIGURE 2.1

LUMPED - MASS MODELS FOR CYLINDRICAL STRUCTURE (REF. 2.2)

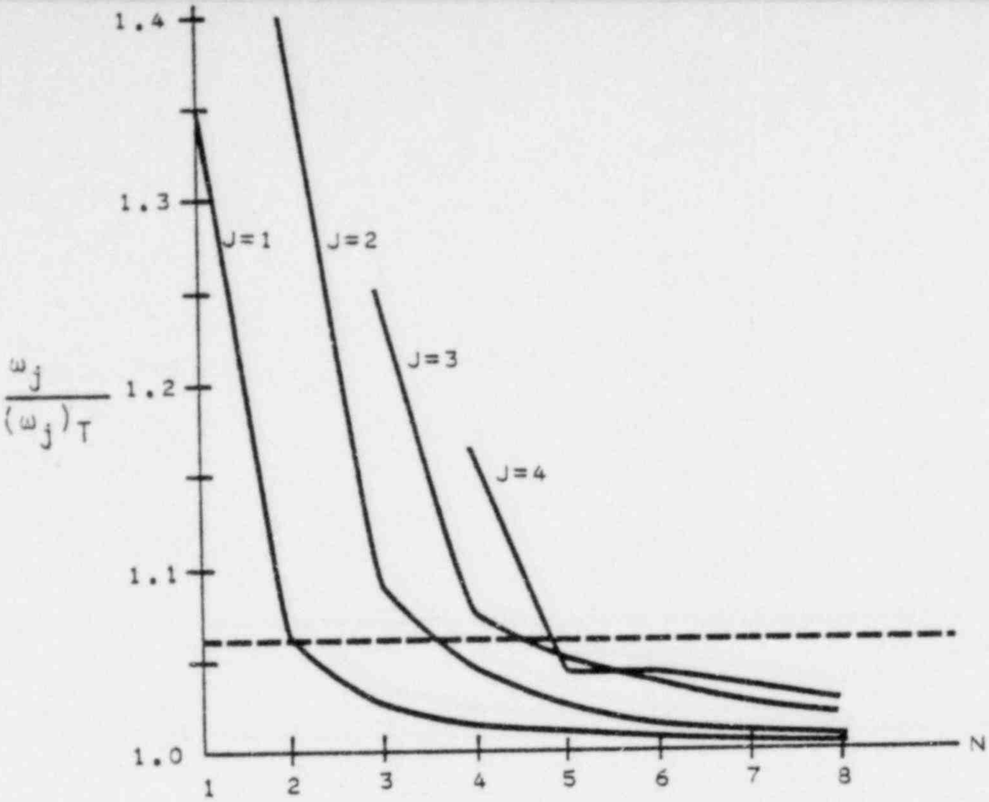

(a) FREQUENCY RATIO $\omega_j/(\omega_j)_T$ VS. N FOR HORIZONTAL VIBRATION OF MODEL (I)

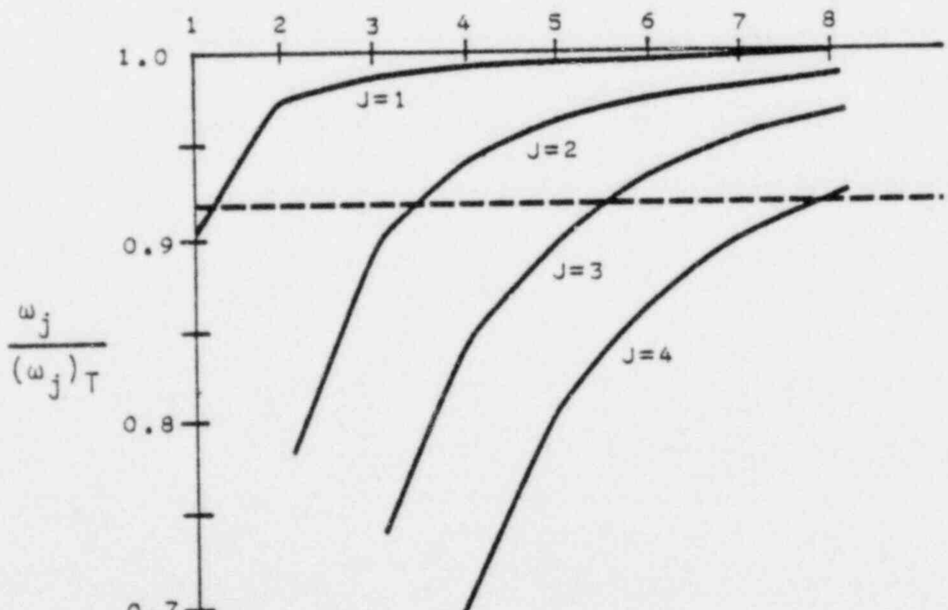

(b) FREQUENCY RATIO $\omega_j/(\omega_j)_T$ VS. N FOR VERTICAL VIBRATION OF MODEL (I)

FIGURE 2.2

FREQUENCY OUTPUT FOR THE MODELS SHOWN IN FIGURE 2.1 (REF. 2.2)

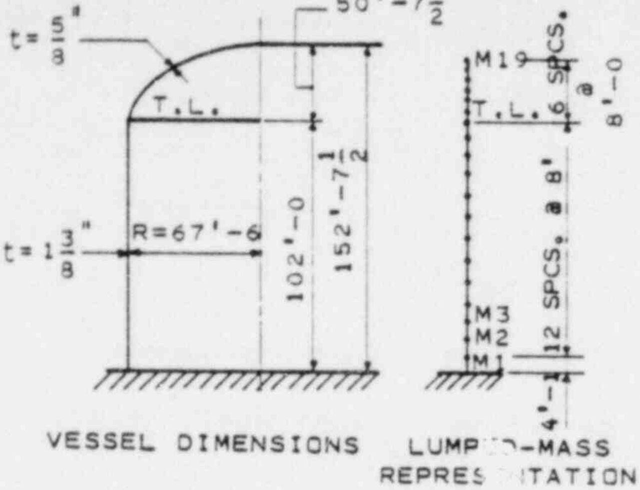

FIGURE 2.3 (a)
LUMPED MASS MODELS (REF. 2.3)

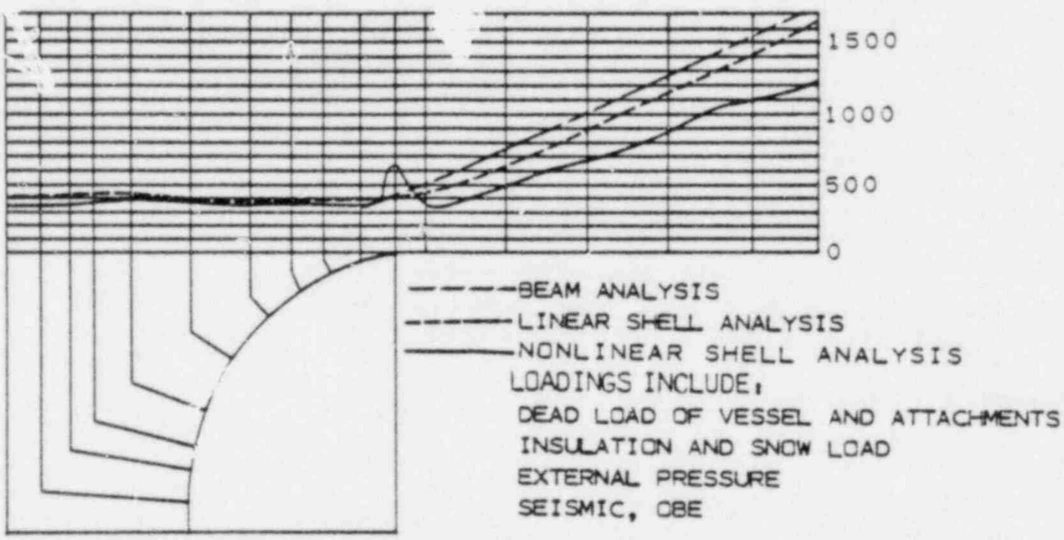

FIGURE 2.3 (b)
LINEAR SPECTRAL STRESS RESULTANTS AND MAXIMUM ABSOLUTE VALUES FOR NONLINEAR STRESS RESULTANTS, MERIDIONAL DIRECTION (REF. 2.3)

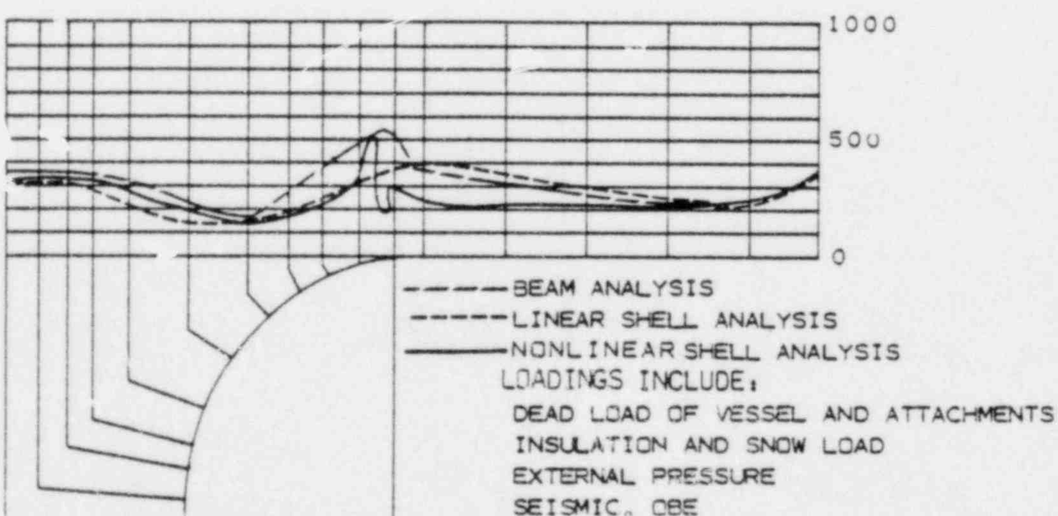

FIGURE 2.3 (c)
LINEAR SPECTRAL STRESS RESULTANTS AND MAXIMUM ABSOLUTE VALUES FOR NONLINEAR STRESS RESULTANTS, CIRCUMFERENTIAL DIRECTION (REF. 2.3)

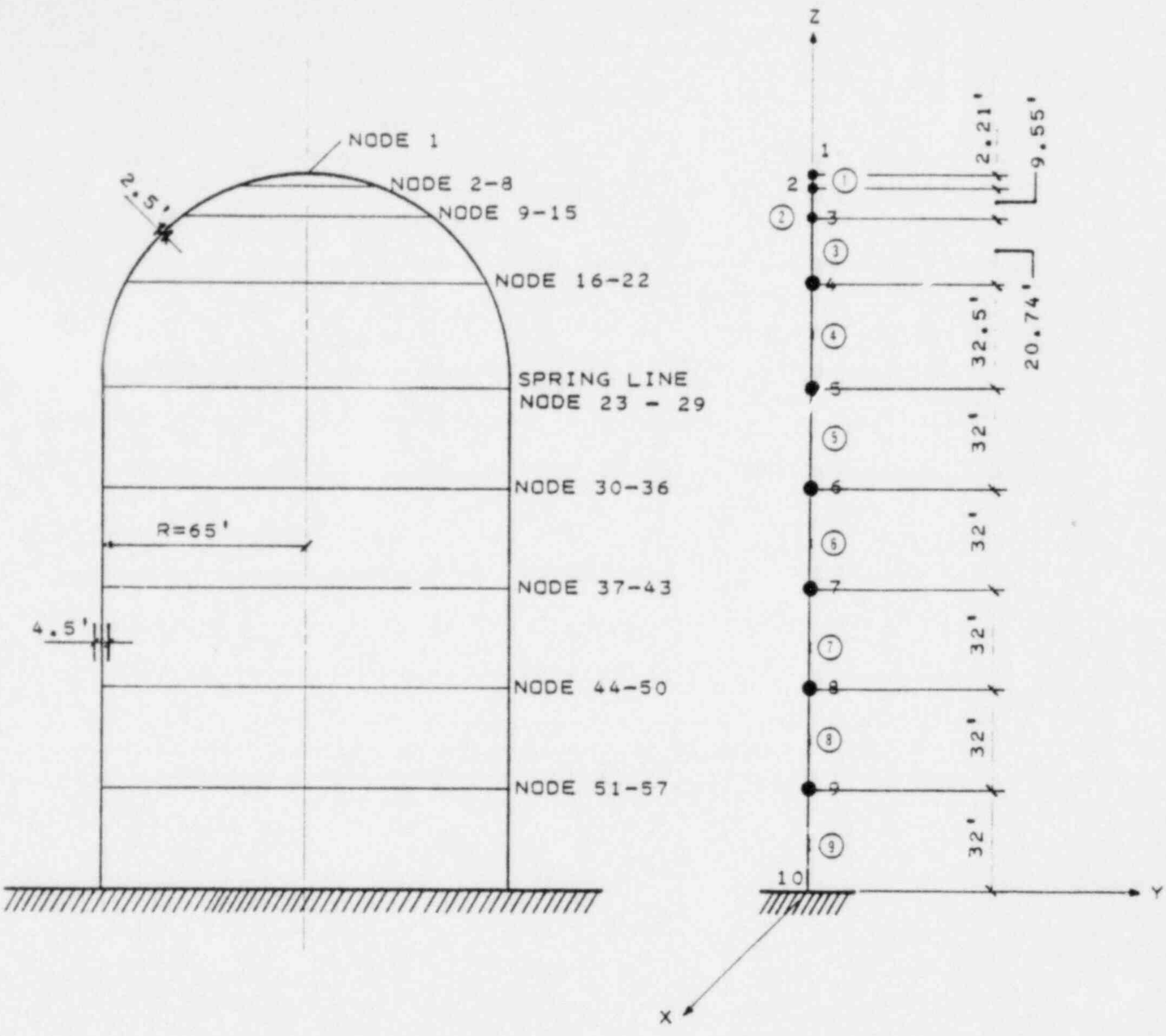

FIGURE 2.4

LUMPED-MASS MODELS FOR AN AXISYMMETRICAL SHELL

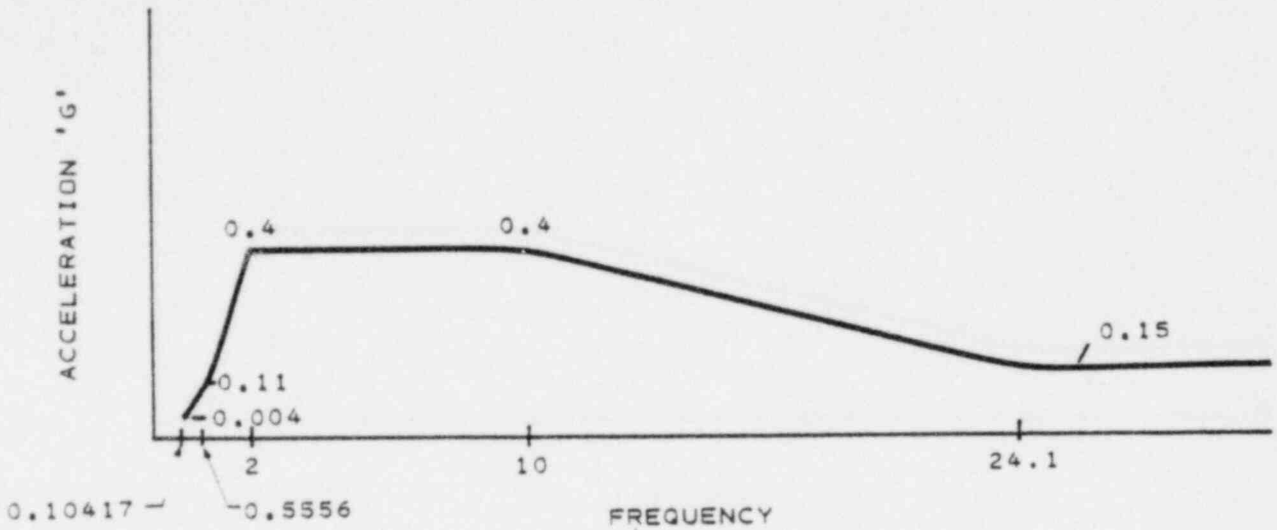

FIGURE 2.5

INPUT RESPONSE SPECTRA

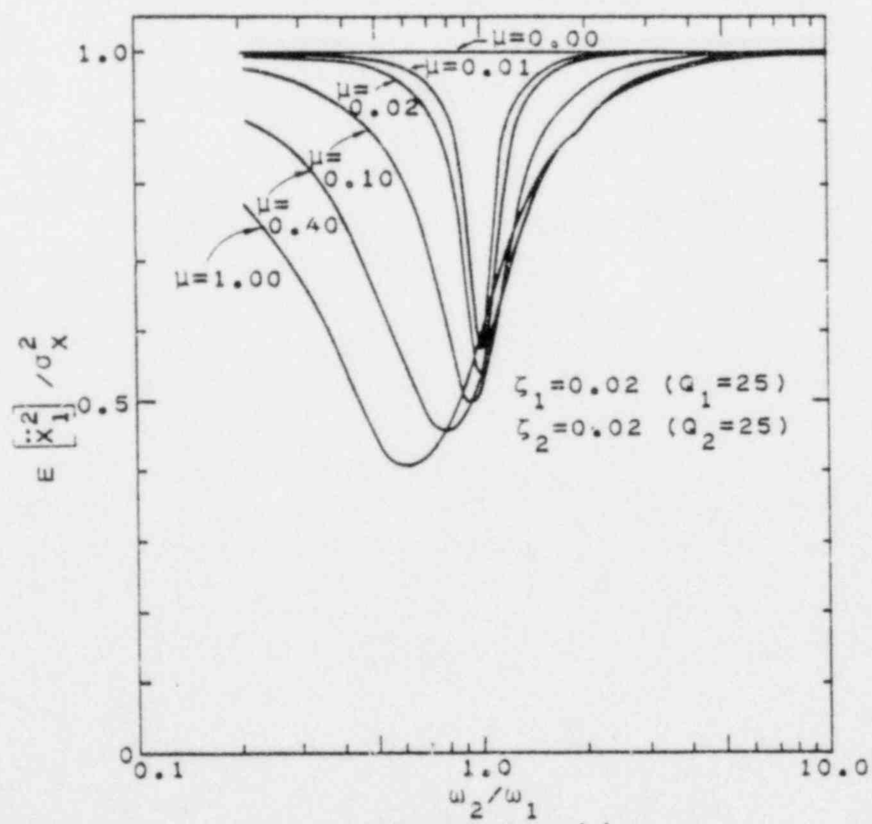

FIGURE 2.6 (a)

MEAN SQUARE ACCELERATION OF m_1 AS A FUNCTION OF SYSTEM PARAMETERS ω_2/ω_1 AND $\mu=m_2/m_1$ FOR $\zeta_1=\zeta_2=0.02$ WHEN EXCITATION IS IDEAL WHITE NOISE ACCELERATION OF FOUNDATION. (REF. 2.5)

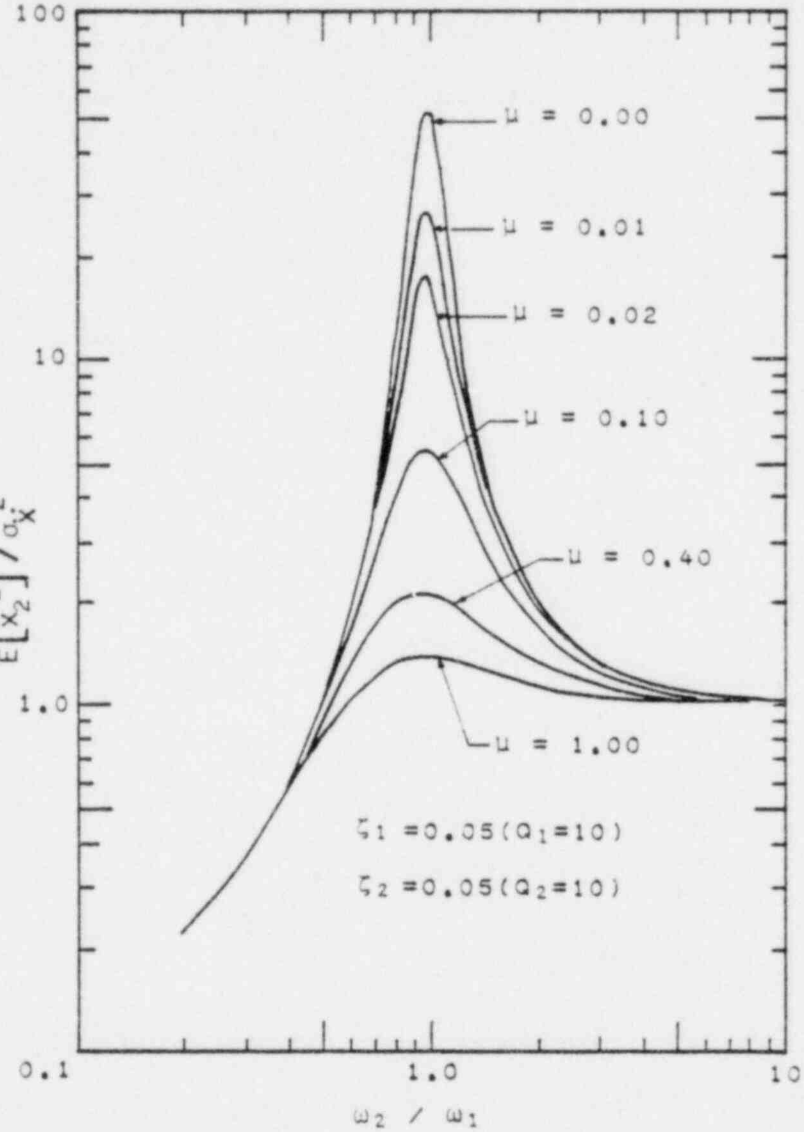

FIGURE 2.6 (b)
MEAN SQUARE ACCELERATION OF m_2 AS A FUNCTION OF SYSTEM PARAMETERS ω_2/ω_1 AND $\mu = m_2/m_1$ FOR $\zeta_1 = \zeta_2 = 0.05$ WHEN EXCITATION IS IDEAL WHITE NOISE ACCELERATION FOUNDATION (REF. 2.5)

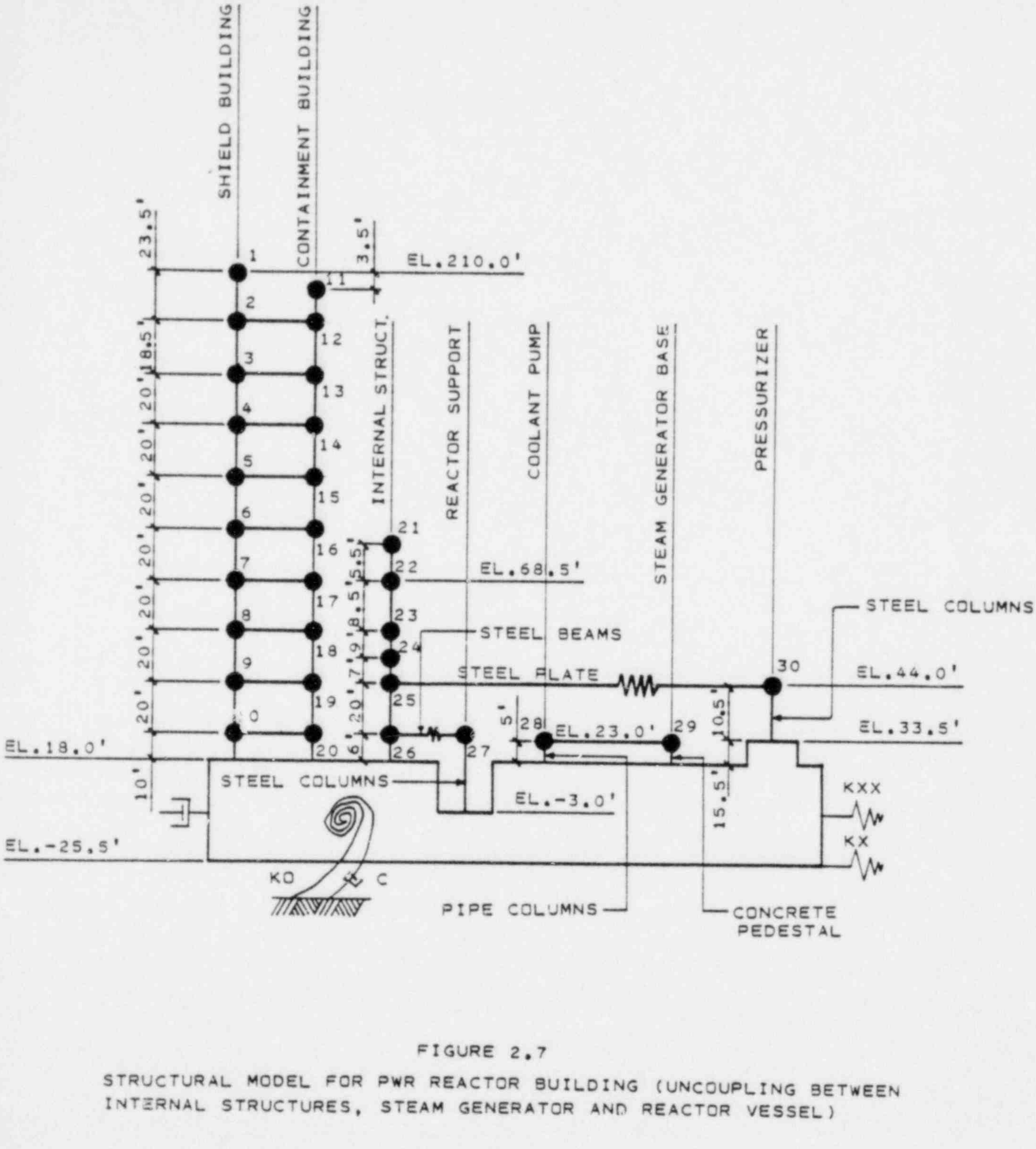

FIGURE 2.7

STRUCTURAL MODEL FOR PWR REACTOR BUILDING (UNCOUPLING BETWEEN INTERNAL STRUCTURES, STEAM GENERATOR AND REACTOR VESSEL)

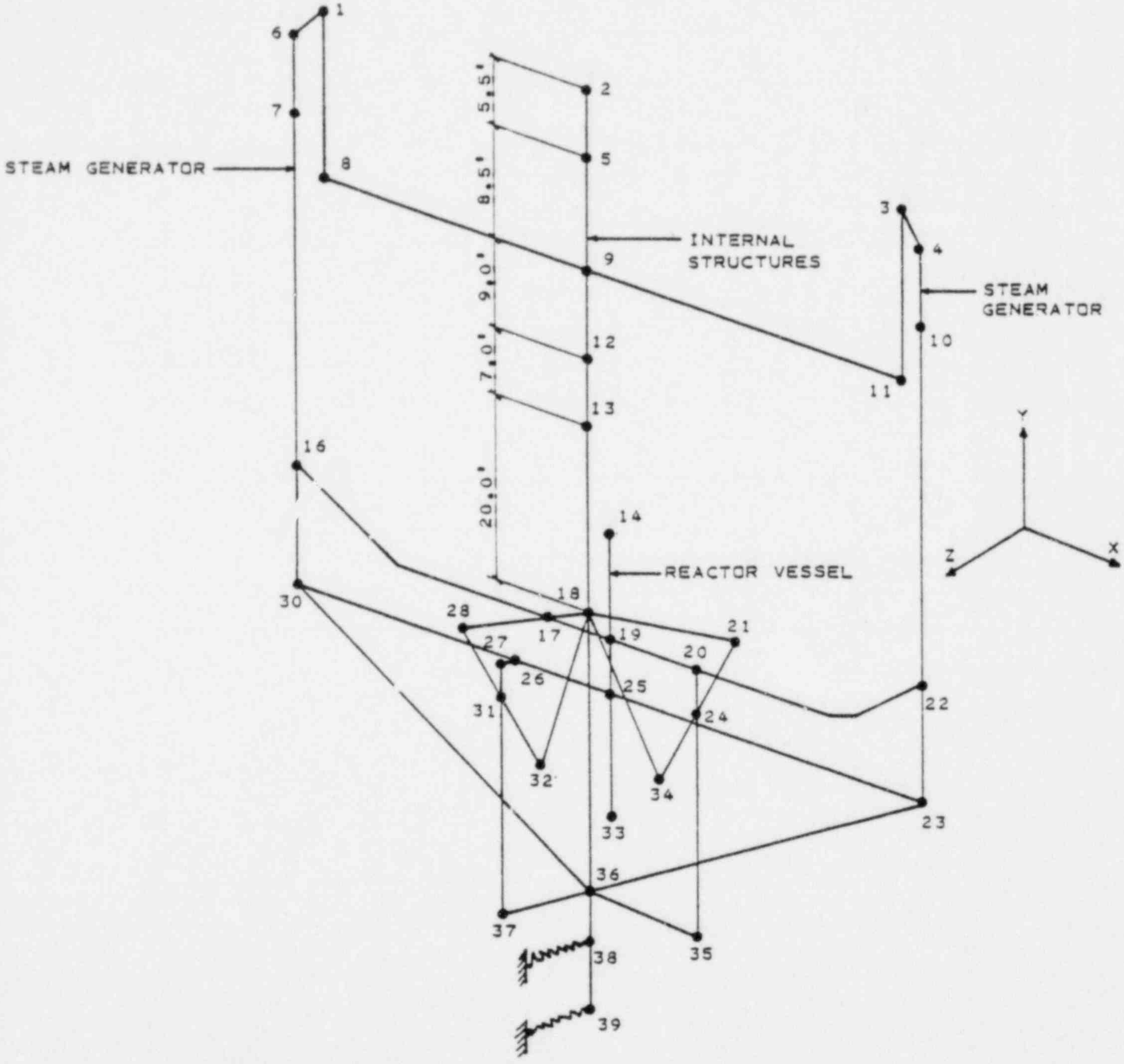

FIGURE 2.8

DETAILED MODEL FOR STEAM GENERATORS, INTERNAL STRUCTURES, AND REACTOR VESSEL

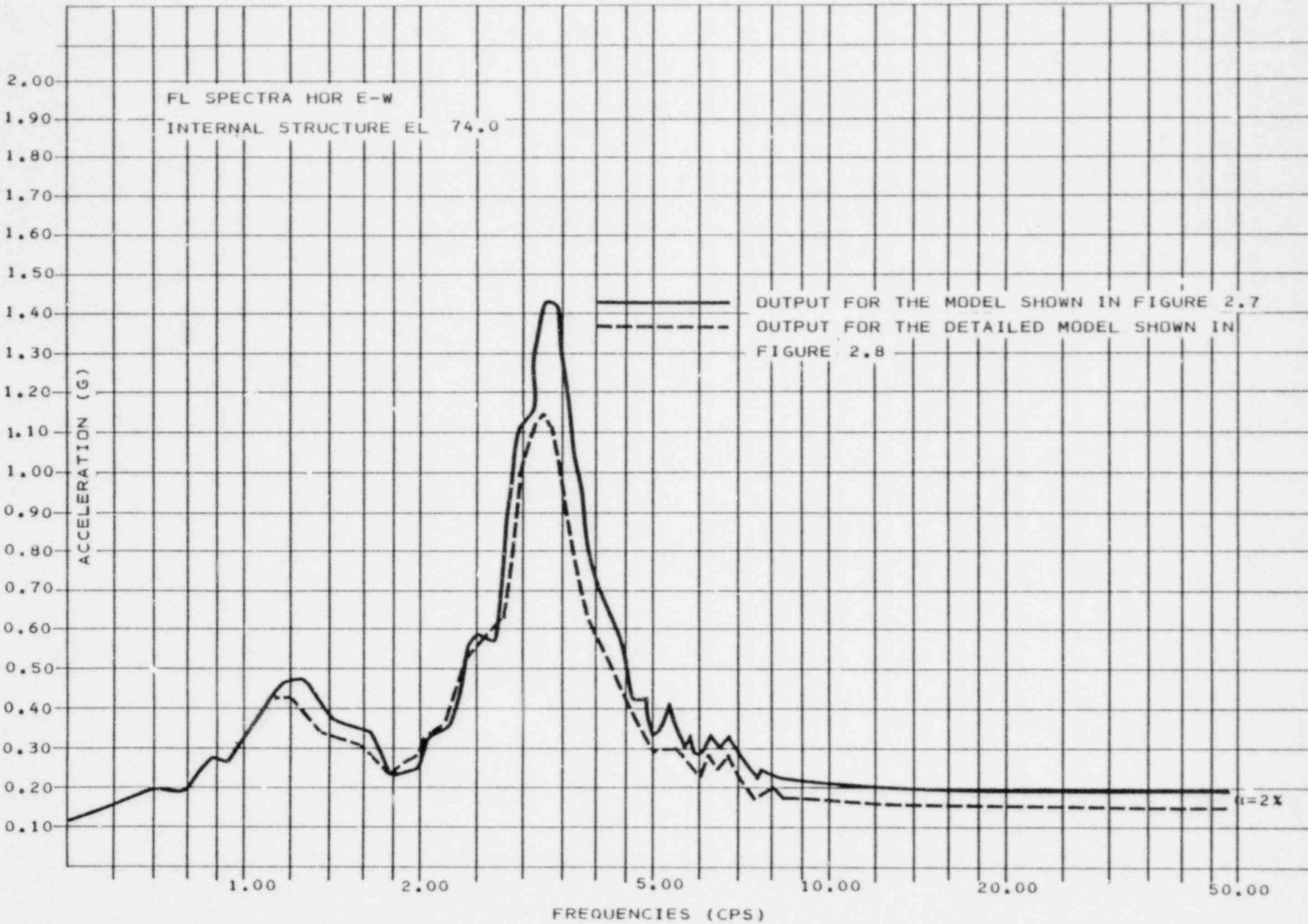

FIGURE 2.9

RESPONSE SPECTRA COMPARISONS BETWEEN OVERALL BUILDING MODEL AND DETAILED MODEL

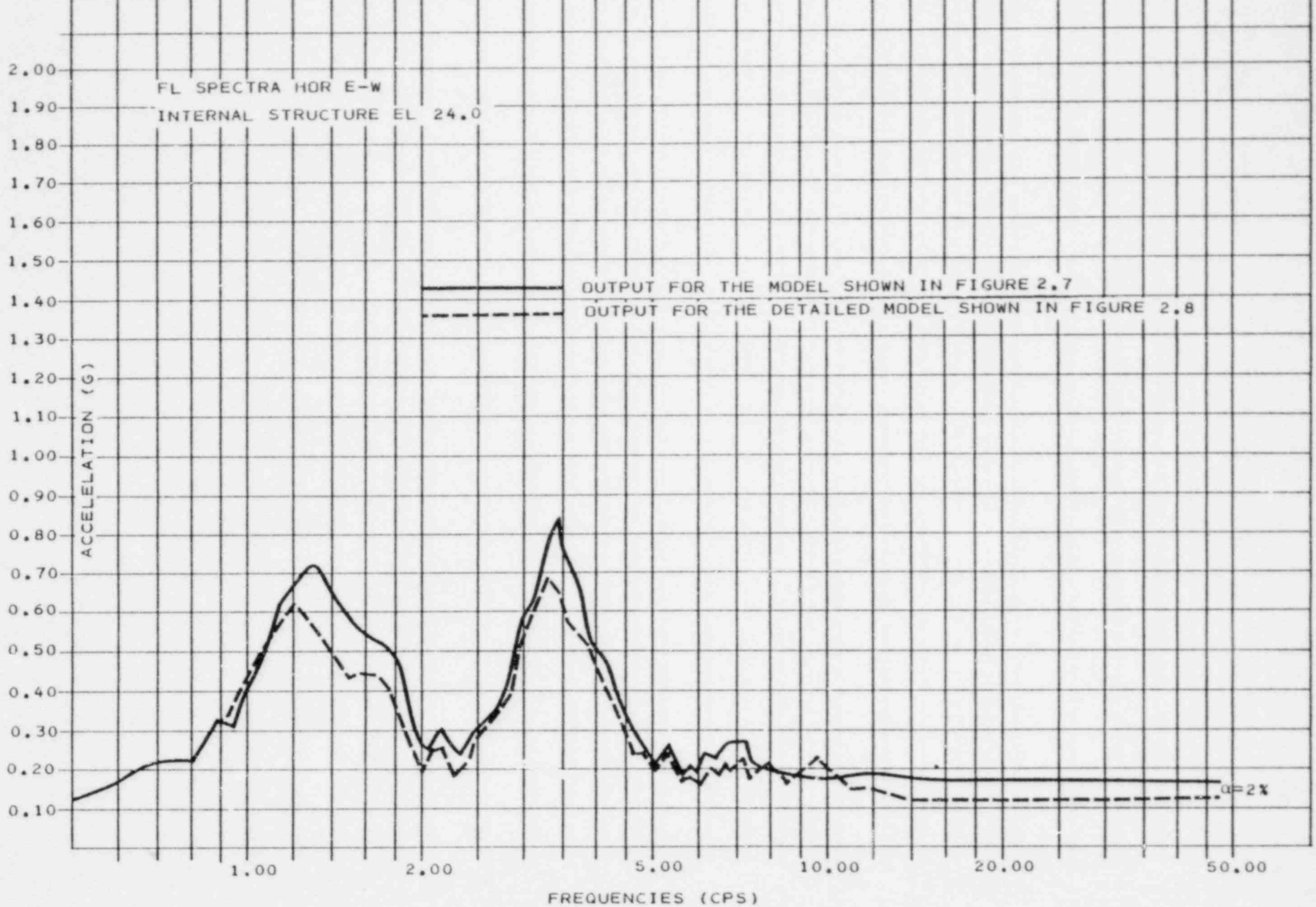

FIGURE 2.10

RESPONSE SPECTRA COMPARISONS BETWEEN OVERALL BUILDING MODEL AND DETAILED MODEL

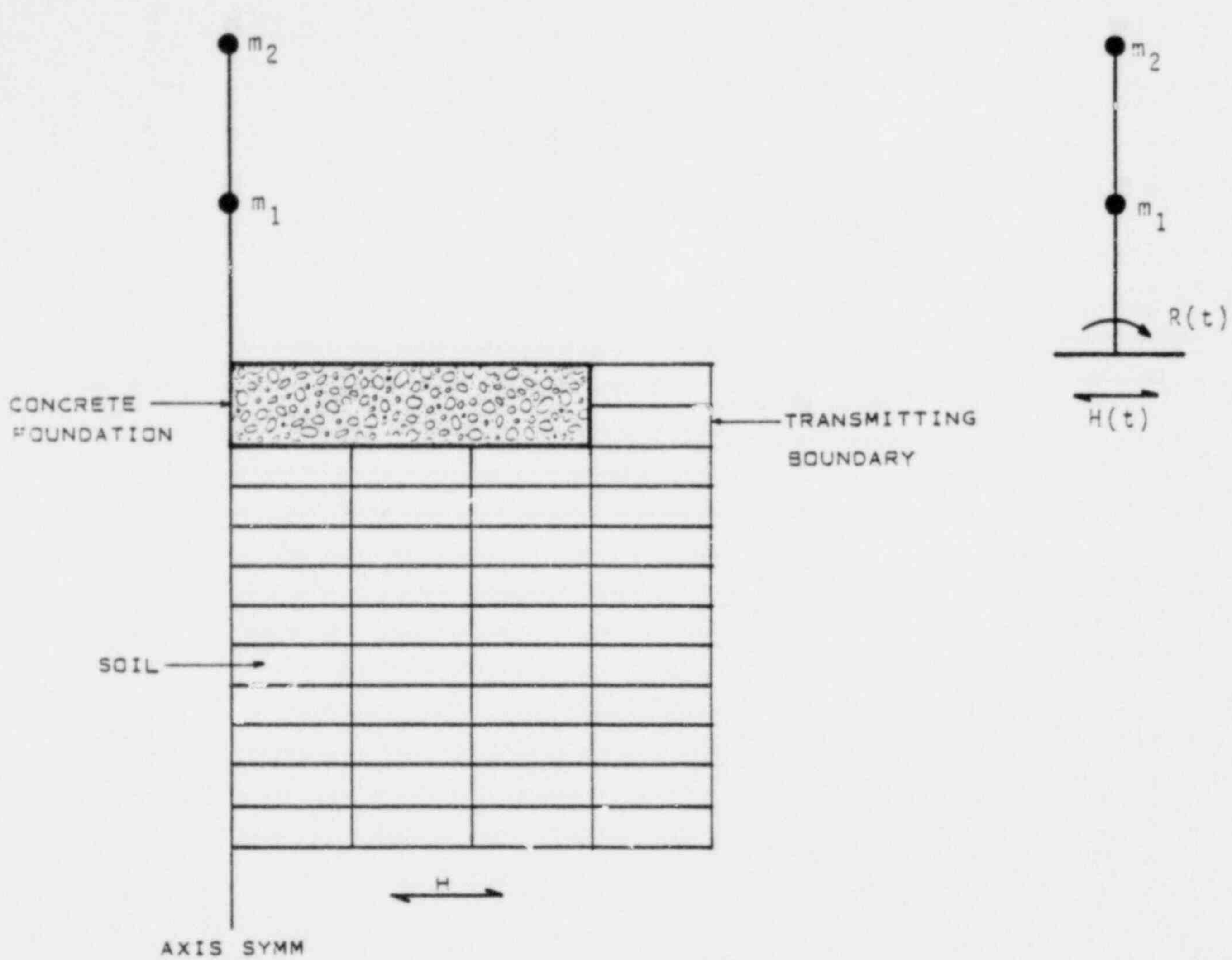

FIGURE 2.11

MODELS FOR SSIA AND DECOUPLED ANALYSIS (FROM SOIL)

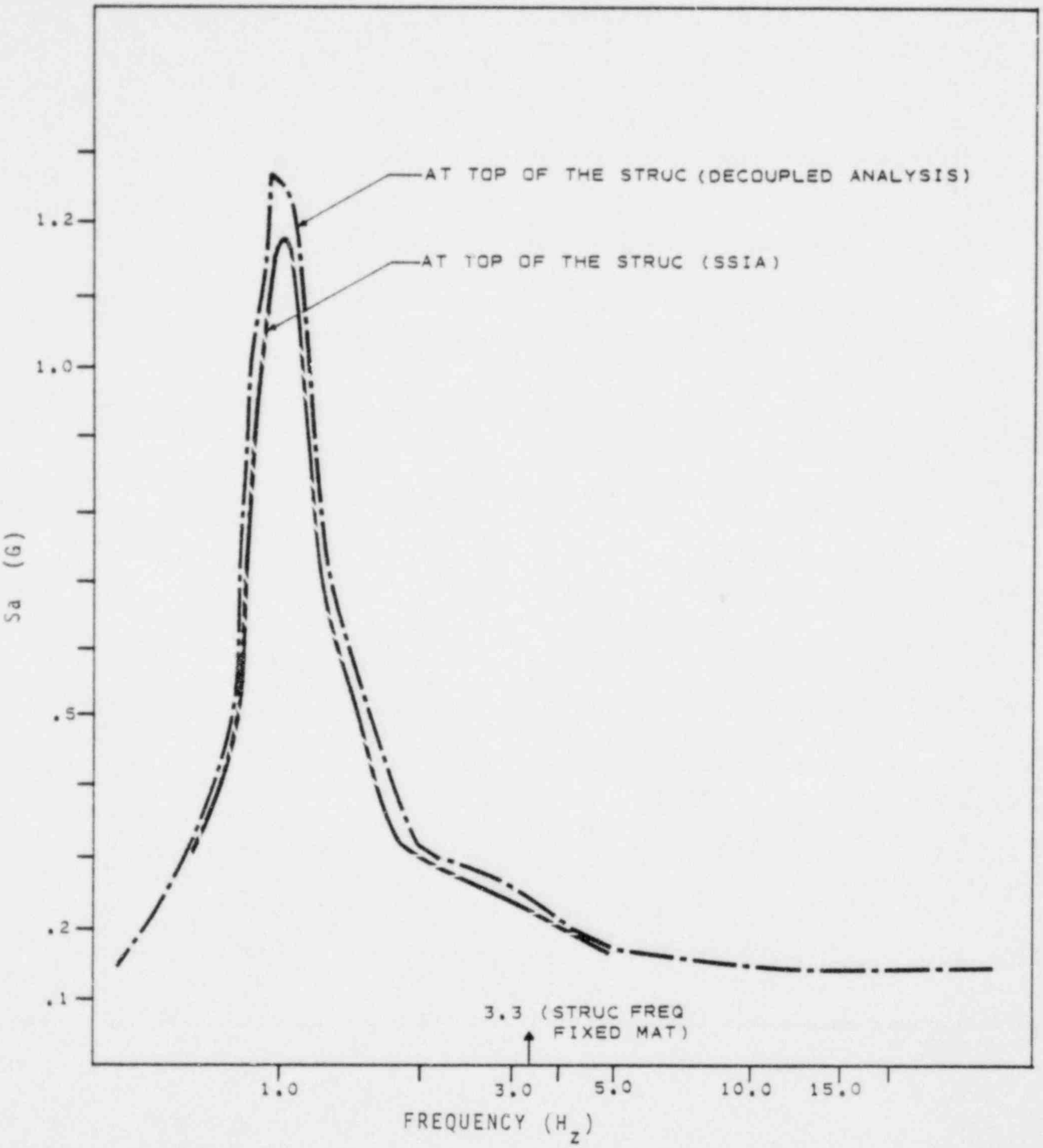

FIGURE 2.12

DECOUPLED ANALYSIS (FROM SOIL) VERSUS SOIL STRUCTURE INTERACTION ANALYSIS (SSIA)

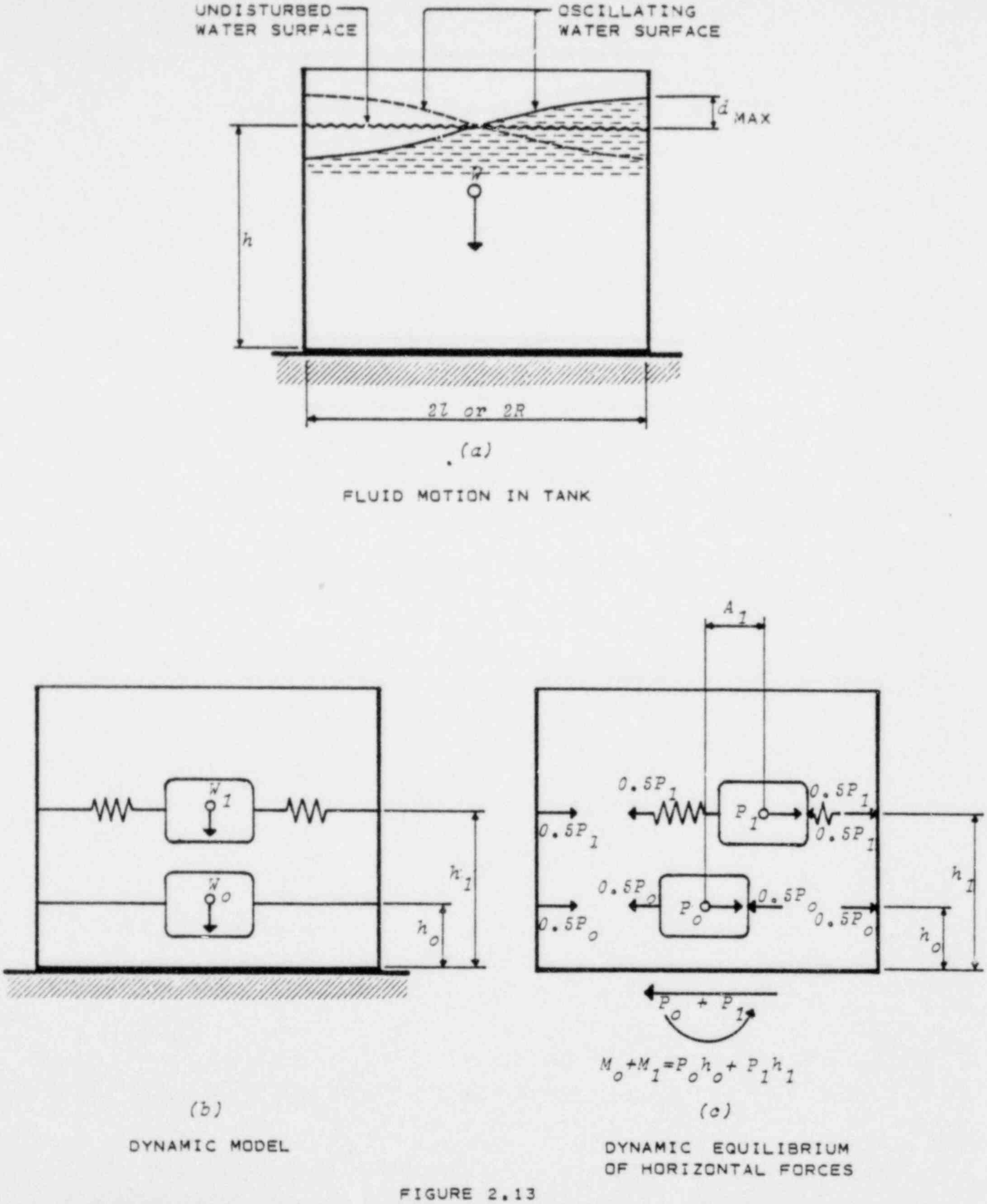

FIGURE 2.13
DYNAMIC MODEL FOR FLUID CONTAINER SUPPORTED ON THE GROUND. (*a*) FLUID MOTION IN TANK. (*b*) DYNAMIC MODEL. (*c*) DYNAMIC EQUILIBRIUM OF HORIZONTAL FORCES. (REF. 2.24)

Chapter 3
Structural Analysis

3.1 Introduction

Struc ural response can be determined by either (a) The time-history approach, or (b) The response spectrum approach. The response spectrum technique involves evaluation of the maximum response for each mode from the input design response spectrum (Ref 3.1). These modal responses are combined according to certain rules since the modal maxima do not necessarily occur at the same instant of time. The information obtained in this manner is not exact and the method cannot be used directly for a nonlinear analysis. In contrast, the time-history approach is theoretically more rigorous. Such analyses are usually accomplished by employing modal superposition or direct numerical integration of the equations of motion. The various analytical methods are treated in this Chapter along with the important topic of damping.

3.2 Time-History Method

The response of a structural system can be described by the differential equation of motion expressed as follows (Refs 3.2 and 3.3):

$$[M]\{\ddot{x}\} + [C]\{\dot{x}\} + [K]\{x\} = \{f(t)\} \tag{3-1}$$

where M is a mass matrix, C is a matrix of viscous damping coefficients, and K is a stiffness matrix, f is a force vector representing external loading and x, $\dot{x}$ and $\ddot{x}$ represent the displacement, velocity and acceleration vectors, respectively. If the system is subjected to a ground motion $\ddot{y}$, then the force vector may be expressed as $-[M]\,\ddot{y}\,a_i$, with $a_i = 1$ if the degree of freedom i is parallel to the direction of y, and $a_i = 0$, otherwise.

There are three methods available to solve Equation (3-1) numerically, namely, modal analysis, complex analysis and the direct integration method. Each of these methods is described below.

3.2.1 Modal Analysis - This discussion will treat both linear and nonlinear systems.

3.2.1.1 Linear Systems - The method of modal analysis assumes that a matrix Φ exists such that

$$[\Phi]^T[M][\Phi] = [I]$$

$$[\Phi]^T[K][\Phi] = [\omega^2]$$

and that the matrix $[C]$ is also diagonalized by,

$$[\Phi]^T[C][\Phi] = [2\xi\omega]$$

where ω is the natural frequency of the structure and ξ is the modal fraction of critical damping.

Let Y be the normal coordinates such that the displacement x can be defined by the transformation

$$\{x\} = [\Phi]\{Y\} \tag{3-3}$$

Equation (3-1) can then be transformed as:

$$\{\ddot{Y}\} + [2\xi\omega]\{\dot{Y}\} + [\omega^2]\{Y\} = [\Phi^T]\{f\} \tag{3-4}$$

Equation (3-4) is a set of decoupled equations, with each individual equation representing a mode. As a result, the response for each mode can be solved individually. The total response for the system involves combining the solutions for all the individual modes. There are limitations on the damping matrix C in order to obtain a set of decoupled equations as shown in Equation (3.4). In Section 3.6, the limitations and methods of solutions are discussed further.

3.2.1.2 Nonlinear Systems - Nonlinearities may be introduced in the system either due to material behavior or large geometric deformation. In either case, one of the coefficient matrices in Equation (3-1) will be nonlinear and hence time dependent. By introducing some new variables $[M_n]$, $[C_n]$ and $[K_n]$, Equation (3-1) can be written as a linear system on the left side, ie,

$$[M_e]\ddot{x} + [C_e]\dot{x} + [K_e]x = \{F(t)\} \tag{3-5}$$

where

$$[M_e] = [M] - [M_n]$$
$$[C_e] = [C] - [C_n] \quad (3\text{-}6)$$
$$[K_e] = [K] - [K_n]$$

and

$$[F(t)] = [f(t)] - [M_n]\ddot{x} - [C_n]\dot{x} - [K_n]x$$

Let $\{\Phi_i\}$ and $\{\omega_i\}$ be the ith orthonormal eigenvector and natural frequency respectively,

$$[M_e]\{\ddot{X}\} + [K_e]\{X\} = 0 \quad (3\text{-}7)$$

A transformation

$$\{X\} = [\Phi]\{Y\} \quad (3\text{-}8)$$

is introduced in Equation (3-5). The resulting uncoupled equation is as follows:

$$[I]\{\ddot{Y}\} + [2\xi_j\omega_j]\{\dot{Y}\} + [\omega_j{}^2]\{Y\} = \{P\} \quad (3\text{-}9)$$

where

$[I]$ = identity matrix

= $[\Phi]^T[M][\Phi]$

$[\Phi]$ = set cf significant eigenvectors

$\{Y\}$ = generalized displacement vector

ξ_j = j^{th} modal damping ratio

ω_j = j^{th} natural frequency

$\{P\}$ = generalized force

= $[\Phi]^T\{F\}$

Equation (3-9) can now be solved by explicit or implicit integration schemes with the condition that the generalized force in Equation (3-9) has to be updated at every time increment. If the initial stiffness matrix has a relatively large bandwidth and a large number of eigenvectors are not required for the analysis, it is likely that the modal superposition approach would be quite economical as compared with the direct integration procedures to be discussed later. The method described in this section was introduced in References 3.4, 3.5 and 3.6. Additional developments have been published in various technical papers which address efficient solutions for specific problems (eg, References 3.36 and 3.37).

3.2.2 Complex Analysis Method - With the concept of complex modulus or stiffness (References 3.7 and 3.8), Equation (3-1) can be written as

$$[M]\{\ddot{X}\} + [K^*]\{X\} = -[m]\{\ddot{y}\} \qquad (3\text{-}10)$$

where $[K^*] = [K_1] + i[K_2]$, is a complex stiffness matrix, which is obtained by including the element damping into the imaginary stiffness formulation as

$$K^* = K\left(1 - 2\beta^2 + i2\beta\sqrt{1 - \beta^2}\right)$$

where,

$i = \sqrt{-1}$
K = element stiffness
β = element damping ratio (≤ 1)

If y is expressed as

$$\ddot{y}(t) = \text{Re} \sum_{S=0}^{N/2} \ddot{Y}_s \exp(i\omega_s t) \qquad (3\text{-}11)$$

and assume that the response X is of the form

$$x(t) = \text{Re} \sum_{S=0}^{N/2} U_s \exp(i\omega_s t) \qquad (3\text{-}12)$$

then by substituting Equations (3-11) and (3-12) into (3-10), the response $[U_s]$ can be solved for each frequency ω_s. By the inverse Fourier transform, x(t) can be found in time domain. This method, of course, can be applied only for linear analysis. For consideration of inelastic material behavior, certain equivalent linear methods such as the effective shear strain concept (Reference 3.9) are employed. The validity of the equivalent linear method is highly dependent upon the selection of the coefficients.

The complex analysis method exhibits a difference in phase lag as compared to the method of modal superposition. By way of background, it will be recalled that the steady-state response of a damped single degree-of-freedom (SDOF) system subjected to a single frequency harmonic excitation has the same frequency as the loading, but it is out of phase with it. The phase angle, θ, by which the response lags behind the applied load, is given by

$$\tan\theta = \frac{2\beta\ \omega/\omega_o}{1-(\omega/\omega_o)^2} \tag{3-12a}$$

where,

β = damping ratio
ω = loading frequency
ω_o = SDOF natural frequency

If the response of the SDOF is again estimated through the complex stiffness method, defined above, the same amplitude will result, but the phase angle will be, (Reference 3.10).

$$\tan\theta^* = \frac{2\beta\sqrt{1-\beta^2}}{1-2\beta^2 - (\omega/\omega_o)^2} \tag{3-12b}$$

Table 3.1 presents the difference $(\theta-\theta^*)$ between both approaches as a function of β and α ($= \omega/\omega_o$). As can be seen from this table, in the quasi-resonant range and for the relatively low levels of damping used in practice, this phase angle difference may be regarded as insignificant.

3.2.3 Direct Integration - The direct integration method can be used for solving either linear or nonlinear systems. For nonlinear analysis, the stiffness or the damping matrix has to be updated at each time step. The method involves integrating the set of the governing equations by means of an acceptable numerical scheme as described in the following section.

3.2.4 Numerical Integration Schemes - Numerical integration techniques can be classified into two groups based on the numerical technique, ie, explicit integration schemes or implicit integration schemes.

3.2.4.1 Explicit Schemes - In this approach, the differential equations of motion are converted to a set of linear algebraic equations with unknown state variables which are independent of one another. The widely used explicit schemes are: (a) Runge-Kutta methods, (b) Predictor-corrector methods, (c) Nordsieck integration method and (d) Central difference methods.

The Runge-Kutta procedures are single-step methods. They do not require any past history of values, and, hence, changing the value of the time step is not a problem. Various formulas have been derived to implement the method, eg, fourth order formula, the third order formula, etc. Higher order derivatives are required depending upon the order of the method. Naturally, the order of magnitude of the errors associated with each formula is different. Details of the various formulations can be found in various texts on numerical procedures (for example, References 3.39, 3.40 and 3.41). The predictor-corrector methods are carried out in two steps. One step is to predict the value of the unknowns based on certain formulas (for example, Adam's method). The second step is to correct the predicted value with a closed formula such as Simpson's rule. Such methods have been well developed and error estimates based on each specific method can be found in the numerical texts referenced above. The central difference method has been widely used in the field of mechanics. The method is popular because its formulation is simple and the procedure for computer programming is straightforward. However, the method has its disadvantages in that it is limited to a constant time step. The Nordsieck integration method was introduced in Reference 3.38. The approach is similar to the predictor methods. However, the formulation is more complicated due to the addition of more parameters and thus, the method is subject to higher-order error. Since the above methods are conditionally stable, they have the inherent disadvantage of requiring that small time steps be employed.

All the explicit schemes have been utilized extensively in dynamic analysis, eg, recently, Garnet and Armen (3.11) solved one-dimensional wave propagation problems with the aid of a predictor-corrector method, ie, the modified Adam's method. In Reference 3.12, the Nordsieck integration scheme is used to solve nonlinear vibration problems in reactor components. Wu and Witmer (3.13) analyzed the problem of large transient elastic-plastic deformation of structures using the central difference method. However, the popular computer programs listed in Table 2.3 are all written based on implicit schemes as covered in the next section.

3.2.4.2 Implicit Schemes - These schemes convert the differential equations of motion to a set of linear simultaneous algebraic equations and require matrix inversion to step the solution forward. The widely used implicit shemes are:

a) Newmark's generalized acceleration method.

b) Wilson-θ-method.

c) Houbolt method.

3.2.4.2.1 Newmark's Generalized Acceleration Method (Reference 3.14) - The nodal point velocities and displacements are given by the following expressions:

$$\{\dot{X}_{n+1}\} = \{\dot{X}_n\} + (1-\gamma)(\Delta t)\{\ddot{X}_n\} + \gamma(\Delta t)\{\ddot{X}_{n+1}\} \quad (3\text{-}13)$$

and

$$\{X_{n+1}\} = \{X_n\} + (\Delta t)\{\dot{X}_n\} + (1/2 - \beta)(\Delta t)^2\{\ddot{X}_n\} + \beta(\Delta t)^2\{\ddot{X}_{n+1}\} \quad (3\text{-}14)$$

With the Equations (3-13) and (3-14) substituted into Equation (3-1), expressed at the present time point (n+1). This gives

$$\left[[M] + \gamma\,(\Delta t)\,[C] + \beta\,(\Delta t)^2\,[K]\right] \ddot{X}_{n+1}$$

$$= \{F_{n+1}\} - \left[(1-\gamma)\,(\Delta t)\,[C] + (1/2-\beta)\,(\Delta t)^2\,[K]\right]\{\ddot{X}_n\} \qquad (3\text{-}15)$$

$$- \left[[C] + (\Delta t)\,[K]\right]\{\dot{X}_n\} - [K]\,\{X_n\}$$

This set of algebraic simultaneous equations in the unknown accelerations is solved and used with Equations (3-13) and (3-14) to obtain the velocity and displacement at the present time. The parameter γ in the above equation is a damping parameter. Artifical positive damping is introduced if $\gamma > 0.5$ and artificial negative damping if $\gamma < 0.5$. For linear problems, the method is unconditionally stable if $\beta > (2\gamma + 1)^2/16$. For $\gamma = 1/2$, $\beta > 1/4$ gives unconditional stability. For systems with nonlinearities and/or nonproportional damping, there is no analytical expression available for unconditional stability. In order to provide a margin of stability for these systems $\beta > 1/4$ is considered for $\gamma = 1/2$. The value of γ slightly larger than 0.5 may be considered to damp out the highest (and least important) modes while preserving the lower ones. The Newmark method for $\gamma = 1/2$ (no numerical damping), and $\beta = 1/6$ (linear acceleration), is conditionally stable.

3.2.4.2.2 Wilson-θ-Method (Reference 3.15) - To obtain the solution at the present time point (n+1), this method assumes the acceleration varies linearly over the time interval $\tau = \theta\Delta t$, where $\theta > 1.0$. With the aid of Equation (3-15), $\beta = 1/6$ and $\gamma = 1/2$, solution at time point $(n+\theta)$, is obtained. Then the acceleration, velocity and displacement at the time point (n+1) are given by the following expressions:

$$\{\ddot{X}_{n+1}\} = (1-1/\theta)\,\{\ddot{X}_n\} + \frac{1}{\theta}\,\{\ddot{X}_{n+\theta}\}$$

$$\{\dot{X}_{n+1}\} = \{\dot{X}_n\} + \frac{\Delta t}{2}\,\{(\ddot{X}_n + \ddot{X}_{n+1})\} \qquad (3\text{-}16)$$

$$\{X_{n+1}\} = \{X_n\} + \Delta t\,\{\dot{X}_n\} + \frac{\Delta t^2}{6}\,\{(\ddot{X}_{n+1} + 2\,\ddot{X}_n)\}$$

The last two equations are obtained from Equations (3-13) and (3-14) with the values of β and γ as specified above. In Reference 3.15 it is indicated that this method is unconditionally stable for $\theta > 1.37$. For $\theta = 1.4$, the numerical damping is less than one percent provided twenty-two steps are taken within the natural period of the mode of interest (Reference 3.16).

3.2.4.2.3 The Houbolt Method (Reference 3.19) - In this method, a third-order interpolation polynomial which fits the known displacements at the three previous time points and the unknown displacement at the present time point is formulated. The expressions for acceleration and velocity are given as:

$$\left\{\ddot{X}_{n+1}\right\} = \frac{1}{(\Delta t)^2}\left[2\left\{X_{n+1}\right\} - 5\left\{X_n\right\} + 4\left\{X_{n+1}\right\} - \left\{X_{n-2}\right\}\right]$$

$$\left\{\dot{X}_{n+1}\right\} = \frac{1}{6(\Delta t)}\left[11\left\{X_{n+1}\right\} - 18\left\{X_n\right\} + 9\left\{X_{n-1}\right\} - 2\left\{X_{n-2}\right\}\right] \qquad (3\text{-}17)$$

Equation (3-17) is substituted in Equation (3-1) expressed at the present time point (n+1). This gives

$$\left[\frac{2}{\Delta t^2}[M] + \frac{11}{6\Delta t}[C] + [K]\right]\left\{X_{n+1}\right\} = \left\{F_{n+1}\right\} + \left[\frac{5}{\Delta t^2}[M] + \frac{3}{\Delta t}[C]\right]\left\{X_n\right\} - \left[\frac{4}{\Delta t^2}[M] + \frac{3}{2\Delta t}[C]\right]\left\{X_{n-1}\right\} + \left[\frac{1}{\Delta t^2}[M] + \frac{1}{3\Delta t}[C]\right]\left\{X_{n-2}\right\} \qquad (3\text{-}18)$$

This set of algebraic simultaneous equations in the unknown displacements is solved and used to find velocity and acceleration.

This method is unconditionally stable for linear problems by introducing artificial damping. The amount of such damping increases with the ratio of time step to period of the natural modes of the system. The artificial damping is less than one percent provided fifty time steps are taken within the natural period of the mode of interest. Thus, the Houbolt method effectively removes higher mode response from the system.

A comparison of these methods for linear problems is shown in Figure 3.1 (Reference 3.15).

For nonlinear systems, the following two steps are suggested to ensure convergence of the solution to the proper value.

1) Iterative schemes, based on the residual force array derived from the equation of motion at the present time point (n+1) may be used to obtain convergence. This residual, obtained by transferring all the terms in equations to the right-hand side, is a measure of how well the dynamic equilibrium is satisfied at the present time point (n+1). The time dependent matrices and force arrays are modified based on the calculated solution at time point (n+1) and the iterative scheme is continued until dynamic equilibrium is satisfied to a prescribed tolerance. References 3.16, 3.17 and 3.18 considered this approach to improve efficiency in nonlinear solutions.

2) Successive computation of the time history, employing successively smaller values of the integration time step, may also be used to ascertain convergence.

3.3 Response Spectrum Method

With the input given in terms of the design spectra, the modal displacement response is directly obtained from the design spectra as

$$q_{j,max} = r_j Sa_j / \omega_j^2 \qquad j = 1,2 \ldots \qquad (3\text{-}19)$$

where Sa_j is the value of the acceleration spectral response at frequency ω_j (or f_j, $f_j = \omega_j / 2\pi$) and for damping β_j. From Equation (3-19), the displacement response per mode at any mass point is:

$$x_{ij,max} = \Phi_{ij} q_{j,max} \qquad (3\text{-}20)$$

Other structural responses per mode, such as shears and moments, can be computed from $x_{ij, max}$ by using the stiffness properties of the structural members. The modal responses are then combined according to the methods described in the following section.

Another aspect of the response spectrum approach which is being developed (eg, References 3.44 and 3.45) are procedures which permit the direct generation of the floor response spectra, based upon the input design spectra, without performing a time-history analysis.

3.4 Combination of Modal Responses

Following the response spectrum approach, only the modal maxima, presumed to occur at different time instants, are known. Therefore, in order to obtain the final response, these modal maxima are combined using statistical rules.

A commonly used method takes the square root of the sum of the squares (SRSS) of the modal maxima, treating these in the manner of random quantities. Good agreement is achieved with respect to the time-history approach, provided that the individual modes are well separated.

The SRSS method tends to yield low values when the frequencies corresponding to two or more significant modes have very close values. The following methods overcome this shortcoming (Reference 3.42):

Grouping Method - Closely spaced modes are divided into groups that include all modes having frequencies lying between the lowest frequency in the group and a frequency 10 percent higher, with no frequency included in more than one group.

Within each group, so defined, the representative value is found through the sum of the absolute values of the modal maxima. The overall final response is found by SRSS combination of each group representative value and the remaining modal responses of the modes that are not closely spaced

Double Sum Method - The final response, R_a, is defined by the below formula

$$R_a = \left[\sum_{K=1}^{N} \sum_{L=1}^{N} R_K R_L \epsilon_{KL} \right]^{1/2}$$

where,

R_K, R_L = modal maxima

ϵ_{K_L} = modal coupling term defined as

$$\epsilon_{KL} = \left\{ 1 + \left[\frac{\omega'_K - \omega'_L}{\beta'_K \omega_K + \beta'_L \omega_L} \right]^2 \right\}^{-1}$$

with

$$\omega'_K = \omega_K \left[1 - \beta_K{}^2 \right]^{1/2}$$

$$\beta'_K = \beta_K + \frac{2}{t_d \omega_K}$$

and,

ω_K = modal frequency of mode

β_K = modal damping of mode

t_d = earthquake duration

Modified Double Sum Method - This method attempts to reduce the number of operations by setting as an acceptable truncation,

$$\epsilon_{KL} \leq 0.10$$

The overall response is set equal to,

$$R_a = \left\{ \left[\sum_{K=1}^{N} R_K{}^2 \right] + 2 \left[\sum_{K=1}^{N} \sum_{L=K+1}^{N_K} R_K R_L \epsilon_{KL} \right] \right\}^{1/2}$$

with

N_K being the limiting coupling mode for mode K

These methods have been adopted into Reference 3.43 in a form which introduces additional conservatism into the results.

In addition, it should be noted that these methods for combining modal responses presume that the modal responses correspond to frequencies between 0.5 cps and 33 cps. Indications are that special considerations are necessary for the conservative inclusion of modal response contributions from outside this range.

3.5 Combination of Effects Due to Triaxial Excitation

In the response spectrum method of analysis, the natural frequencies, mode shapes, and the load for each mode are first determined. The load for each mode for unit generalized response is the product of the force matrix, the mode shapes and the mode participation factors. When this product is multiplied by the generalized response determined from the spectrum curves, the load for each natural mode results.

The following basic considerations are recognized in combining the loads of each natural mode and for each direction:

i) The peak responses of the different modes due to any one excitation do not occur at the same time.

ii) The peak generalized responses due to the three different earthquake excitations for the same mode do not occur at the same time.

The nonsimultaneous occurrence of the peaks permits the use of the square root of the sum of squares (SRSS) method to compute the resultant responses. It is important to recognize that in order to implement the basic principles, it is necessary to use the SRSS on scalar components.

The following general procedure should be used to combine the seismic responses due to triaxial excitation:

$$R_{ij} = \pm\left[\sum_{k=1}^{3} R_{ijk}^{2}\right]^{1/2} \qquad (3\text{-}21)$$

where R_{ijk} = Maximum, codirectional seismic response of interest (strain, displacement, stress, moment, shear, etc) associated with coordinates "i" and "j" due to earthquake excitation in the "k"th direction.

R_{ij} = Seismic response of interest for design (strain, displacement, stress, moment, shear, etc) obtained by the square root of the sum of squares (SRSS) rule to account for the nonsimultaneous occurence of the R_{ijk} responses.

When the time-history method is used for seismic analysis, two different approaches are generally employed for combining responses. If the maximum responses due to each of the three components of the seismic motion are calculated separately, the method of analysis is the same as that described above. When the time-history responses from each of the three components of the earthquake motion are calculated by the step-by-step method and combined algebraically at each time step, the maximum responses are obtained from the combined time solution provided that the seismic motions in each direction are statistically independent from each other.

3.6 Damping

For structural dynamic analysis, it is commonly assumed that the phenomenon of energy dissipation can be modeled by including viscous damping in the dynamic system (References 3.20, 3.21 and 3.22). There are various damping sources: internal friction within the material(s), slip at structural connections, etc.

In structural analysis methods, the two basic mathematical idealizations are viscous damping and hysteretic damping. These approaches can be described as follows:

a) Viscous damping:

$$\{D\} = [C]\{\dot{X}\} \tag{3-22}$$

where $[C]$ is a viscous damping matrix. The damping force is proportional to the velocity.

b) Hysteretic damping:

$$\{D\} = \nu \, [K] \, \{|x|\} \, \frac{\{\dot{x}\}}{\{|\dot{x}|\}} = i \nu \left[K\right] \{X\} \qquad (3\text{-}23)$$

where ν represents the structural damping factor. This damping is also called complex damping. The damping force is proportional to the amplitude of the displacement and is opposite in direction to the velocity.

For a nonlinear SDOF system, the percentage of the damping of type (a) and type (b) may be expressed as (Reference 3.2)

$$D^1 = \frac{H_1\ (y) + H\ (y)}{2\pi\, K(y)\ y^2} = D + \frac{H(y)}{2\pi\, K(y)\ y^2} \qquad (3\text{-}24)$$

where H_1 (y) = energy dissipated in damping per cycle under steady-state harmonic oscillations of amplitude y.

H(y) = energy dissipated in hysteresis per cycle of amplitude y.

K(y) = secant stiffness at deformation y.

Based on experimental tests, the damping value for a system can be theoretically determined at a given stress level. Nevertheless, the damping values obtained from experimental tests may vary. As an example, the critical damping values obtained from Reference 3.23 are reprinted in Table 3.2.

In nuclear plant structural design, Newmark, et al, recommended the set of damping values listed in Table 3.3 (References 3.24 and 6.49). It seems the approach given in Reference 3.25 is more precise by expressing the energy loss per cycle in terms of the ratio of the stress level and the fatigue strength of the material. Naturally, in order to determine such a function, both analytical investigations and experimental studies are required.

To treat the damping matrix mathematically, the methods can be grouped in two categories, proportional damping and nonproportional damping. The equations of motion for systems with proportional damping (Section 3.6.1) can be readily uncoupled since the damping coefficients can be expressed as a linear combination of the mass and/or stiffness constant. For nonproportional damping, additional mathematical considerations are necessary as will be described in Section 3.6.2.

3.6.1 Proportional Damping - Consider a viscously damped system of the following form

$$[M]\{\ddot{X}\} + [C]\{\dot{X}\} + [K]\{X\} = \{F\} \qquad (3\text{-}25)$$

Let $[\Phi]$ be the modal matrix of the undamped system of

$$[M]\{\ddot{X}\} + [K]\{X\} = \{0\} \qquad (3\text{-}26)$$

such that

$$[\Phi]^T [M] [\Phi] = [I]$$

and

$$[\Phi]^T [K] [\Phi] = [\omega^2] \qquad (3\text{-}27)$$

where

$[\Phi]^T$ is the transpose of the matrix $[\Phi]$

$[I]$ is an identity matrix and

$[\omega^2]$ is a diagonal matrix and ω_i's are circular frequencies

The matrix [C] can be diagonalized if it is a linear combination of the [M] and [K] matrices. This is called Rayleigh damping. More general cases were derived later in Reference 3.34 for which the [C] can be diagonalized. The following is a description of how [C] is treated in the available computer codes based on either mass and stiffness or orthogonal modes.

3.6.1.1 <u>Mass and Stiffness Damping</u> (Reference 3.8) - With this method, the matrix [C] is assumed to be proportional either to the mass matrix [M] or to the stiffness matrix [K] or to a linear combination of the two. That is,

$$\left[C\right] = \alpha\left[M\right] + \beta\left[K\right] \tag{3-28}$$

where α and β are two real constants. α [M] is called the mass damping and β [K] the stiffness damping.

To apply this method in dynamic analysis, damping values of the entire system are determined by the two constants α and β. To determine the values for α and β, one can control the damping ratios for two frequencies.

Let ω_r and ω_s be the two frequencies that we want to have a damping ratio of ξ_r and ξ_s respectively. Then α and β can be determined as

$$\alpha = 2\omega_r\, \omega_s\, (\xi_s\, \omega_r - \xi_r\, \omega_s)/(\omega_r^{\,2} - \omega_s^{\,2}) \tag{3-29a}$$

$$\beta = 2\, (\xi_r\, \omega_r - \xi_s\, \omega_s)/(\omega_r^{\,2} - \omega_s^{\,2}) \tag{3-29b}$$

Then, for an arbitrary frequency, ω_i, the damping ratio, ξ_i, can be computed by eliminating α and β , and is given as:

$$\xi_i = \frac{1}{(\omega_r^{\,2} - \omega_s^{\,2})} \left[\frac{\omega_r\, \omega_s}{\omega_i} (\xi_s\, \omega_r - \xi_r\, \omega_s) + \omega_i(\xi_r\, \omega_r - \xi_s\, \omega_s)\right] \tag{3-30}$$

where

$$\frac{1}{(\omega_r^2 - \omega_s^2)} \cdot \frac{\omega_r \omega_s}{\omega_i} (\xi_s \omega_r - \xi_r \omega_s)$$ is due to mass damping

and

$$\frac{1}{(\omega_r^2 - \omega_s^2)} \cdot \omega_i (\xi_r \omega_r - \xi_s \omega_s)$$ is due to stiffness damping.

3.6.1.2 Orthogonal Modal Damping - When using the orthogonal modal damping approach (Reference 3.26), the system damping is defined once the differential equations have been decoupled after solving the eigenvalue problem. The following set of equations is thus established with the second term added to account for the damping:

$$\ddot{q}_i + \xi_i (2\omega_i) \dot{q}_i + \omega_i^2 q_i = f_i \qquad i = 1, 2, ---, N \qquad (3\text{-}31)$$

The damping ratio for each frequency is assigned by the analyst without any mathematical restriction. The damping ratio for any individual mode will have no effect on the damping ratios of the others since the modes are orthogonal. Conventional modal damping recommendations can be employed for this purpose.

3.6.2 Nonproportional Damping

3.6.2.1 General - For a system which is composed of different materials such as reactor coolant loops and soil foundations modeled with the containment structures, the methods described above are not adequate. Either the damping matrix cannot be diagonalized or modal damping values cannot be specified. To solve the problem practically, many papers have been published (References 3.27 to 3.33).

3.6.2.2 Composite Damping - The concept of composite damping can be linked directly with the energy dissipation. Let D be the energy dissipation of a system, then

$$D = \frac{1}{2} \sum_{i=1}^{nc} (\alpha_i \{\dot{X}\}_i^T [M]_i \{\dot{X}\}_i + \beta_i \{\dot{X}\}_i^T [K]_i \{\dot{X}\}_i) \qquad (3\text{-}32)$$

where $[M]_i$ and $[K]_i$ are mass and stiffness matrices of subsystems i, α_i and β_i are mass and stiffness proportional constants of subsystem i, and nc is equal to number of subsystems. The constants α_i and β_i can be determined based on the previous method for any subsystem, ie, the frequencies and modes of the free undamped vibration of the ith subsystem are used as a basis.

The mathematical process involved is similar to the one of stiffness and mass damping described above except the constants α_i and β_i are different for each material or subsystem.

Using Equation (3-32), the equation of motion of a viscously damped system has the following form:

$$[M] \{\ddot{X}\} + \sum_{i=1}^{nc} (\alpha_i [M]_i + \beta_i [K]_i) \{\dot{X}\} + [K]\{X\} = \{F\} \qquad (3\text{-}33)$$

Equation (3-33) can be integrated directly to obtain the response. On the other hand, if the normal mode method is used, Equation (3-33) can only be solved by neglecting the modal coupling effect to decouple the equations of motion on the normal mode basis.

Let $[\Phi]$ be the modal matrix of the undamped system of Equation (3-33) and $[\Phi_j]$ be the jth modal vector. With the aid of the orthogonality conditions, the equation of motion for the jth mode can be written in the following form:

$$\{\phi_j\}^T [M] \{\phi_j\} \ddot{q}_j + \{\phi_j\}^T \sum_{i=1}^{n} (\alpha_i [M]_i + \beta_i [K]_i) [\phi] \{\dot{q}_j\} + \{\phi_j\}^T [K] \{\phi_j\} q_j = \{\phi_j\}^T \{F\} \qquad (3\text{-}34)$$

where q_j is the jth generalized coordinate. The second term on the left-hand side of Equation (3-34) contains the coupling terms. If these coupling terms are neglected, Equation (3-34) reduces to the following equation:

$$\{\phi_j\}^T [M] \{\phi_j\} \ddot{q}_j + \{\phi_j\}^T \sum_{i=1}^{n} (\alpha_i [M]_i + \beta_i [K]_i) \{\phi_j\} \dot{q}_j + \{\phi_j\}^T [K] \{\phi_j\} q_j = \{\phi_j\}^T \{F\} \tag{3-35}$$

Or, one may write

$$\ddot{q}_j + 2\omega_j \left(\frac{\sum_{i=1}^{nc} \{\phi_j\}^T \alpha_i [M]_i \{\phi_j\}}{2\omega_j \{\phi_j\}^T [M] \{\phi_j\}} + \frac{\sum_{i=1}^{nc} \omega_j \{\phi_j\}^T \beta_i [K]_i \{\phi\}_j}{2 \{\phi_j\}^T [K] \{\phi_j\}} \right) \dot{q}_j + \omega_j^2 q_j = \frac{\{\phi_j\}^T \{F\}}{\{\phi_j\}^T [M] \{\phi_j\}} \tag{3-36}$$

Consequently, the effective damping for the jth mode is

$$\xi_j = \frac{\sum_{i=1}^{nc} \{\phi_j\}^T \alpha_i [M]_i \{\phi_j\}}{2\omega_j \{\phi_j\}^T [M] \{\phi_j\}} + \frac{\sum_{i=1}^{nc} \omega_j \{\phi_j\}^T \beta_i [K]_i \{\phi_j\}}{2 \{\phi_j\}^T [K] \{\phi_j\}} \tag{3-37}$$

or

$$\xi_j = \frac{\sum_{i=1}^{nc} \alpha_i \text{[MAX. K.E. for ith subsystem in the jth mode]}}{2\omega_j \text{[MAX K.E. for the system]}} + \omega_j \frac{\sum_{i=1}^{nc} \beta_i \text{[MAX. S.E. for ith subsystem in the jth mode]}}{2 \text{[MAX. S.E. for the system]}} \tag{3-38}$$

Once the damping ratio ξ_j is known, the analysis can be carried out using the time-history method or response spectrum technique.

Another refined heuristic version of the composite modal damping formulation can be found in Reference 3.31. On the other hand, Reference 3.30 presents a nonproportional coupled damping matrix suitable for a direct-integration numerical scheme.

In Ebasco (Reference 3.33), a comparative study has been made to find the modal damping factor with different methods on various types of soil (Table 3.4). For the example, based on a 3-mass cantilever model, the two basic approaches, kinetic and strain energy dependent, show little difference. However, the strain energy approach requires less computing time and is less sensitive to the foundation rocking mode.

References (Chapter 3)

3.1 Biggs, J M and Roesset, J M, "Seismic Analysis of Equipment on a Massive Structure," Dept of Civil Engineering, MIT, 1969.

3.2 Newmark, N M and Rosenblueth, E, Fundamentals of Earthquake Engineering, Prentice-Hall, Inc, 1971.

3.3 Clough, R W and Penzien, J, Dynamics of Structures, McGraw-Hill Co, 1975.

3.4 Riead, H D, "Nonlinear Response Using Normal Modes," AIAA 12th Aerospace Sciences Meeting, Paper No. 74-138, January 1974.

3.5 Stricklin, J A and Haisler, W E, "Survey of Solution Procedures for Nonlinear Static and Dynamic Analysis," SAE Conference on Vehicle Structural Mechanics, Detroit, Michigan, March 26-28, 1974, pp 1-17.

3.6 O'Hara, G J and Cunniff, P F, "Numerical Method for Structural Shock Response," Journal of the Engineering Mechanics Division, ASCE, Vol 90, EM2, April 1964, pp 51-82.

3.7 Lysmer, J, et al, "FLUSH Manual," EERC Report 75-30, University of California, November 1975.

3.8 Hwang, R N, "Seismic Response of Embedded Structures," PhD Dissertation, University of California, Berkeley, 1974.

3.9 Seed, H B and Idriss, I M, "Soil Moduli and Damping Factors for Dynamic Response Analysis," EERC Report 70-10, University of California, 1970.

3.10 Lysmer, J, "Modal Damping and Complex Stiffness," Dept of Geotechnical Engineering, University of California, Personal Communication, August 1973.

3.11 Garnet, H and Armen, H, "Evaluation of Numerical Time Integration Methods as Applied to Elastic-Plastic Dynamic Problems Involving Wave Propagation," Grumman Research Department Report, RE-475, March 1974.

3.12 Nahavandi, A N and Bohm, G J, "A Solution of Nonlinear Vibration Problems in Reactor Components," Nuclear Science and Engineering: 26, 1966, pp 80-89.

3.13 Wu, R W H and Witmer, E A, "Nonlinear Transient Responses of Structures by the Spatial Finite-Element Method," AIAA, Vol II, No. 8, 1973, pp 1110-1117.

3.14 Newmark, N N, "A Method of Computation for Structural Dynamics," Journal of the Engineering Mechanics Division, ASCE, EM3, June 1959, pp 67-94.

3.15 Bathe, K J and Wilson, E L, "Stability and Accuracy Analysis of Direct Integration Methods," International Journal of Earthquake Engineering and Structural Dynamics, Vol 1, 1973, pp 283-291.

3.16 Wilson, E L Farhoomand, I and Bathe, K J, "Nonlinear Dynamics Analysis of Complex Structure," Earthquake Engineering and Structural Dynamics, Vol 1, 1973, pp 241-252.

3.17 McNamara, J F and Marcal, P V, "Incremental Stiffness Method for the Finite Element Analysis of the Nonlinear Dynamic Problem," ONR Symposium, "Numerical and Computer Methods in Structural Mechanics," Urbana, Illinois, September 1971.

3.18 Nagarajan, J and Popov, E P, Elastic-Plastic Dynamic Analysis of Axisymmetric Solids," NTIS, AD 764244, July 1973.

3.19 Houbolt, J C, "A Recurrence Matrix Solution for the Dynamic Response of Elastic Aircraft," Journal of Aeronautical Science, Vol 17, 1950, pp 540-550.

3.20 Thompson, W J, Mechanical Vibrations, Prentice-Hall, 1965.

3.21 Meirovitch, L, Analytical Methods in Vibrations, The Macmillan Co, New York, New York, 1967, p 403.

3.22 Biggs, J M, Introduction to Structural Dynamics, McGraw-Hill, 1964.

3.23 Sharpe, R L, et al, "Behavior of Structural Systems Under Dynamic Loads." Building Practices for Disaster Mitigation, Building Sciences Series 146, National Bureau of Standards, February 1973, pp 352-394.

3.24 Regulatory Guide 1.61, US Atomic Energy Commission, Government Printing Office, Washington, DC, 1973.

3.25 Lazan, B J and Goodman, L E, "Material and Interface Damping," in Shock and Vibration Handbook, (Harris & Crede, ed), Vol A, Chapter 31, McGraw-Hill, 1961.

3.26 Wilson, E L and Penzient, J, "Evaluation of Orthogonal Damping Matrices," International Journal for Numerical Methods in Engineering Vol 4, 1972, pp 5-10.

3.27 Hurty, W C, "Dynamic Analysis of Structural Systems Using Component Modes," Journal, American Institute of Aeronautics and Astronautics, AIAA, Vol 3, No. 4, April 1965, pp 678-675.

3.28 Koss, Paul, "Element Associated Damping by Modal Synthesis," National Topical Meeting, Water Reactor Safety, Salt Lake City, Utah, March 1973.

3.29 Wiley, J W, Schechter, K M, Price, D L, Koss, P W, "Seismic Analysis and Design of the San Onofre Nuclear Generation Station, Units 2 & 3 Containment," Electric Power and Civil Engineer, ASCE, 1974.

3.30 Pajuhesh, J and Hadjian, A H, "Determination of Composite Damping Matrices," Fifth World Conference on Earthquake Engineering, Rome, 1973.

3.31 Roesset, J M, Whitman, R V, Dobry, R, "Modal Analysis for Structures with Foundation Interaction," Journal of the Structural Division, ST3, ASCE, March 1973, pp 399-416.

3.32 U S Nuclear Regulatory Commission, Standard Review Plan, Section 3.7.2, 1975.

3.33 Chiu, K D and Kuo, H J, "Modal Damping in Dynamic Analysis of Structures," ASCE, Specialty Conference on Structural Design of Nuclear Plant Facilities, Chicago, 1973.

3.34 Caughey, T K, "Classical Normal Modes in Damped Linear Dynamic Systems," Journal of Applied Physics, 27, 1960.

3.35 Whitman, R V, "Soil-Structure Interaction," Seismic Design for Nuclear Power Plants, MIT Press, Cambridge, Massachusetts, 1970, pp 241-269.

3.36 Shah, J N, et al, "Modal Superposition Method for Computationally Economical Nonlinear Structural Analysis," Transactions, ASME, Vol 101, May 1979.

3.37 Molnar, A J, et al, "Application of Normal Mode Theory and Pseudo-force Methods to Solve Problems with Nonlinearities," Transactions, ASME, Vol 96, May 1976.

3.38 Nordsieck, A, "On Numerical Integration of Ordinary Differential Equations," Journal of Mathematics of Computations, 1962, Vol 16, pp 22-27.

3.39 Lapidus, L and Seinfeild, J H, <u>Numerical Solution of Ordinary Differential Equations</u>, Academic Press, 1971.

3.40 Collatz, <u>The Numerical Treatment of Differential Equations</u>, Springer, 1960.

3.41 Arden, B W and Astill, K N, <u>Numerical Algorithms: Origins and Applications</u>, Addison-Wesley, 1971.

3.42 Singh, A K, et al, "Influence of Closely Spaced Modes in Response Spectrum Method of Analysis," ASCE, Specialty Conference on Structural Design of Nuclear Plant Facilities, Chicago, Vol. II, 1973.

3.43 U S Nuclear Regulatory Commission Regulatory Guide 1.92, Rev 1, February 1976.

3.44 Singh, M P, "Generation of Seismic Floor Spectra," Journal of the Engineering Mechanics Division, ASCE, Vol 101, No. EM5, October 1975, pp 593-607.

3.45 Singh, M P, "Seismic Design Input for Secondary Systems," Civil Engineering and Nuclear Power, Vol II, ASCE National Convention Boston, April 1979.

TABLE 3.1
PHASE LAG IN DIFFERENCE BETWEEN THE MODAL SUPERPOSITION AND COMPLEX ANALYSIS METHODS (REF.3.10)

β	.05	.10	.15	.20	.25
$\alpha = 0$	5.73°	11.48°	17.25°	23.07°	28.95°
$\alpha = .2$	4.78°	9.57°	14.38°	19.24°	24.16°
$\alpha = .4$	4.09°	8.20°	12.33°	16.50°	20.71°
$\alpha = .6$	3.58°	7.18°	10.79°	14.43°	18.12°
$\alpha = .8$	3.18°	6.38°	9.59°	12.82°	16.09°
$\alpha = 1.0$	2.87°	5.74°	8.63°	11.54°	14.48°
$\alpha = 1.2$	2.61°	5.22°	7.84°	10.48°	13.15°
$\alpha = 1.4$	2.39°	4.78°	7.19°	9.61°	12.05°
$\alpha = 1.6$	2.20°	4.41°	6.63°	8.87°	11.12°
$\alpha = 1.8$	2.05°	4.10°	6.16°	8.23°	10.32°
$\alpha = 2.0$	1.91°	3.82°	5.75°	7.68°	9.63°

β=DAMPING RATIO

$\alpha=\omega/\omega_0$, ω=FORCING FUNCTION FREQUENCY
ω_0=SYSTEM FREQUENCY

TABLE 3.2

OBSERVED BUILDING-AS-A-UNIT MODAL DAMPING

(REF. 3.23)

STRUCTURE NUMBER	DESCRIPTION	TEST DIRECTION	DAMPING (PERCENT OF CRITICAL) VARIATION	AVERAGE
1	ONE-STORY ADOBE HOUSE	TRANSVERSE	4-7	5.7
2	TWO-STORY FRAME HOUSE	TRANSVERSE	4-10	6.0
3	ONE-STORY FRAME HOUSE	LONGITUDINAL	0-30	*
4	ONE-STORY CONCRETE HOUSE	LONGITUDINAL	**	5**
5	FREE-STANDING CHIMNEY	LONGITUDINAL	2.5 - 4.0	3.0

* APPROXIMATELY 30% DAMPING OBSERVED IN FIRST CYCLE, THEREAFTER DAMPING WAS 0 - 2%

**APPROXIMATELY -- RECORD TOO NOISY TO OBTAIN DAMPING FOR INDIVIDUAL PEAKS.

TABLE 3.3

DAMPING VALUES[1]

(PERCENT OF CRITICAL DAMPING)
(REF. 6.49)

STRUCTURE OR COMPONENT	OPERATING BASIS EARTHQUAKE OR 1/2 SAFE SHUTDOWN EARTHQUAKE[2]	SAFE SHUTDOWN EARTHQUAKE
EQUIPMENT AND LARGE-DIAMETER PIPING SYSTEMS[3], PIPE DIAMETER GREATER THAN 12 IN.	2	3
SMALL-DIAMETER PIPING SYSTEMS, DIAMETER EQUAL TO OR LESS THAN 12 IN.	1	2
WELDED STEEL STRUCTURES	2	4
BOLTED STEEL STRUCTURES	4	7
PRESTRESSED CONCRETE STRUCTURES	2	5
REINFORCED CONCRETE STRUCTURES	4	7

[1]TABLE 1 IS DERIVED FROM THE RECOMMENDATIONS GIVEN IN REFERENCE 1.

[2]IN THE DYNAMIC ANALYSIS OF ACTIVE COMPONENTS AS DEFINED IN REGULATORY GUIDE 1.48, THESE VALUES SHOULD ALSO BE USED FOR SSE.

[3]INCLUDES BOTH MATERIAL AND STRUCTURAL DAMPING. IF THE PIPING SYSTEM CONSISTS OF ONLY ONE OR TWO SPANS WITH LITTLE STRUCTURAL DAMPING, USE VALUES FOR SMALL-DIAMETER PIPING.

TABLE 3.4

MODAL DAMPING FACTORS (REF. 3.33) CALCULATED FROM DIFFERENT METHODS

MODAL DAMPING FACTORS OF THREE MASS MODEL

STRUCTURE	HARD								MEDIUM								SOFT							
SOIL	SOFT				HARD				SOFT				HARD				SOFT				HARD			
MODE	1	2	3		1	2	3		1	2	3		1	2	3		1	2	3		1	2	3	
1	.095	.100	.100		.097	100	.100		.076	.099	.100		.090	.096	.096		.061	.099	.099		.071	.081	.082	
2	.075	.098	.099		.053	.056	.056		.077	.098	.099		.060	.064	.065		.090	.099	.099		.079	.080	.080	
3	.077	.062	.051		.050	.050	.050		.050	.050	.050		.050	.050	.050		.050	.050	.050		.050	.050	.050	
4	.050	.050	.050		.097	.100	.094		.096	.165	.052		.050	.050	.050		.050	.050	.050		.050	.050	.050	
5	.050	.050	.050		.050	.050	.050		.050	.050	.050		.100	.203	.089		.098	.290	.052		.099	.327	.087	
6	.051	.051	.050		.051	.051	.050		.051	.052	.050		.051	.053	.060		.051	.053	.050		.051	.053	.050	
7	.050	.050	.050		.050	.050	.050		.050	.050	.050		.050	.050	.050		.050	.051	.050		.050	.051	.050	
8	.050	.050	.050		.050	.050	.050		.050	.050	.050		.050	.050	.050		.050	.050	.050		.050	.050	.050	

(1) KINETIC DISSIPATED ENERGY - MASS ASSOCIATED DAMPING

(2) KINETIC DISSIPATED ENERGY - DISPLACEMENT ASSOCIATED DAMPING

(3) STRAIN DISSIPATED ENERGY (WHITMAN GIVES SAME RESULTS FOR THIS EXAMPLE) (REF. 3.35)

WHERE, FOR (1) AND (2)

$$\beta_n = \frac{\sum_{i=1}^{N} \{\phi_n\}_i^T \; \beta_i [M]_i \; \{\phi_n\}_i}{\{\phi_n\}^T \; [M_T] \; \{\phi_n\}}$$

(2) CONSIDERS ONLY RELATIVE DISPLACEMENTS IN DEFINING ϕ, WHILE IN (1), ϕ INVOLVES THE RIGID BODY MOTIONS OF THE SUPERSTRUCTURE

AND, FOR (3)

$$\beta_n = \frac{\sum_{i=1}^{N} \{\phi_n\}_i^T \; \beta_i [K]_i \; \{\phi_n\}_i}{\{\phi_n\}^T \; [K_T] \; \{\phi_n\}}$$

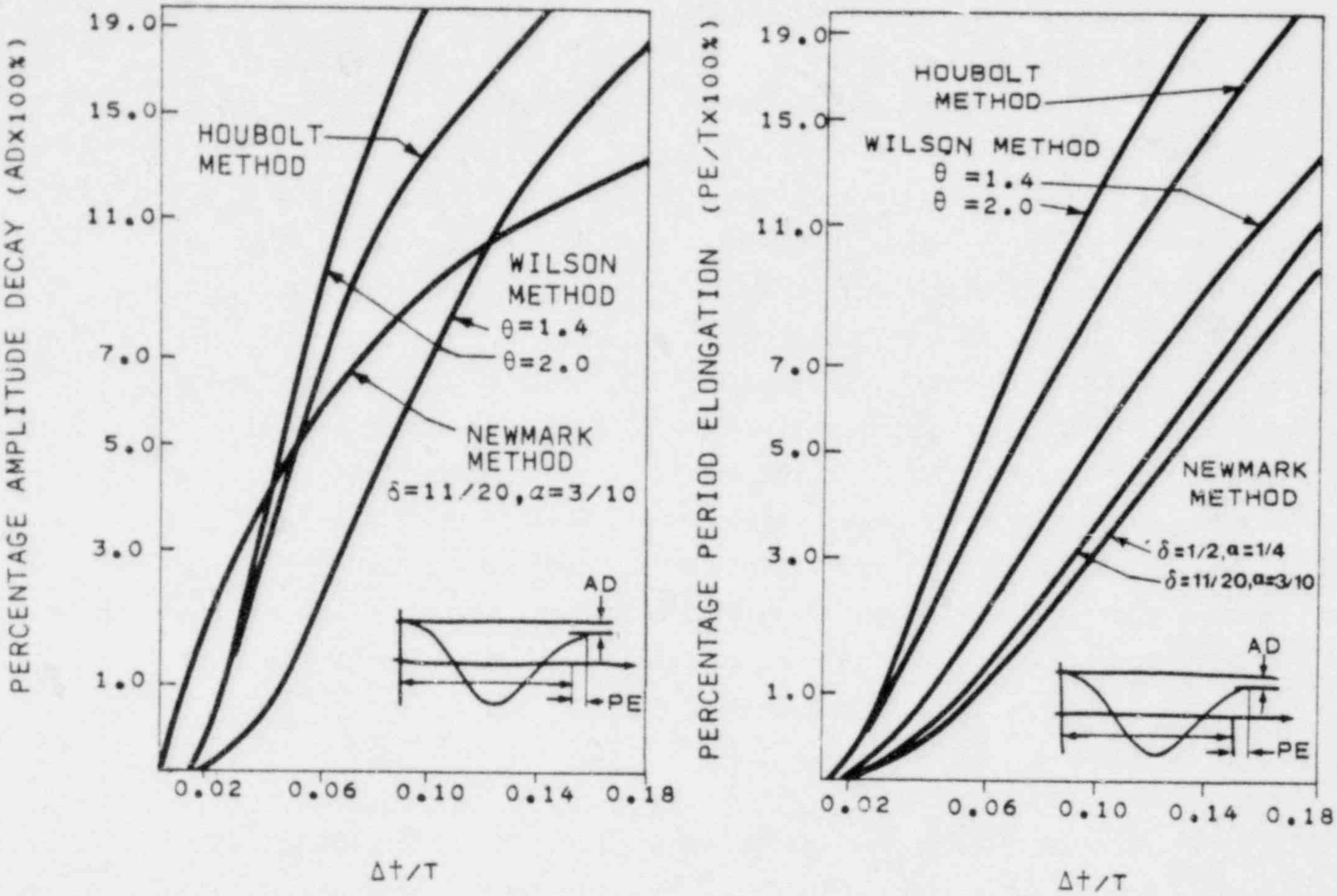

FIGURE 3.1

COMPARISONS ON THE PERCENTAGE OF AMPLITUDE DECAY AND PERIOD ELONGATIONS AMONG THREE IMPLICIT SCHEMES. (REF.3.15)

Chapter 4
Nonlinear Behavior of Materials and Structures

4.1 General

The nonlinear behavior of a structural system may be related to various factors including nonlinearity in the stress-strain relationships, the development of large deformations, and the support conditions. These factors can be conveniently considered in two general categories - material nonlinearities and geometric nonlinearities. For nuclear power plants, the structures are usually of three types, ie, (a) Frame structures, eg, turbine building; (b) Shearwall-frame structures, eg, reactor auxiliary building and fuel-handling building; and (c) Shell structures, eg, reactor building. Geometric nonlinearities due to large deformation are unlikely to occur considering the sizes and dimensions of nuclear plant structures. Hence, only material nonlinear behavior is described in detail in this review. The algorithms for nonlinear dynamic analysis are discussed including various approaches for linearizing simple systems. Such equivalent linear approaches may potentially play an important role in engineering practice from the standpoint of computational economy.

4.2 Nonlinear Material Behavior

The nonlinear behavior of a multiple degree-of-freedom system is usually quite complicated. For this reason, in dynamic analysis, nonlinear material characteristics are simulated with simple idealized force deformation curves. The principal features of nonlinear behavior are described below:

4.2.1 Lumped Plasticity - For a frame-type structure, such as shown in Figure 4.1, constructed with ductile materials, a plastic hinge will form when the maximum bending moment reaches the yield moment. If the material is of the strain-hardening type or with a shape factor larger than 1.0, the plastic deformation will be distributed over a finite length of the member. For further increases in load, more hinges may be formed and the stresses will be redistributed. Details of the phenomenon can be found from various texts, eg, in References 4.1, 4.2 and 4.3. The plastic hinge concept can be generalized to beam-column members by considering biaxial bending and axial forces. In that case, the yield surface should be established as the one sketched in Figure 4.2.

4.2.2 Distributed Plasticity - In reality, plasticity is distributed over a finite region of a structural member. Hence, in order to consider such nonlinear behavior accurately, the analytical method must be able to follow the spreading of plastic zones near the yield location (References 4.3 and 4.4). For shearwall-type members, such inelastic behavior may be found when it is subjected to high levels of seismic loading. The plastic distribution is, in general, not uniform over the member and it plays an important role in stress redistribution through the structure.

As an example, the formation of plastic regions in a shearwall is shown in Figures 4.3 and 4.4 when the wall is subjected to severe seismic load. These results will be further discussed in Section 4.4, Structural Nonlinear Behavior.

4.2.3 Stiffness Degradation - For concrete structures, reduction of stiffness may appear due to concrete cracking. For repeated loads like seismic excitations, stiffness degradation can be substantial and can increase considerably the capacity for energy disipation. An example is shown in Figure 4.5 of the force-displacement relationships of a hysteretic frame (References 4.5 and 4.14). The first four cycles of the measured results (Figure 4.13) show quite large differences in stiffness measured by the slope of a line drawn through the points on the hysteretic curve corresponding to maximum and minimum displacements.

4.3 Nonlinear Force-Deformation Relationships

Nonlinear material behavior can be elastic or inelastic (Reference 4.1). The stress-strain relationships may be established directly from tests, eg, Figure 4.8 depicts a typical "skeleton" curve for a nonlinear system, ie, the static force deformation curve on first loading. Typical shapes of other nonlinear curves are shown in Figures 4.6 and 4.7 for concrete and steel, respectively, for repeated loading cycles. Based on these relationships, the proper force-displacement relationship for the structural model can be constructed based on the material characteristics and boundary conditions for each structural component. Material nonlinearity in steel is conveniently treated by a bilinear curve in conjunction with a material flow rule. The stiffness is varied by iterative or incremental techniques following the post-yield material behavior. Concrete nonlinear behavior is complicated by its anisotropic character with different properties in tension and compression. Incremental procedures are generally employed to account for the formation of cracks and subsequent yielding of reinforcing steel by changing the stiffness of the individual elements based on the internal forces at each load step.

The following is a summary of selected idealized force-displacement curves commonly used to represent various types of structural systems.

4.3.1 Elastic Systems - This special type of nonlinear system can be characterized by a variety of nonlinear load-deformation curves (Figures 4.8 and 4.9) with the important distinction that upon unloading the behavior follows the same curve as that for the loading sequence. Problems of geometric nonlinearity often fall in this category. Another example is a bilinear system with zero stiffness in the second branch (Figure 4.9(c)) which can represent the behavior of a prestressed concrete frame failing in tension due to flexure. In such cases, the nonlinear character of the load-deformation curve arises from the opening of flexural cracks that close again upon unloading. Since the hysteretic loops for this type of behavior are small, idealized elastic behavior may be utilized to depict the real structure.

4.3.2 Elastic-Plastic System - The elastic-plastic system with the force-deformation curve shown in Figure 4.10 is the most frequently employed relationship. Many studies have been performed to (a) evaluate the adequacy of elastic-plastic representations for the analysis of single degree-of-freedom (SDOF) systems subjected to earthquake excitation, and (b) to calibrate the method by comparing it with actual measured responses. The application of SDOF analyses to elastic-plastic curves involves the determination of equivalent period and equivalent damping values (eg, Equation 3.24).

Figures 4.11 and 4.12 show the comparison of undamped and damped elastic-plastic systems with various maximum ductility ratios with the equivalent linear system ($\mu=1$) whose natural period and damping correspond to that of the inital linear branch of the elastic-plastic system. These results indicate that the degree of conservatism in such elastic-plastic solutions, as compared to linear system responses, varies with the earthquake duration, degree of damping and the frequency characteristics of the structure.

4.3.3 Stiffness-Degrading System - As described earlier, the cracking of concrete walls reduces the stiffness of the member and, consequently, in dynamic analysis may cause shifts in natural frequencies. The force-deformation relations for this type of behavior may be depicted by the curve shown in Figure 4.13. As can be seen from the figure, the initial stiffness of the system is reduced after the first cycle of loading and unloading. The stiffness is decreased as a function of the maximum deformation imposed in the previous cycles. In Reference 4.5, the measured results for the first four cycles of the loading deformation shapes were plotted for a reinforced concrete structure frame. Different ways to model such complicated behavior will be discussed further in Section 4.4. One of the simplest approaches was suggested in Reference 4.5 in which the unloading path of the degrading system with an empirical expression, $\gamma(\frac{1}{\mu})^{\alpha}$, in terms of the following parameters: ductility factor (μ), the slope (γ) corresponding to fully cracked section and constant (α) recommended as 0.5. The equivalent damping ratio is also proposed in terms of the ductility factor (as sketched with the dotted line in Figure 4.14). The proposed method can simplify the analytical procedures, nevertheless, the solution may not be that accurate as can be seen from Figure 4.14 in which the proposed damping values are compared to experimental results. In general, while equivalent viscous damping is a useful concept for developing an intuitive feeling for the behavior of an inelastic system, it cannot, in itself produce meaningful quantitative results.

In addition, the behavior of some specific strucutral systems are being modeled by other idealizations which do not necessarily fall into any of the three basic categories of elastic, elastic-plastic or stiffness-degrading systems. For example, a braced system as shown in Figure 4.15

(Reference 4.1) may be represented by the sample model shown in Figure 4.16. Naturally, the likelihood of finding a suitable model depends upon the goal of the analysis, the degree of sophistication in the system as well as the experience of the analyst.

4.4 Structural Nonlinear Behavior

Inelastic structural response can be evaluated based on the idealized force-deformation curves described in Section 4.2. For comparison, the elastic and inelastic response spectra are computed in References 4.1 and 4.6, and reprinted in Figures 4.11 and 4.12. As described earlier, these response spectra were generated for a single degree-of-freedom system with an elastic-plastic type material behavior and various ductility factors. Based on References 4.1, 4.6, 4.7, 4.8, 4.9, 4.10 and 4.14 the "ductility factor" concept was extensively investigated based on seismic studies. Recommendations for utilizing the ductility factor to predict the inelastic response spectra from an elastic one were suggested as follows, (Reference 4.9): (a) the inelastic response spectra to be reduced by $1/\mu$ at frequencies less than 2 Hz; (b) the inelastic response spectra to be reduced by $1/\sqrt{2\mu-1}$ roughly between 2 Hz and 8 Hz; (c) no reduction between inelastic response spectra and elastic response spectra for frequencies higher than 33 Hz. The development of a "ductility factor" method for multiple degree-of-freedom (MDOF) structures, by means of approximate modal analyses, is described in Reference 4.35.

For complicated structures, the ductility factor approach is not generally sufficient and a dynamic nonlinear analysis is required. The input material behavior for the dynamic analysis may be based on the force-deformation relations of the subassemblages for both the translational and rotational directions. The calculations proceed by carrying out an incremental step-by-step analysis of the equations of motion for very short time intervals during each of which the structure is treated as a linear element. At each time step, changes in geometry or material or connectivity properties of the structure are made by modifying the appropriate mass, damping or stiffness values.

Some results of interest to this study are as follows: In Reference 4.11, experimental tests were performed to compare the force-deformation relationships of a subassemblage (Figure 4.17) to the analytically simulated ones. The results show quite close agreement and are reprinted in Figure 4.18. Similarly, based on such input material behavior, inelastic dynamic behavior of both open frame and shearwall frame hi-rise systems were considered in Reference 4.3. The structural geometry and member characteristics are tabulated in Figure 4.19. The output is shown in Figures 4.20 and 4.21. For the open frame case, both the elastic and inelastic displacements are plotted for each floor. It seems the displacements are quite close, based on the input earthquake records. The ductility factors, on the other hand, are quite different for each case, especially at the upper level. If the ductility factor method is applied to the inelastic analysis, the solutions are shown in Figure 4.20 (Reference 4.3). It can be concluded that this method is very effective as a design aid, however, it may not be able to predict local behavior. For the shearwall frame-type structures, the maximum displacements, the ductility factors for both the columns and girders, and the reactions for columns and walls are also reprinted in Figure 4.21 from Reference 4.12. Again, no definite conclusions can be drawn to predict the inelastic behavior of a system like this. As mentioned earlier in the chapter, the turbine building is typically a frame-type structure. As such, turbine building behavior could be close to the example mentioned except the turbine building usually is lower in elevation and generally with stiffer members. A study was made and published in Reference 4.13. The geometry and the force-deformation curves for the structures selected for investigation are shown in Figure 4.22. The seismic input motion was based on a postulated time history with 0.5 g maximum acceleration and corresponding with the Newmark-Hall's inelastic response spectra modification curves. By varying the member sectional properties, cases with different ductility factors (μ), (ie, μ = 3, μ = 4 and μ = 6), are simulated. The yield mechanism of the structure is shown in Figure 4.23 for μ = 6. The displacement time histories for the roof level are shown in Figure 4.24. The shapes look quite similar but the maximum displacements can not readily be seen without considering the shifts of periods and the stress redistribution in the portion of the structural system.

There have been numerous investigations of the lateral load performance of shearwall systems. One of the most interesting available results from Kobori et al (Reference 4.4) is described below. The dynamic analysis was performed with the finite element method on a single-story frame filled with wall. All the elements were assumed to follow the von Mises yield condition. The seismic input was excited at the base mat and based on the El Centro, 1940 record N-S component. The structural model is shown in Figure 4.3. The width-height ratio of wall was 2/3. Two types of walls were analyzed - one with the thickness-depth ratio equal to 1/2 (Type 1), and the other with the ratio equal to 1/4 (Type 2). The hardening coefficient was set at 0.1 for both cases. The formation of the plastic zones were discussed earlier as shown in Figure 4.4. An interesting fact is that the plastic zones are confined to the lower part of the system in Type 1 but spread over the entire area of the wall in Type 2. By varying the hardening coefficients, the stiffness and strength of the members are also changed. The effects on horizontal displacements at the top of the walls are shown in Figure 4.25, as a function of time. These results illustrate the difference between elastic and inelastic solutions. For a particular type of sturcture, eg, shell structures, dynamic analysis has to be performed based on proper simulation.

4.5 Nonlinear Analysis

From the previous descriptions, it can be concluded that nonlinear analysis is inevitable for finding the dynamic behavior of a structural system when subjected to high levels of seismic excitation. Reference 4.32 provides a general review of the overall problem, and current status of approaches being taken in the structural and mechanical areas to develop suitable methods of inelastic analysis. The methods can be broadly categorized as follows: (a) detailed multiple degree-of-freedom (MDOF) inelastic calculations, (b) 1-dimensional inelastic methods, and (c) MDOF elastic type analyses. The simplified inelastic analysis of SDOF systems, as will be discussed below, have found wide usage and potential applicability to design situations. Important general characteristics of inelastic response of structures can often be understood through study of the response of such SDOF systems to the extent that, in the first approximation, the response of inelastic systems can be represented by the fundamental mode of vibration. Efforts are underway to extend the range of application of such analyses by establishing guidelines whereby these results can be conservatively related to the MDOF problem (eg, Reference 4.36). The impetus for such development efforts is the time-consuming and costly nature of detailed 3-dimensional inelastic dynamic analyses.

Computational stability and economy are among the main concerns in the performance of a nonlinear analysis. For these reasons, the following two sections discuss the algorithms for nonlinear dynamic analysis and the equivalent linear analysis approach.

4.5.1 Algorithms for Nonlinear Dynamic Analysis - A number of the commercially available computer programs suitable for determining the seismic response of nonlinear structures by step-by-step numerical integration procedures have been developed with the implicit integration scheme. The preferred scheme for a particular application is dependent upon the method of stiffness formulation, the type of elements selected for a particular problem, the type of excitation (frequency content, duration), etc. The literature contains numerous references to the degree of success achieved with the various integration schemes, eg, References 4.24 through 4.27 with respect to the explicit scheme and References 4.28 and 4.29 with regard to stability and convergence based on results obtained with the implicit methods described in Section 3.2.4.2. Due to theoretical difficulties in justifying the stability conditions for nonlinear operators, new schemes are still being proposed, eg, the Park stiffly-stable method (Reference 4.30).

4.5.2 Equivalent Linear Approach - For simple hysteretic structures, the equivalent linear approach is quite valuable. In this approach to SDOF analysis, any equivalent linear system is developed such that its response is matched, by various alternative measures, to the response of the subject nonlinear system. This method has several inherent and other potentially attractive features, eg, (a) the approach is considerably more economical than detailed nonlinear dynamic computations, (b) such equivalent linear calculations provide important insights into the nature of structural system response which can be invaluable for preliminary design, (c) the approach is readily compatible with the input loading specified as a design response spectrum, and (d) the equivalent linear approach should be useful in the development of practical response spectrum methods for MDOF analysis.

As indicated above, the basic concept is to replace the equation of motion of a SDOF system (Reference 4.15):

$$\ddot{X} + 2\ \xi_o\ \omega_o\ \dot{X} + \omega_o^{\ 2}\ f(X) = -a(t) \tag{4-1}$$

in which $\xi_o = \dfrac{C_o}{2\sqrt{K_o\ M_o}}$ and $\omega_o^{\ 2} = \dfrac{K_o}{M_o} = \left(\dfrac{2\pi}{T_o}\right)^2$ (4-1a)

and

$f(X)$ = restoring force/K_o

C_o = viscous damping coefficients

K_o = stiffness coefficients

T_o = period

M_o = the mass of the system

by an approximate linear system:

$$\ddot{X} + 2\ \xi_e\ \omega_e\ \dot{X} + \omega_e^{\ 2}\ X = -a(t) \tag{4-2}$$

in which

ξ_e, ω_e, K_e, M_e, T_e = the quantities in the effective or equivalent system.

In the main, the mass is often taken to be the same in the equivalent and in the nonlinear system. Hence the fundamental equivalent parameters are the effective linear system damping and period.

The methods of developing the equivalent linear system can be categorized in terms of the three basic types of input motion, ie, harmonic, random (white noise) and earthquake loading. Since the equivalent stiffness and damping are themselves functions of the response, the response of a series of linear systems is often used in an iterative manner to calculate equivalent stiffness and damping. The three basic categories are discussed separately in the subsequent sections.

4.5.2.1 Methods Based on Harmonic Response - In order to relate the results of the harmonic analysis method described below to the earthquake response problem, the assumption is usually made that the seismic response is quasi-harmonic. In this way, the peak response is equal to the maximum response amplitude. For steady-state response to harmonic input, expressions for the equivalent linear stiffness and damping can be developed in closed form.

There are various methods falling in this category. The representative methods are Harmonic Equivalent Linearization (HEL) (Reference 4.17), Resonant Amplitude Matching (RAM) (Reference 4.20), Dynamic Mass (DM) (Reference 4.20), Constant Critical Damping (CCD) (Reference 4.20), Geometric Stiffness (GS) (References 4.21 and 4.22) and Geometric Energy (GE) (Reference 4.19). A brief description of each method is given below:

a. HEL Method - This method is to minimize the difference between Equations (4-1) and (4-2) with respect to the parameters ω_e^2 and $\xi_e \omega_e$ for all the solutions of the form:

$$X(t) = X_m \operatorname{Cos} (\omega t - \emptyset) = X_m \operatorname{Cos} \theta \qquad (4\text{-}3)$$

in which

X_m = amplitude of the steady-state oscillation

ω = forcing frequency

$\emptyset$ = phase angle of the response.

If the minimization is performed on the mean square of the difference averaged over one cycle of oscillation, then the equivalent damping and frequency would have the form:

$$\xi_e = \frac{\omega_o}{\omega_e} \xi_e - \left(\frac{\omega_o}{\omega_e}\right)^2 \frac{S(X_m)}{X_m} \qquad (4\text{-}4a)$$

$$\omega_e^2 = \omega_o^2 \frac{C(X_m)}{X_m} \qquad (4\text{-}4b)$$

in which

$$S(X_m) = \frac{1}{\pi} \int_0^{2\pi} f(X_m \cos\theta) \sin\theta \, d\theta \tag{4-4c}$$

and

$$C(X_m) = \frac{1}{\pi} \int_0^{2\pi} f(X_m \cos\theta) \cos\theta \, d\theta \tag{4-4d}$$

b. RAM Method - This method ignores the shift of the frequency but equates the energy dissipated per cycle for the linearized and the hysteretic system at resonance, ie,

$$\omega_e = \omega_o \tag{4-5a}$$

$$\xi_e = \frac{\Delta W (X_m)}{2\pi K_o X_m^2} \tag{4-5b}$$

where $\Delta W (X_m)$ = the total energy dissipated per cycle.

c. DM Method - In this method the stiffness of the linearized system is kept at the nominal stiffness of the hysteretic system but the mass is varied to keep the resonant frequency of the linearized system consistent with the observed hysteretic system.

d. CCD Method - This method equates the critical damping for both systems, ie,

$$K_o M_o = K_e M_e = \frac{K_e^2}{\omega_e^2} \tag{4-6a}$$

and let

$$\xi_e = \frac{\Delta W (X_m)}{2\pi K_e X_m^2} \tag{4-6b}$$

e. GS Method - In this method, the secant stiffness, $K(X_m)$, is set equal to the stiffness of the effective linear system, ie,

$$\omega_e = \frac{2\pi}{T_e} = \omega_o \sqrt{\frac{K(X_m)}{X_o}} \tag{4-7a}$$

and

$$\xi_e = \frac{\Delta W(X_m)}{2\pi K (X_m)^2} \qquad (4\text{-}7b)$$

f. GE Method - This method defines the effective damping as

$$\xi_e = \frac{1}{4\pi} \frac{\Delta W(X_m)}{W(X_m)} \qquad (4\text{-}8a)$$

where

$W(X_m)$ = denotes the maximum strain energy stored during one cycle of oscillation with amplitude X_m.

The effective period and viscous damping for this method are plotted in Figure 4.26 along with the methods to be described in the following section. In general, the fits vary considerable for different ductility ratios.

4.5.2.2 Methods Based on Random Response - The methods based on random response can be computed with the actual earthquake records or the assumed excitation with a stationary process. (A nonstationary approach, such as presented in Reference 4.31, has also been initiated in this area.) These methods are: Stationary Random Equivalent Linearization (SREL) (Reference 4.16), Averaged Period and Damping (APD) (Reference 4.1), and Average Stiffness and Energy (ASE) (Reference 4.18). Following are brief descriptions of these approaches:

a. SREL Method - This method is similar to the HEL Method described above except in a probabilistic format. By assuming that

$$X(t) = A(t) \cos\left[\omega t - \emptyset(t)\right] \qquad (4\text{-}9a)$$

is a narrow band Gaussian distribution, with $A(t)$ and $\emptyset(t)$ representing the amplitude and phase lag. For Gaussian white noise input, closed form expressions cannot be developed thereby necessitating the numerical evaluation of integral expressions. Similar to Equations (4-4a) and (4-4b), the damping and frequency are taken as:

$$\xi_e = \frac{\omega_o}{\omega_e} \xi_o - \left(\frac{\omega_o}{\omega_e}\right)^2 \frac{E\left[AS(A)\right]}{E\left[A^2\right]} \quad (4\text{-}9b)$$

$$\omega_e^2 = \omega_o^2 \frac{E\left[AC(A)\right]}{E\left[A^2\right]} \quad (4\text{-}9c)$$

in which $E\left[g(a)\right]$ denotes the expected value of $g(a)$ and where $S(A)$ and $C(A)$ are the same expression as defined in Equations (4-4c) and (4-4d). For this narrow band Gaussian response process, the probability density function of the response amplitude, A, is approximated by a Rayleigh distribution. Hence, the expected value of a function $g(A)$ is,

$$E\left[g(a)\right] = \int_{-\alpha}^{+\alpha} \frac{Ag(A)}{\sigma^2} \exp\left(\frac{-A^2}{2\sigma^2}\right) dA \quad (4\text{-}9d)$$

where σ = the rms value of the response, $X(t)$ and $S(A)$ and $C(A)$ have the same expression as (4c) and (4d). σ is the rms value of the response $X(t)$.

b. APD Method - In this method the equivalent period (T_e) and equivalent damping ξ_e are found from the effective period (T_e') and damping (ξ_e') in terms of the amplitude (A) of the oscillation as defined in Equations (4-7a) and (4-6b). Thus,

$$T_e = \frac{2\pi}{\omega_e} = \frac{1}{X_m} \int_o^{X_m} T_e' \; (A) \; dA \quad (4\text{-}10a)$$

$$\xi_e = \frac{1}{X_m} \int_o^{X_m} \xi_e' \; (A) \; dA \quad (4\text{-}10b)$$

c. ASE Method - This method is similar to the Averaged Period and Damping Method (APD) except the parameters are based on stiffness and energy, ie,

$$K_e \; (X_m) = \frac{1}{X_m} \int_o^{X_m} K(A) da \quad (4\text{-}11a)$$

and

$$\Delta W_e \; (X_m) = \frac{1}{X_m} \int_o^{X_m} \Delta W(A) da \quad (4\text{-}11b)$$

with $K(A)$ and $\Delta W(A)$ equal to the cyclic secant stiffness and energy dissipated for harmonic oscillation of amplitude A.

4.5.2.3 Method Based on Earthquake Excitation - As compared to the previous two general categories, less material is available on the development of the equivalent linear approach explicitly for application to SDOF systems excited by earthquake motions. Reference 4.5 provides simple expressions for equivalent parameters based on experimental results for reinforced concrete portal frames. Reference 4.33 develops equivalent linear stiffness and damping expressions in terms of the maximum seismic response for elastic-plastic systems with bilinear hardening. This approach is based on the definition of a pseudo steady-state harmonic response having a response representative of the actual transient response in that it has corresponding values of equivalent linear stiffness and damping. In this manner, the closed form expression developed by Caughey (Reference 4.17) can then be utilized for the case of earthquake excitation. In order to account for the transient rather than the harmonic nature of the loading, the pseudo steady-state response is equated to the rms transient response. Reference 4.33 describes the present status of this approach and compares the results with some extensive series of numerical response computations. This equivalent linear approach provides good prediction of the maximum response of a SDOF system with bilinear hysteresis with the agreement depending upon the hardening coefficient, the ductility ratio and frequency. The accuracy increases for increasing values of the hardening coefficient and for ductility ratios greater than 4.0.

4.5.2.4 Comparison of Various Methods - In order to compare the estimates provided by the various harmonic response and random response methods described above (Sections 4.5.2.1 and 4.5.2.2), a set of optimum linear system parameters were developed, as described in Reference 4.15. These optimum effective linear system parameters (OLES) were established as those parameters that minimize the mean square difference between the pseudo-velocity response spectrum and the candidate linear system. Hence, these parameters are considered to provide the best estimate of the maximum seismic response of the system over the frequency raise of interest.

The results were compared for the case of a bilinear hysteretic (BLH) system with the OLES parameters based upon a computer simulation study. The original hysteretic and effective linear systems were compared on the basis of their averaged response spectra. Numerical results for the effective period shift and effective viscous damping versus ductility are presented in Figure 4.26 for the various methods described previously and for the optimum effective system parameters. These results indicate that in terms of period shift, the methods based on harmonic response considerably overestimate the period shift while the averaging methods (ASE, APD) give more realistic estimates. With respect to damping, all of the approximate methods overestimate the effective damping. The amplitude averaging methods provide the best prediction for low ductility levels while the ASE provides better estimates for moderate to large ductility. Overall, the ASE method provided the best overall set of parameters as compared to the OLES values and that, in general, the results from random response methods are better than those from harmonic response methods.

In addition, the seismic response of four different degrading systems (Figure 4.27) was also examined to illustrate the accuracy of the ASE method. Table 3 presents a summary of the results with the range of the rms average spectral error, ϵ, varying from 4 percent to 17 percent for all cases. As indicated in Reference 4.15, the degree of accuracy of this approximate method is quite reasonable and illustrates the utility of such a method for estimating inelastic response.

4.5.3 Discussion

Under current practice, and for economical reasons, the complicated structural systems of nuclear power plants are treated by linear seismic analyses. For example, analyses of concrete structures are treated with both gross properties and fully cracked properties. The cracked properties are usually estimated based on the conservative forces developed for the uncracked linear models. This analytical approach assumingly brackets the true nonlinear response. An Ebasco-developed cracking program, Ebasco-Nastran, has the capability to handle nonlinear cracking time-history analysis. No such analysis has been performed on a large-scale model, however, because it is economically unfeasible.

Considering the inherent difficulties and penalties associated with detailed nonlinear dynamic analyses of MDOF systems, the development of practical, simplified approaches for such nonlinear response calculations is a necessity. As illustrated in Section 4.5.2, the equivalent linear approach provides an attractive means of developing basic response data for use in design. In addition, such approaches should, with further development and calibration, furnish better estimates of MDOF inelastic response and provide a basis and guidelines for workable procedures to provide realistic estimates of nonlinear response at high levels of seismic loading.

References (Chapter 4)

4.1 Newmark, N M and Rosenblueth, E, Fundamentals of Earthquake Engineering, Prentice-Hall, Inc, 1971.

4.2 Powell, G H, "Inelastic Dynamic alysis of Tall Buildings," Earthquake Resistant Design of Engineering Structures, ASCE, Conference, July 19-30, 1972.

4.3 Clough, R W and Benuska, K L, "FHA Study of Seismic Design Criteria for Hi-rise Buildings," Report HUD IS-3, Federal Housing Administration, Washington, DC, August 1966.

4.4 Kobori, Takuji, et al, "Elastic-plastic Earthquake Response of Frames with Shearwall," Proceedings, World Conference of Earthquake Engineering, Meerut, India, Vol VIII, 1977, pp 3037-3042.

4.5 Gulkan, P and Sozen, M A, "Inelastic Responses of Reinforced Concrete Structures to Earthquake Motions," ACI Journal, December 1974.

4.6 Veletsos, A S and Newmark, N M, "Effect of Inelastic Behavior on the Response of Simple Systems to Earthquake Motions," Proceedings, Second World Conference of Earthquake Engineering, Tokyo, Japan, 1960.

4.7 Newmark N M, "Seismic Design Criteria for Structures and Facilities," Trans-Alaska Pipeline System, Proceedings, U S National Conference on Earthquake Engineering, Ann Arbor, Michigan FERI, June 1975.

4.8 Newmark, N M, "A Response Spectrum Approach for Inelastic Seismic Design of Nuclear Facilities," Transactions, Fourth International Conference on Structural Mechanics in Reactor Techonlogy, San Francisco, California, Paper K 4/1, August 1977.

4.9 Newmark, N M and Hall, W J, "Comments on Inelastic Seismic Capacity of Nuclear Reactor Structures," ASCE Convention, Boston, April 1979.

4.10 Veletsos, A S, "Maximum Deformations of Certain Nonlinear Systems," Proceedings, Fourth World Conference on Earthquake Engineering, Santiago, Chile, 2, A-4, 1969.

4.11 Clough, R W and Bertero, V V, "Laboratory Model Testing for Earthquake Loading," Journal of the Engineering Mechanics Division, ASCE, Vol 103, EM6, December 1977.

4.12 Fintel, M, Handbook of Concrete Engineering, Van Nostrand Reinhold, New York 1974.

4.13 Hsiu, F J and Hanson, R D, "Inelastic Seismic Response of Turbine Buildings," Transactions, Third International Conference on Structural Mechanics in Reactor Technology, San Francisco, California, Paper K 4/3, August 1977.

4.14 Penzien, J and Liu, S C, "Nondeterministic Analysis of Nonlinear Structures Subjected to Earthquake Excitations," Proceedings, Fourth World Conference on Earthquake Engineering, Santiago, Chile 1, A-1, 1969.

4.15 Iwan, W D, and Gates, N C, "Estimating Earthquake Response of Simple Hysteretic Structures," Journal of the Engineering Mechanics Division, Vol 105, EM3, ASCE, June 1979.

4.16 Caughey, T L, "Random Excitation of a System with Bilinear Hysteresis," Journal of Applied Mechanics, American Society of Mechanical Engineers, Vol 27, No. 4, December 1960, pp 649-652.

4.17 Caughey, T K, "Sinusoidal Excitation of a System with Bilinear Hysteresis," Journal of Applied Mechanics, American Society of Mechanical Engineers, Vol 27, No. 4, December 1960, pp 640-643.

4.18 Gates, N C, "The Earthquake Response of Deteriorating Systems," thesis presented to the California Institute of Technology, Pasadena, California, in 1977, in partial fulfillment of the requirements for the degree of Doctor of Philosophy.

4.19 Jacobsen, L S, "Damping in Composite Structures," Proceedings," Second World Conference on Earthquake Engineering, Tokyo and Kyoto, Japan, Vol 2, 1960, pp 1029-1044.

4.20 Jennings, P C, "Equivalent Viscous Damping for Yielding Structures," Journal of the Engineering Mechanics Division, ASCE, Vol 94, No. EM1, Proc Paper 5793, February 1968, pp 103-116.

4.21 Rosenblueth, E and Herrera, I, "On a Kind of Hysteretic Damping," Journal of the Engineering Mechanics Division, ASCE, Vol 90, No. EM4, Proc Paper 3999, August 1964, pp 37-48.

4.22 Berg, G V, "A Study of the Earthquake Response of Inelastic Systems," Proceedings, Thirty-Fourth Convention of the Structural Engineers Association of California, Coronado, California, October 1965, pp 63-67.

4.23 Newmark, N M, "A Response Spectrum Approach/for Inelastic Seismic Design of Nuclear Reactor Facilities," Transactions, Third International Conference on Structural Mechanics in Reactor Technology, London, England, Paper K 5/1, June 1975.

4.24 Archer, R R and Large, C G "Nonlinear Dynamic Behavior of Shallow Shells," AIAA, No. 3, 1965, p 2113.

4.25 Kreig, R D, "Unconditional Stability in Numerical Time Integration Methods," Sandia Corp, Report No. SC-DR-70-400, 1970.

4.26 Mescall, J and Tsui, T, "Influence of Damping in Dynamic Stability of Spherical Caps Under Step Pressure Loading," AIAA, No. 9, 1971, p 1244.

4.27 Belytschko, T and Schoeberle, D F, "On the Conditional Stability of an Implicit Algorithm for Nonlinear Dynamics," Journal of Applied Mechanics, Vol 42, 1975, p 865.

4.28 Stricklin, J A, et al, "Nonlinear Analysis of Shells of Revolution by the Matrix Displacement Method," AIAA, No. 6, 1968, p 2306.

4.29 Weeks, G, "Temporal Operators for Nonlinear Structural Dynamics Problems," Journal of the Engineering Mechanics Division, ASCE, Vol 98, EM5, October 1972.

4.30 Adeli, H, Gere, J M and Weaver, W, Jr, "Algorithms for Nonlinear Structural Dynamics," Journal of the Structural Division, ASCE, Vol 104, ST2, February 1978, pp 263-280.

4.31 Wen, Yi-Kei, "Stochastic Response Analysis of Hysteretic Structures," Probabilistic Mechanics and Structural Reliability, Edited by A H-S Ang and M Shinozuka, ASCE Specialty Conference, Tucson, Arizona, January 10-12, 1979.

4.32 Nickell, W E, "A Survey of Simplified Inelastic Analysis Method," Welding Research Council, Bulletin 253, October 1979.

4.33 Transirikongkol, V, and Pecknold, D A, "Equivalent Linear SDF Response to Earthquakes," Journal of the Structural Division, ASCE, Vol 105, ST12, December 1979, pp 2529-2545.

4.34 Iwan, W D, "Application of Nonlinear Analysis Techniques," Applied Mechanics in Earthquake Engineering, W D Iwan, ed, Applied Mechanics Symposium Series, ASME, New York, AMD, Vol 8, 1974.

4.35 Shibata, A and Sozen, M A, "Substitute-Structure Method for Seismic Design in R/C," Journal of the Structural Division, ASCE, Vol 102, ST1, January 1976, pp 1-18.

4.36 Anagnostopoulos, S A, Haviland, R W and Biggs, J M, "Use of Inelastic Spectra in Aseismic Design," Journal of the Structural Division, ASCE, Vol 104, ST1, January 1978, pp 95-109.

TABLE 4.1

MAXIMUM GENERALIZED STRESS OF FRAME ELEMENTS (REF. 4.4)

	TYPE 1	TYPE 2
H'=1.0	2.409×10^{-1}	2.653×10^{-1}
0.7	1.932	1.661
0.3	1.908	1.578
0.1	1.905	1.521

TABLE 4.2

AVERAGE SPECTRAL ERROR AND EFFECTIVE PERIOD AND DAMPING FROM ASE METHOD FOR FOUR DIFFERENT DEGRADING STIFFNESS SYSTEMS (REF. 4.15)

System	Ductility Ratio, μ			
	1.5	2.0	4.0	8.0
02-06-10				
T_e/T_0	0.887	0.951	1.190	1.479
ζ_e, as a percentage	7.84	8.75	13.43	14.61
ϵ, as a percentage	7.8	7.8	8.3	11.1
02-10-10				
T_e/T_0	0.998	1.090	1.350	1.678
ζ_e, as a percentage	8.01	9.57	11.40	10.93
ϵ, as a percentage	4.6	4.6	6.0	6.3
02-10-00				
T_e/T_0	1.130	1.240	1.526	1.876
ζ_e, as a percentage	5.11	8.25	12.48	12.59
ϵ, as a percentage	5.3	9.4	10.3	9.4
10-10-00				
T_e/T_0	1.055	1.138	1.381	1.698
ζ_e, as a percentage	6.47	10.80	16.48	16.73
ϵ, as a percentage	9.8	16.4	16.8	14.3

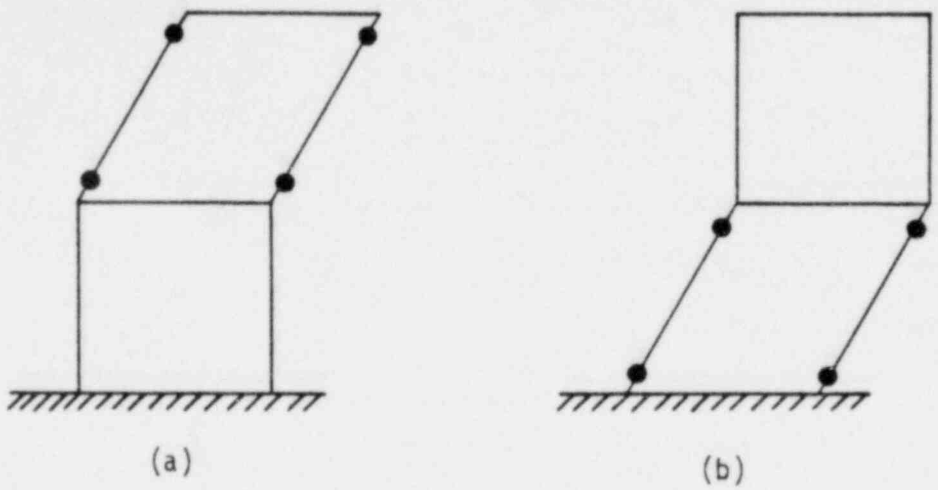

FIGURE 4.1
FORMATION OF PLASTIC HINGES FOR A FRAME STRUCTURE WHEN SUBJECTED TO LATERAL LOADS

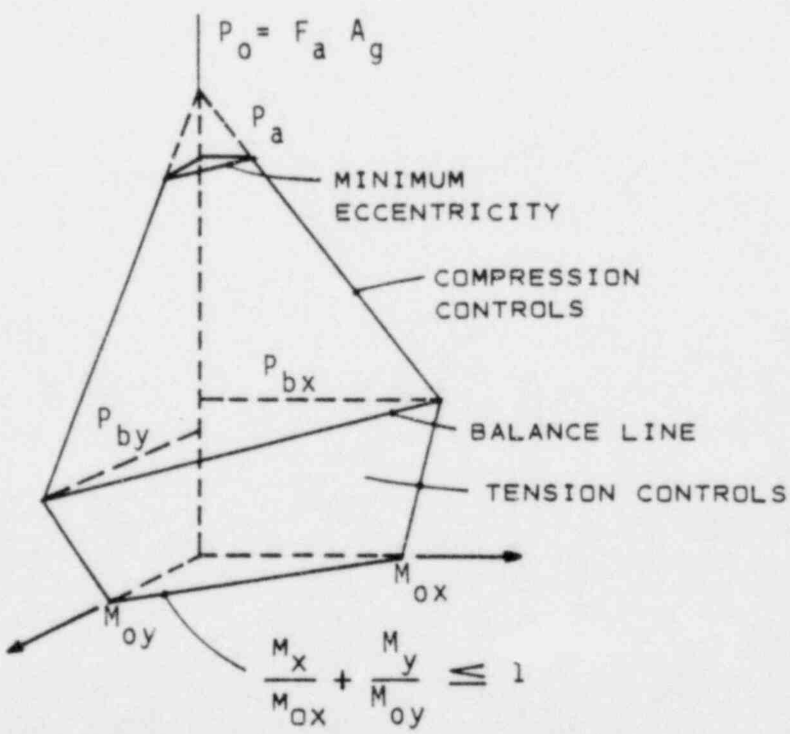

FIGURE 4.2
WORKING STRESS INTERACTION SURFACE FOR RECTANGULAR SECTIONS

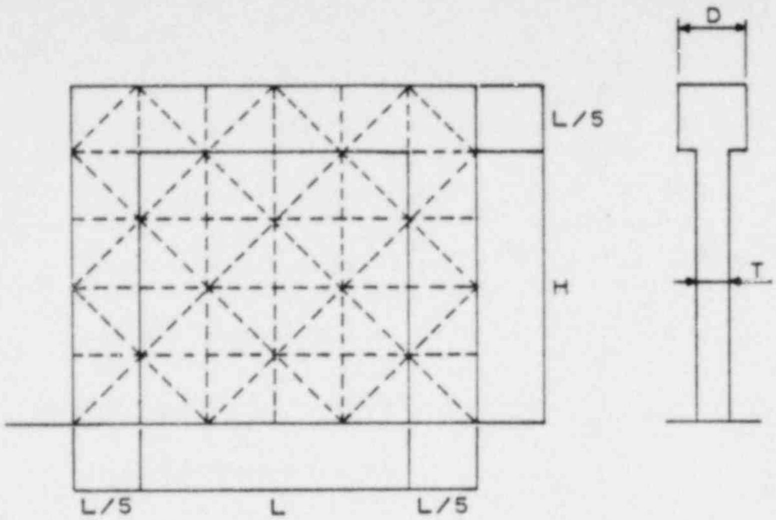

FIGURE 4.3

STRUCTURAL MODEL (REF. 4.4)

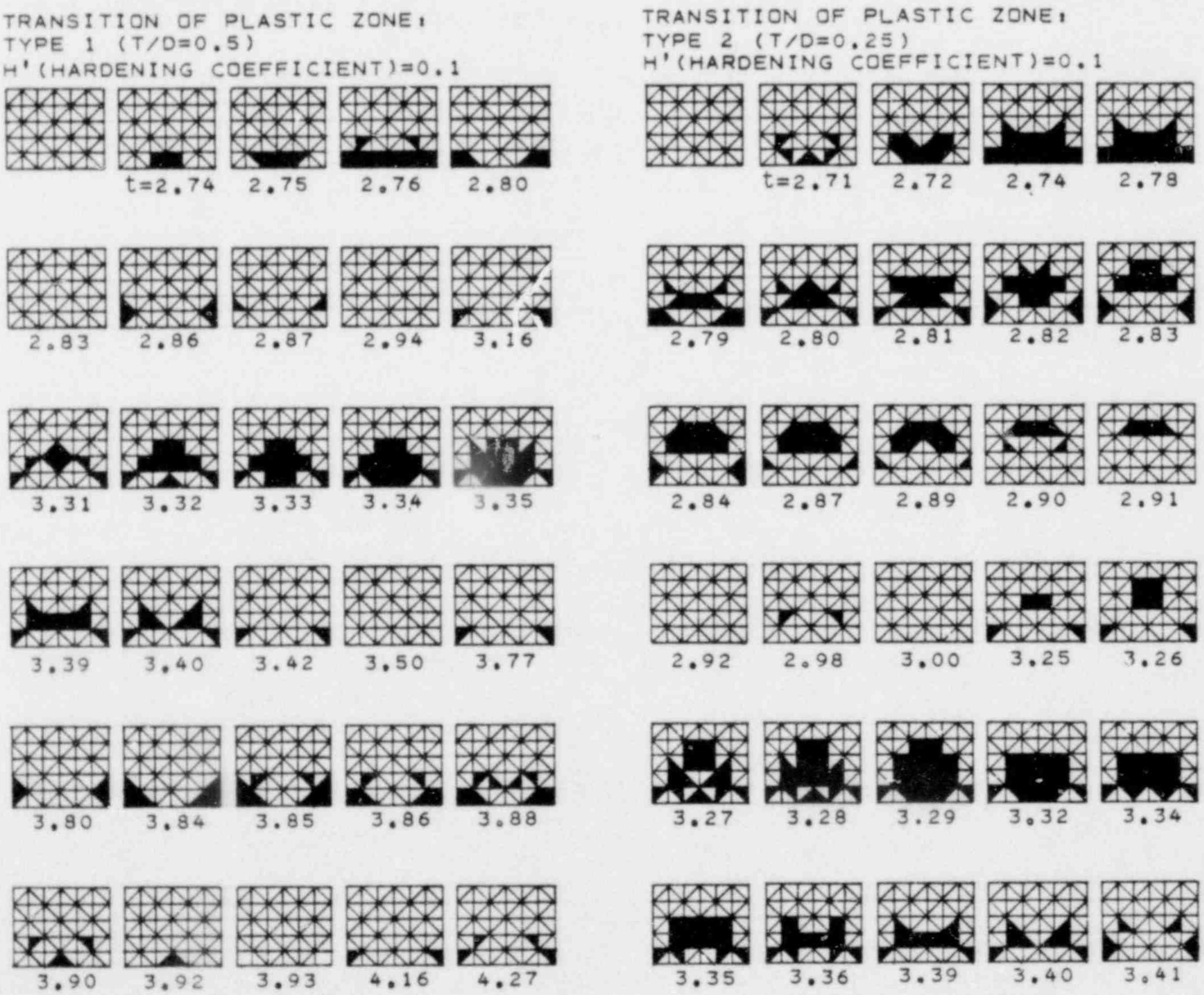

FIGURE 4.4

TRANSITION OF PLASTIC ZONE (REF. 4.4)

(MAXIMUM GENERALIZED STRESSES - SEE TABLE 4.1)

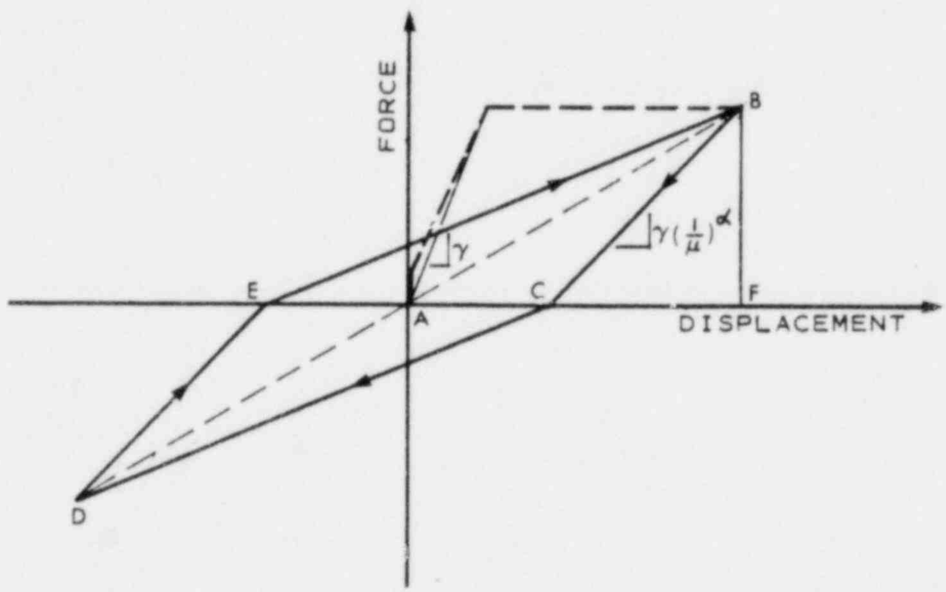

FIGURE 4.5

STIFFNESS DEGRADING SYSTEM, AFTER PENZIEN AND LIU (1969)(REF. 4.5)

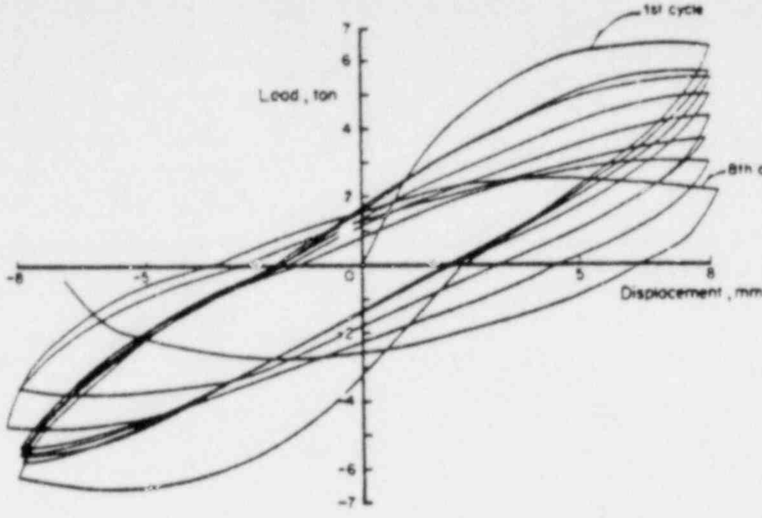

FIGURE 4.6(a)
LOAD - DEFORMATION RELATIONS FOR REINFORCED - CONCRETE COLUMNS (REF.4.4)

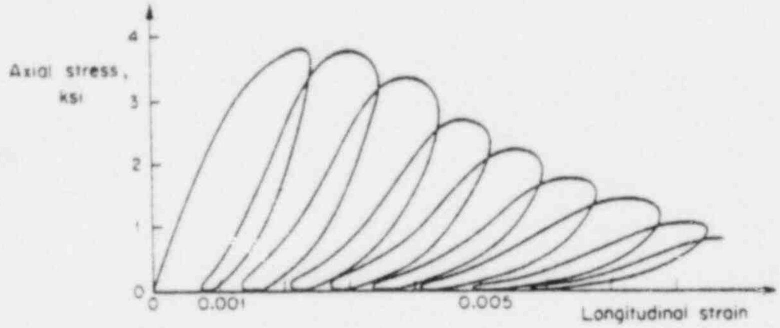

FIGURE 4.6(b)
REPEATED LOADING OF PLAIN CONCRETE IN COMPRESSION (REF. 4.4)

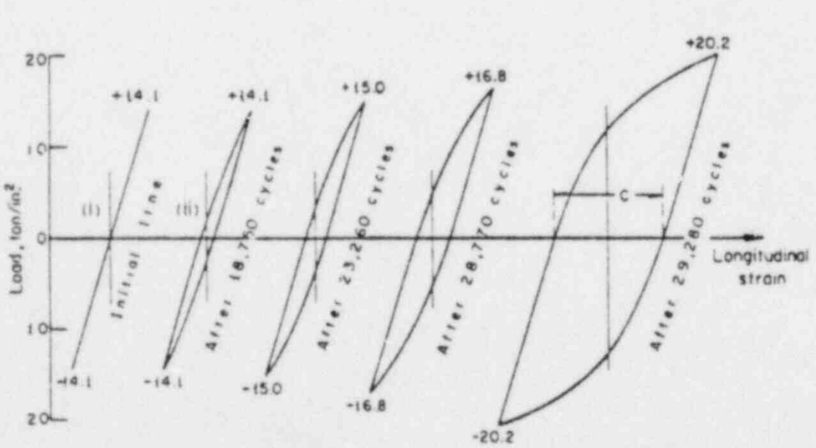

FIGURE 4.7
REPEATED LOADING OF AXLE STEEL (REF. 4.1)

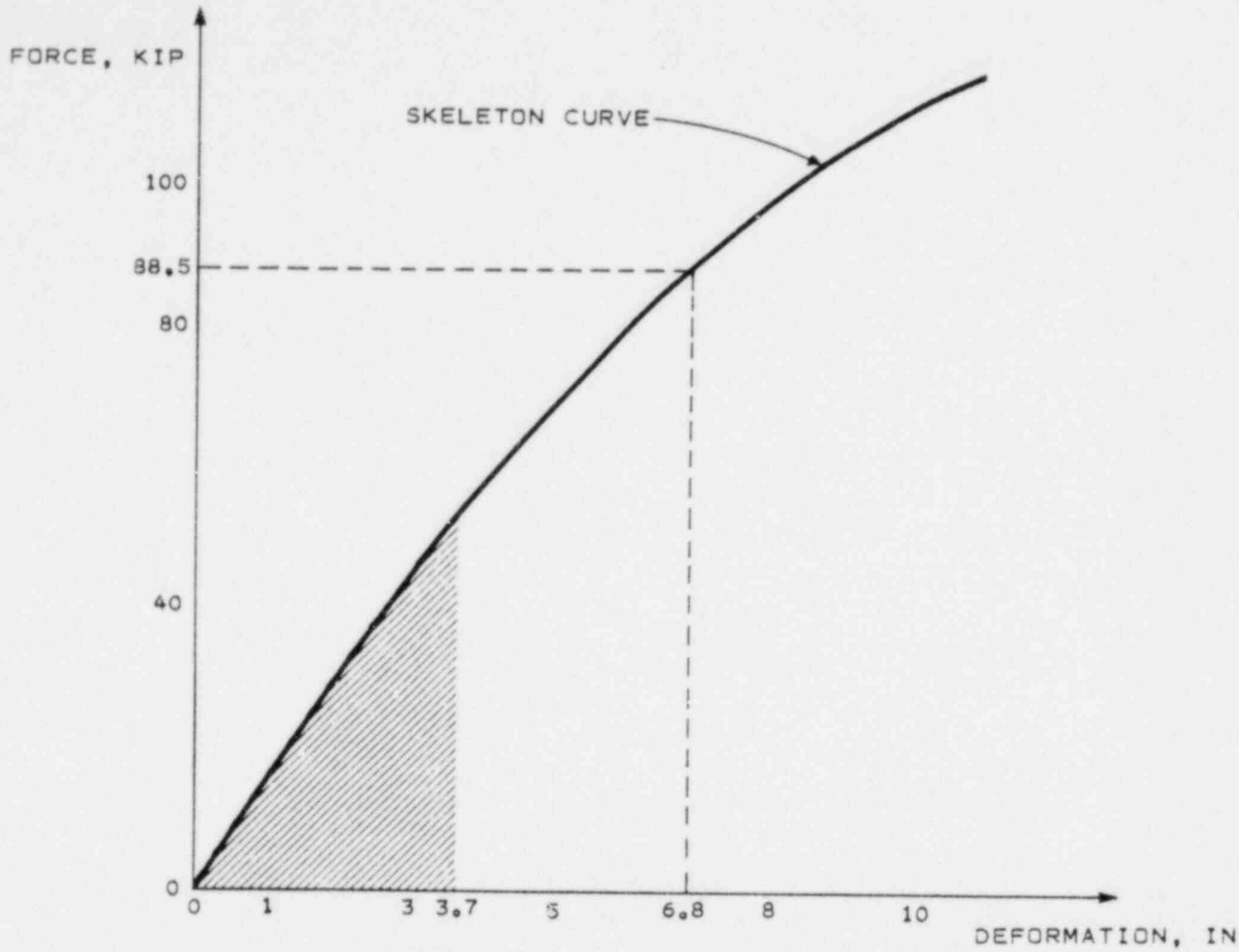

FIGURE 4.8
EXAMPLE OF SKELETON CURVE OF NONLINEAR SYSTEM

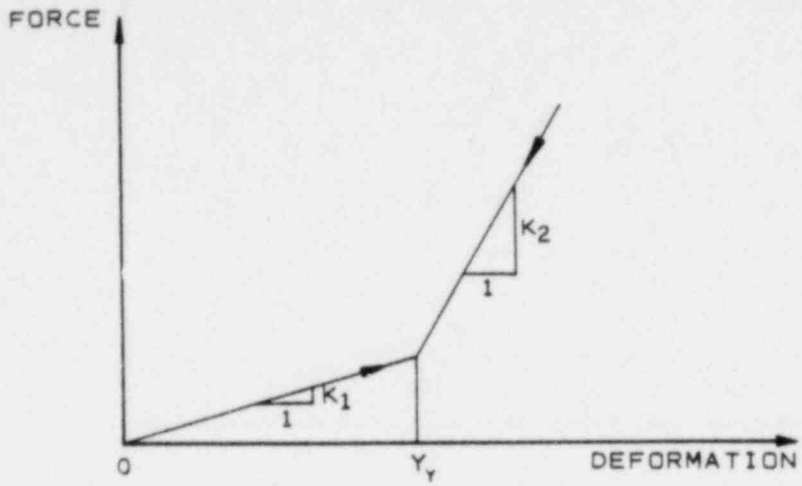

(a) HARDENING SYSTEM

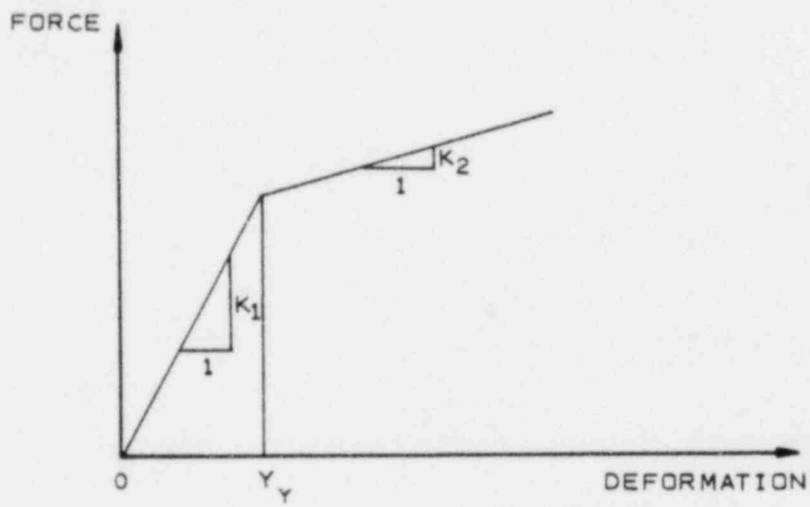

(b) SOFTENING SYSTEM

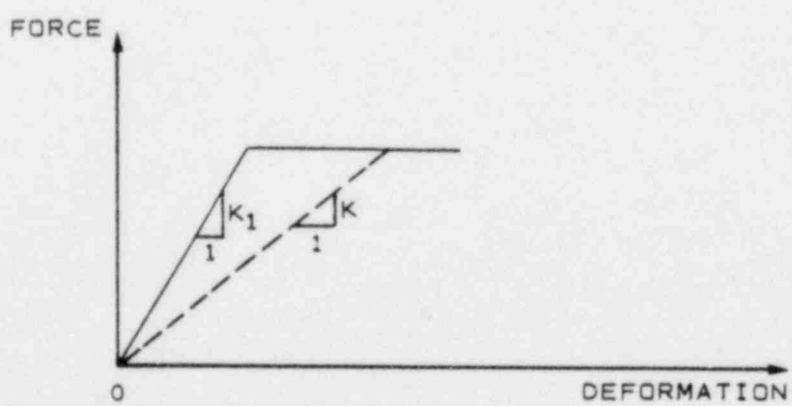

(c) SYSTEM WITH ZERO STIFFNESS IN SECOND BRANCH

FIGURE 4.9
BILINEAR SYSTEMS

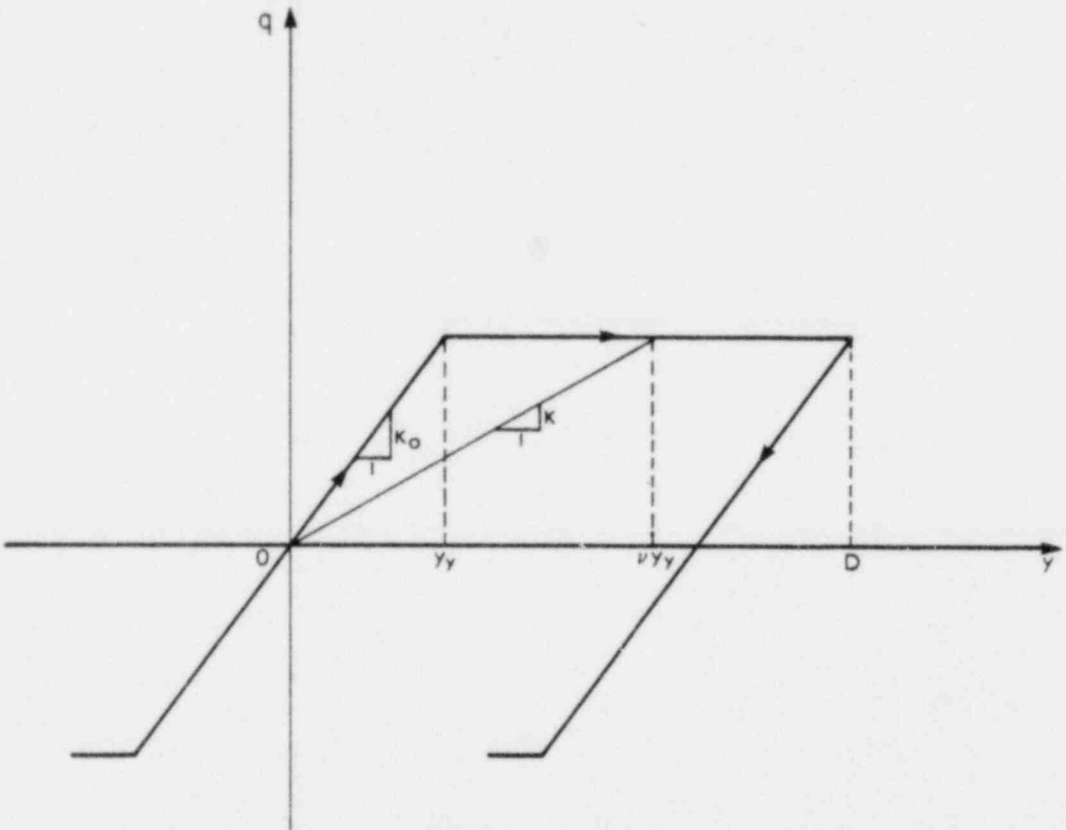

FIGURE 4.10

FORCE - DEFORMATION CURVE OF ELASTOPLASTIC SYSTEM (REF. 4.1)

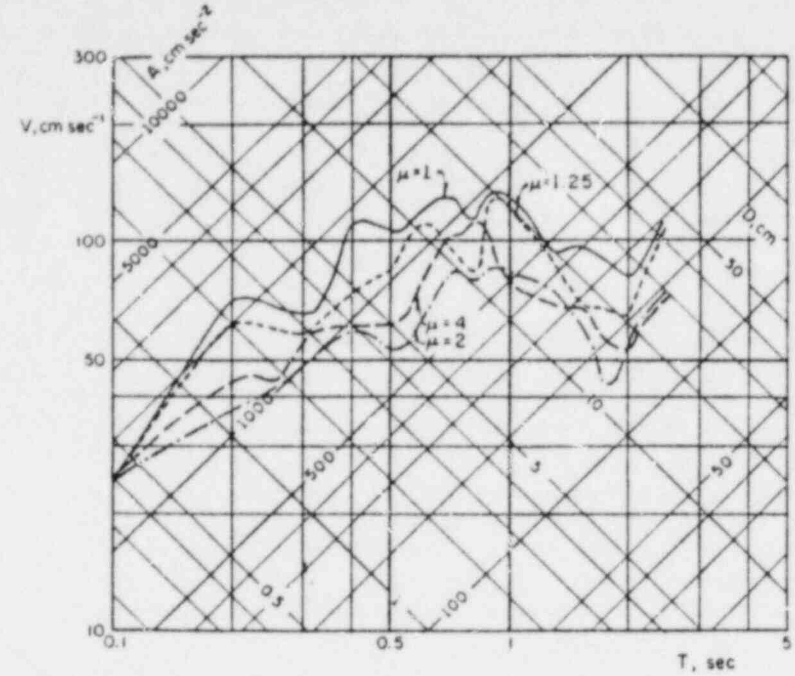

FIGURE 4.11
COMPARISON OF UNDAMPED ELASTOPLASTIC SPECTRA.
DATA AFTER VELETSOS AND NEWMARK (1960)
(REFS. 4.1, 4.6)

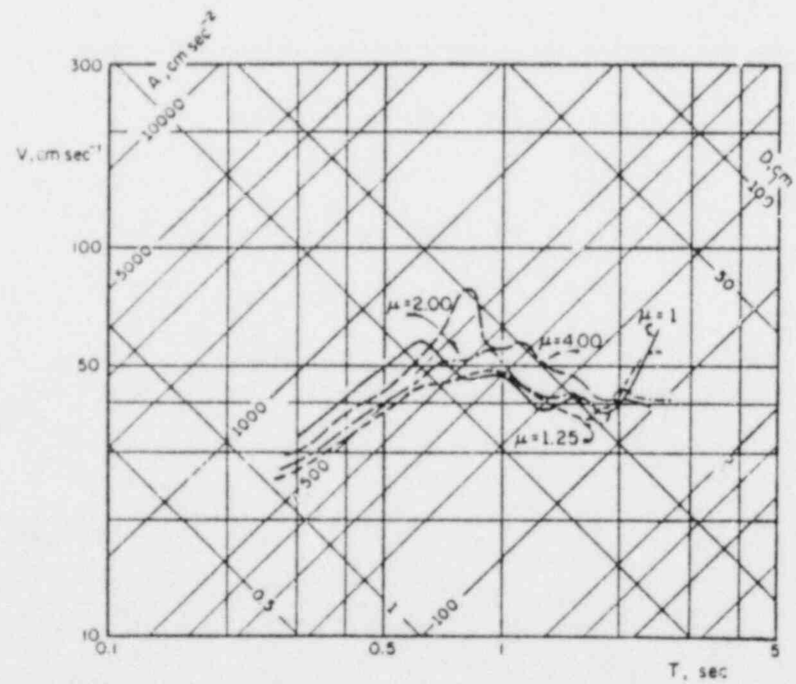

FIGURE 4.12
COMPARISON OF DAMPED ELASTOPLASTIC SPECTRA HAVING
10 PERCENT CRITICAL DAMPING. DATA AFTER VELETSOS
AND NEWMARK (1960) (REFS. 4.1, 4.6)

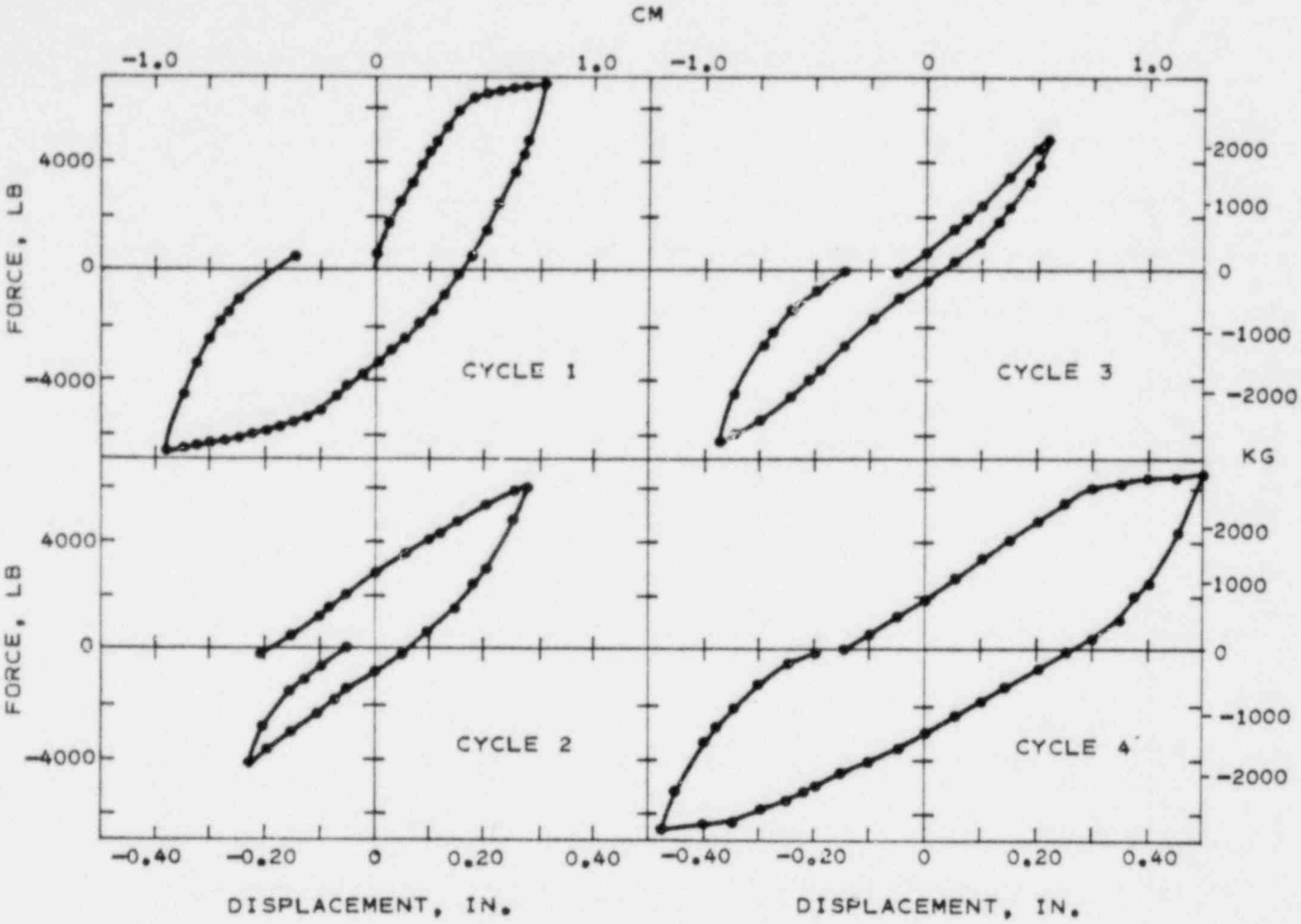

FIGURE 4.13
MEASURED FORCE - DISPLACEMENT RELATIONSHIP FOR FRAME
(FIRST FOUR CYCLES. "STATIC" LOADINGS.) (REF. 4.5)

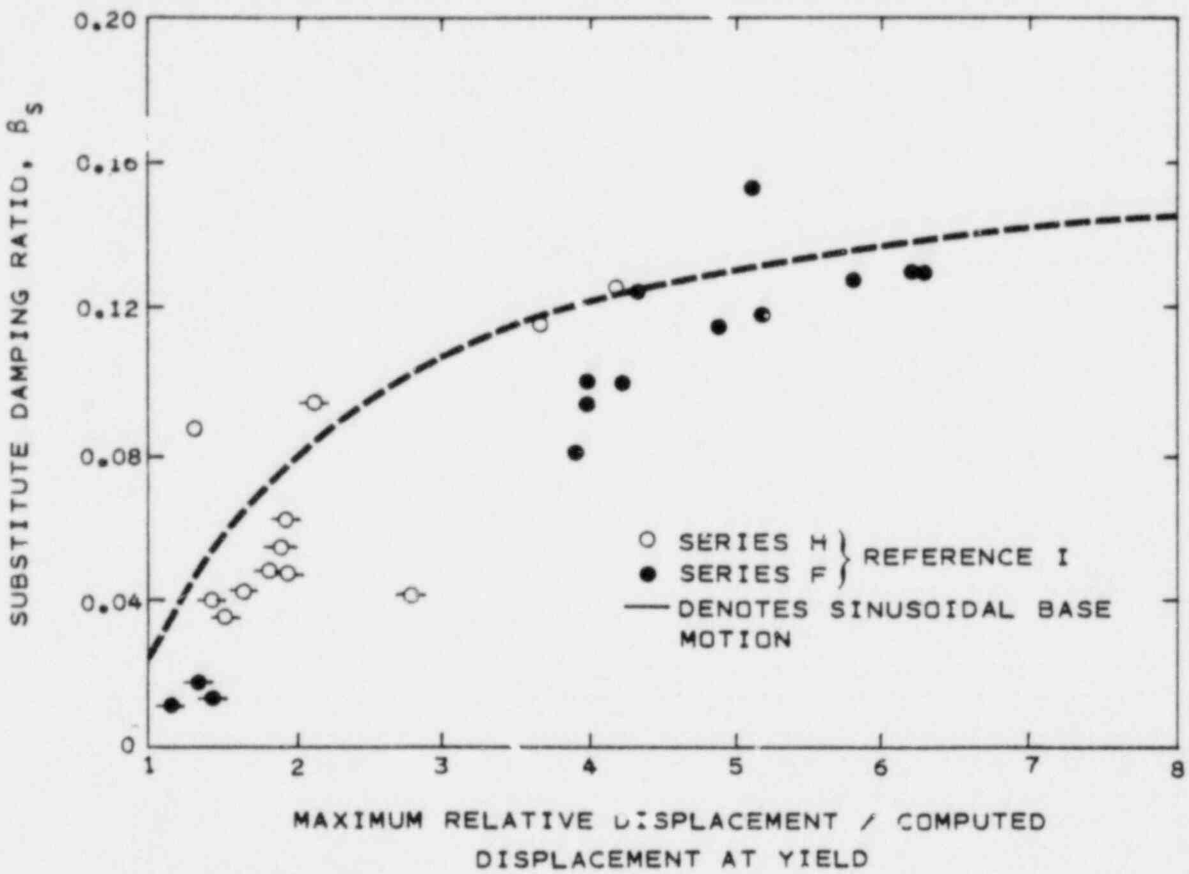

FIGURE 4.14

VARIATION OF MEASURED AVERAGE SUBSTITUTE - DAMPING RATIO, β_S, WITH THE DUCTILITY RATIO, μ (REF. 4.5)

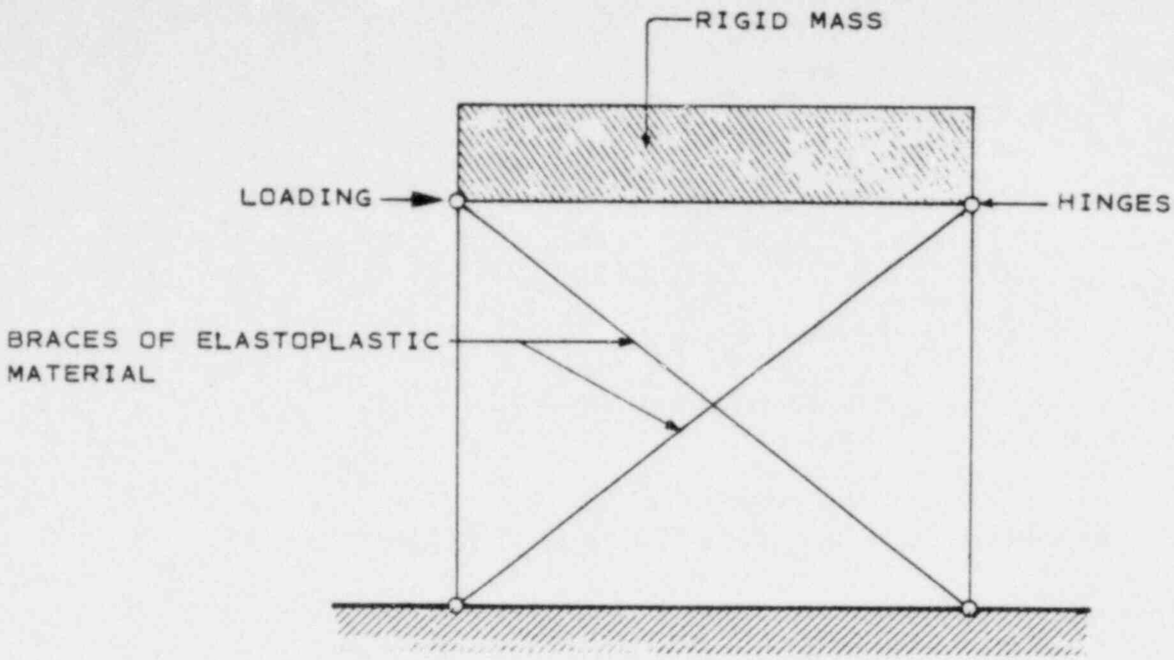

FIGURE 4.15
X - BRACED FRAME (REF. 4.1)

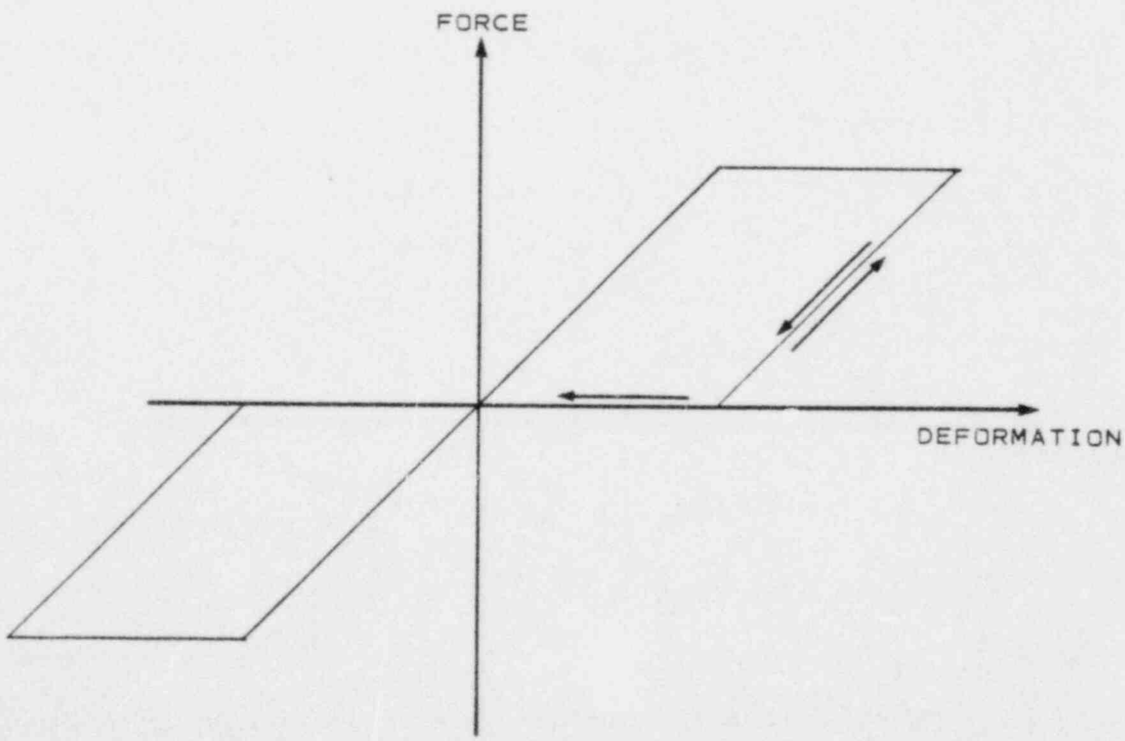

FIGURE 4.16
IDEALIZED FORCE - DEFORMATION CURVE (REFS. 4.1, 4.6)

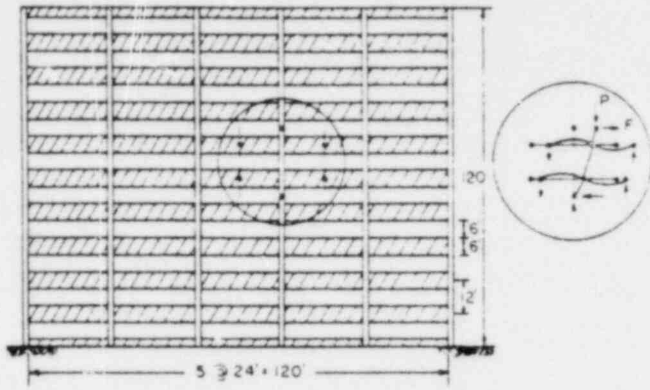

FIGURE 4.17
FRAME, SUBASSEMBLAGE, AND LATERAL DISPLACEMENT PATTERN (REF. 4.11)

Θ_{bw} =FLEXURAL ROTATION OF BEAM
Θ_{pw} =PULLOUT ROTATION

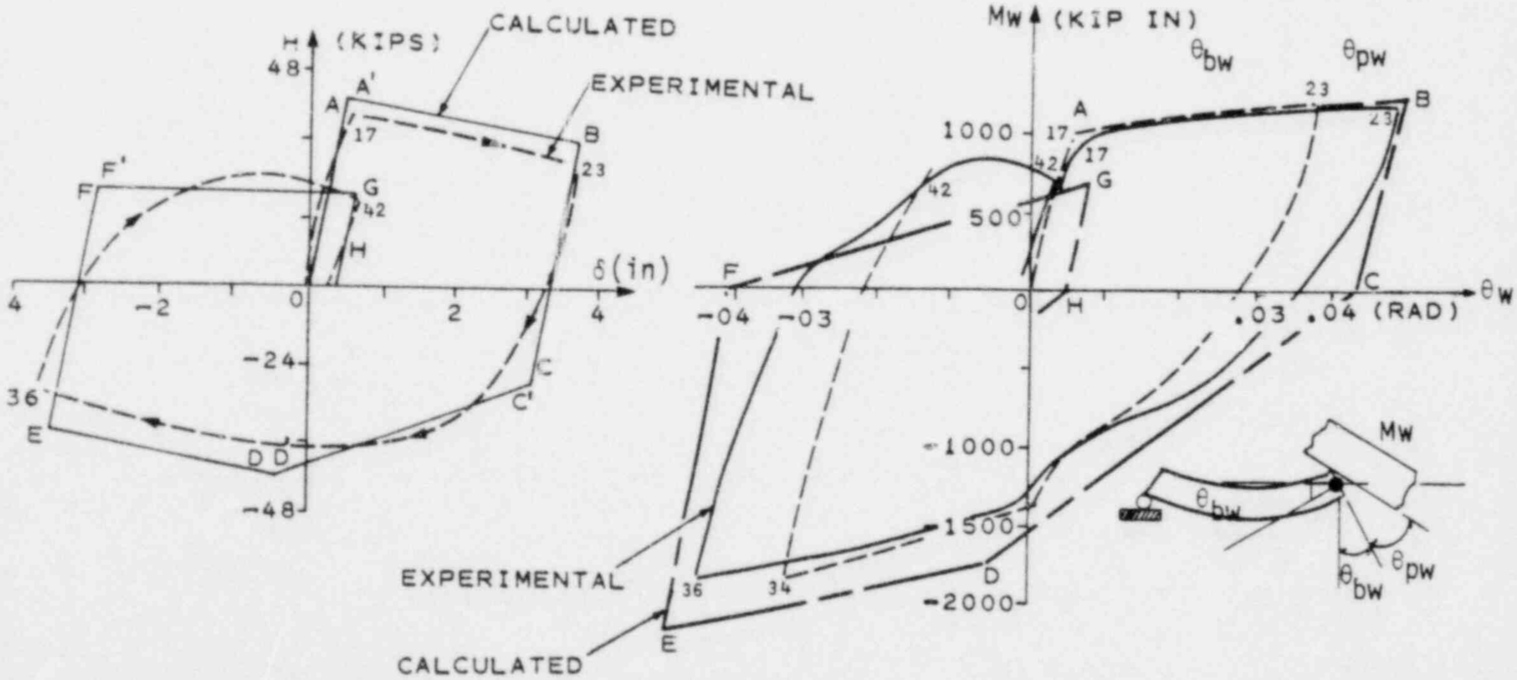

FIGURE 4.18
CORRELATION OF COMPUTED AND MEASURED RESULTS (REF. 4.11)

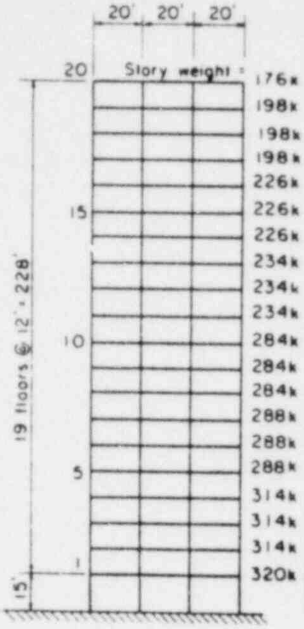

(a) Frames spaced at 25'

Ratio (EI) : (EI)$_0$

Columns: Exterior	Columns: Interior	Girders
1.0	2.0	4.0
1.5	3.0	6.0
3.0	6.0	
4.5	9.0	8.0
6.0	12.0	
10.0	20.0	10.0
12.0	24.0	

(b) Relative stiffness of columns and girders

Fundamental period, 2.2 sec.
$(EI)_0 = 133{,}500$ k-ft^2

(a)

PROPERTIES OF STANDARD OPEN-FRAME STRUCTURE

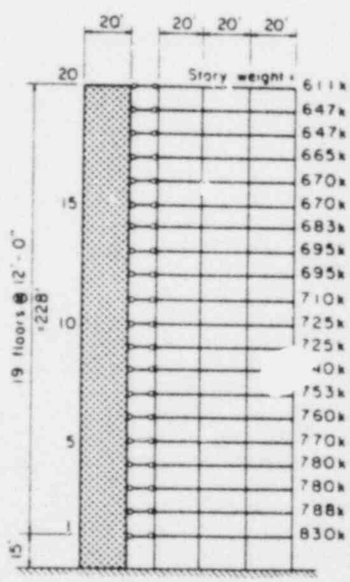

(a) 4 frames spaced at 25' per shear wall

Ratio (EI) : (EI)$_0$

Columns: Exterior	Columns: Interior	20 ft shear wall	Girders
0.3	0.6	1000	1.0
0.9	1.8	1200	
1.5	3.0	1400	
2.1	4.2	1700	
2.7	5.4	2000	
3.3	6.6	2200	
4.0	8.0	2400	

(b) Relative stiffness of columns and girders

Fundamental period, 2.2 sec
$(EI)_0 = 390{,}000$ k-ft^2

(b)

PROPERTIES OF STANDARD FRAME-SHEAR WALL STRUCTURE

FIGURE 4.19
STANDARD OPEN-FRAME AND FRAME-SHEAR WALL STRUCTURES CONSIDERED IN STUDY (REF. 4.3)

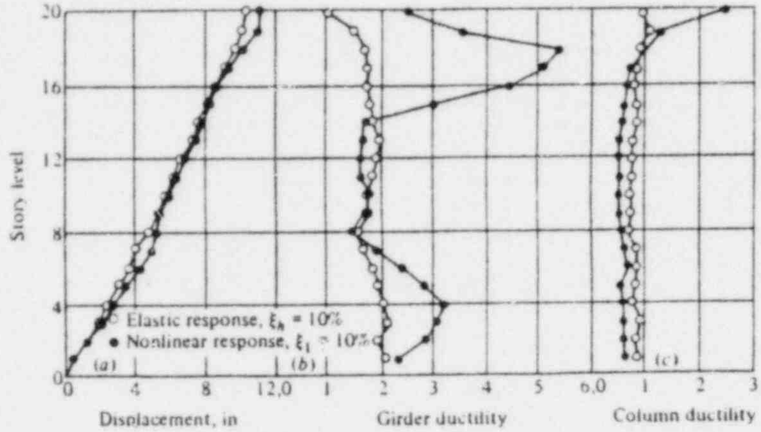

(a)

COMPARISON OF ELASTIC AND NONLINEAR DYNAMIC EARTHQUAKE RESPONSE

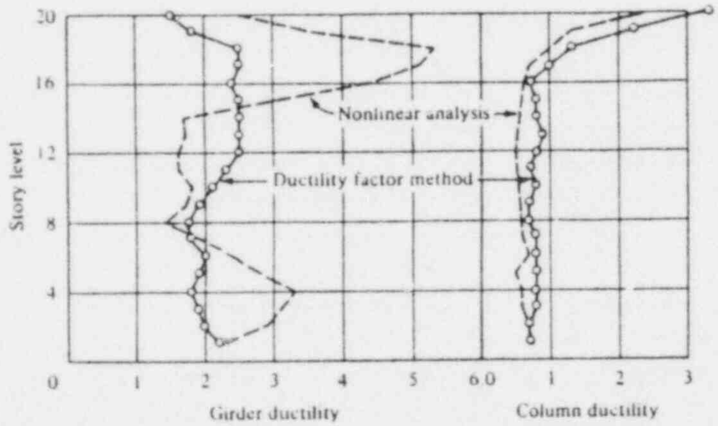

(b)

APPROXIMATE MEMBER DUCTILITY COMPARED WITH EXACT

FIGURE 4.20

ANALYTICAL RESULTS FOR OPEN-FRAME STRUCTURE SHOWN IN FIG. 4.19 (REFS 4.3,4.12)

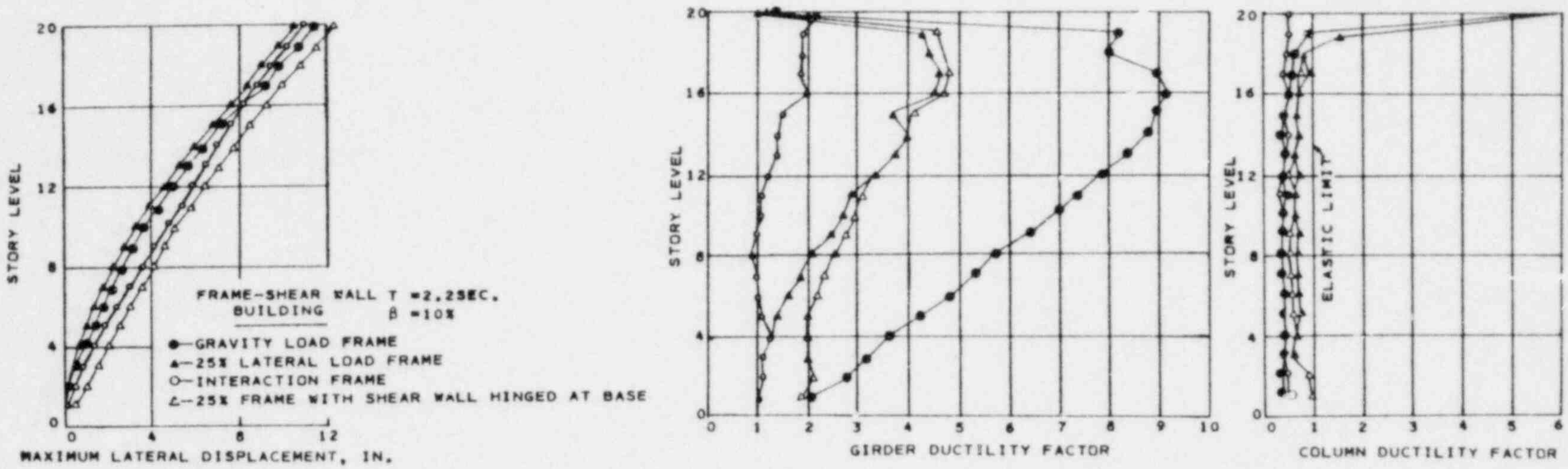

FIGURE 4.21

EFFECT OF DESIGN ASSUMPTION ON DISTRIBUTION OF LATERAL FORCES BETWEEN FRAME AND SHEAR WALL (REFS. 4.3, 4.12)

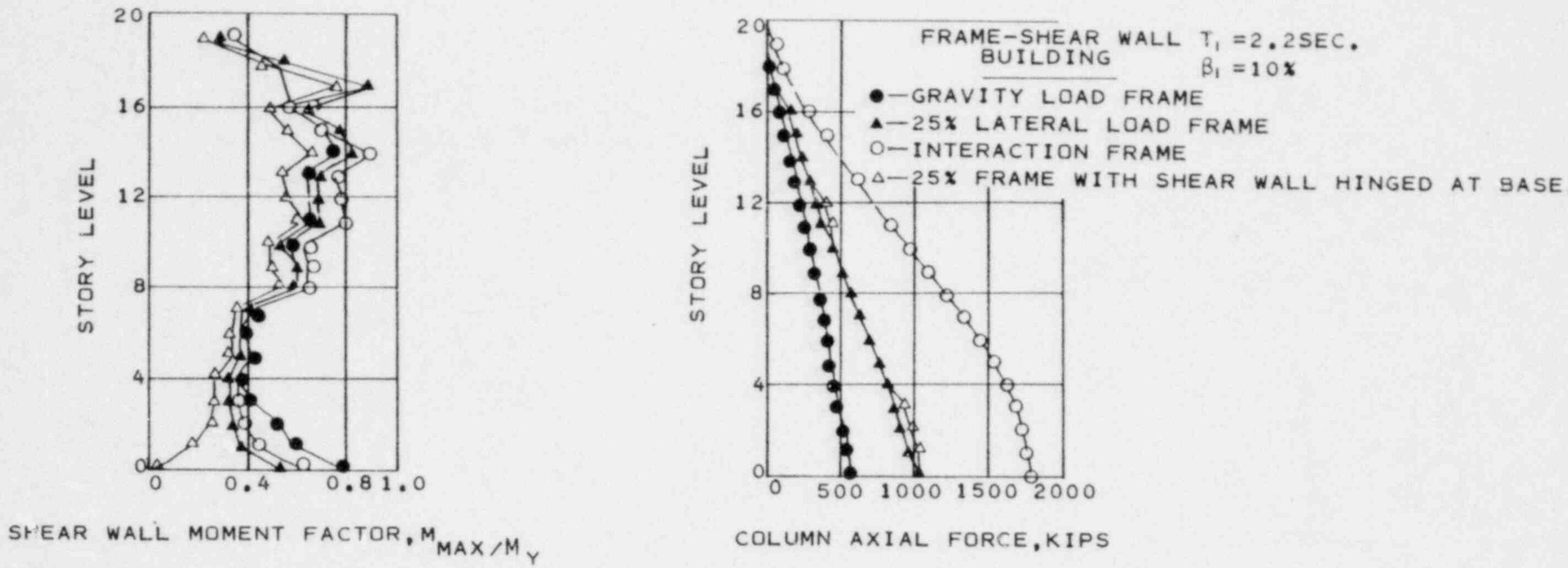

FIGURE 4.21 (CONTINUED)

EFFECT OF DESIGN ASSUMPTION ON DISTRIBUTION OF LATERAL FORCES BETWEEN FRAME AND SHEAR WALL (REFS 4.3, 4.12)

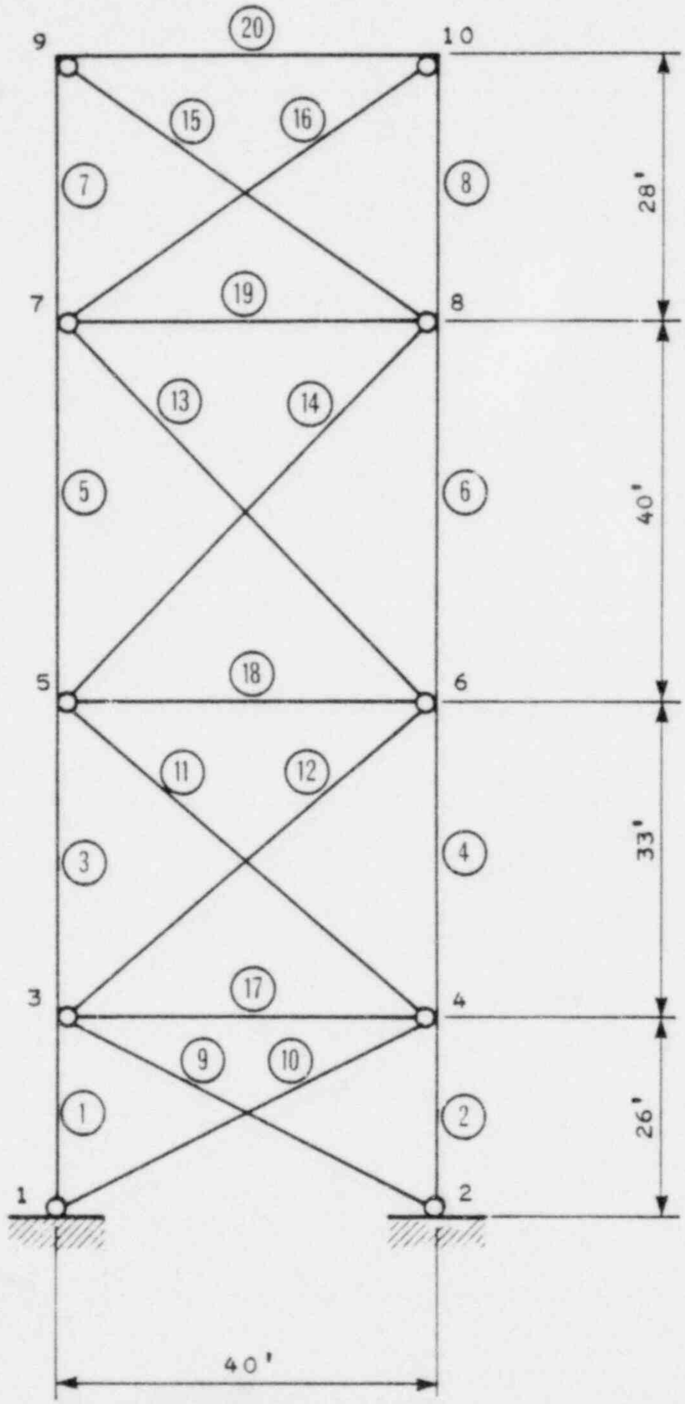

FIGURE 4.22 (a)
STRUCTURE MATHEMATICAL MODEL (REF. 4.13)

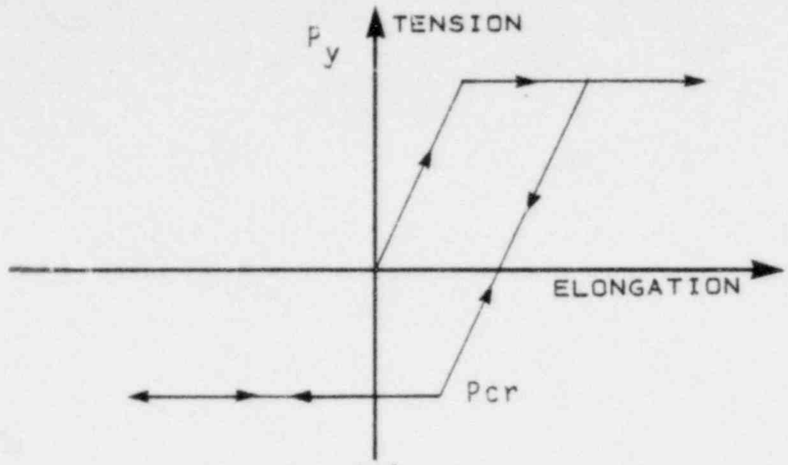

(a)

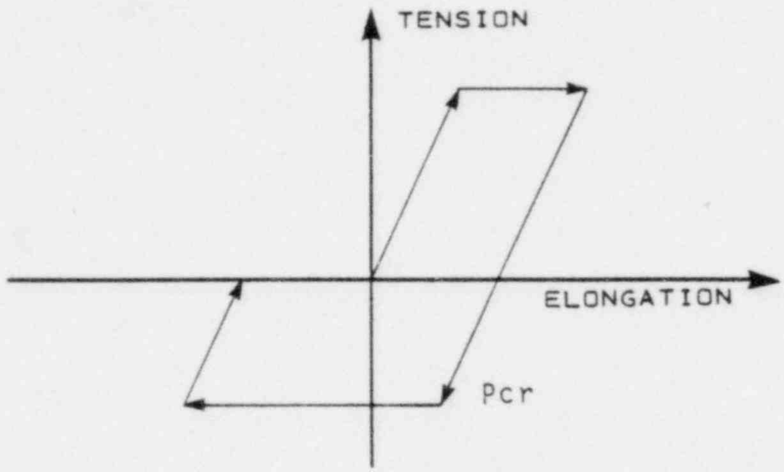

(b)

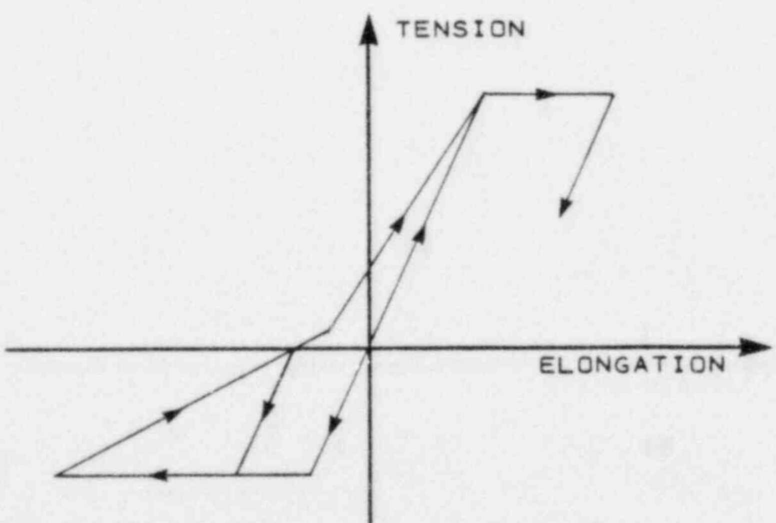

(c)

FIGURE 4.22(b)

ANALYTICAL MODELS OF BRACING MEMBER BEHAVIOR (REF. 4.13)

(a) TENSION YIELDING ELASTIC BUCKLING MODEL

(b) FULL CYCLE MODEL

(c) SINGH MODEL, 1976

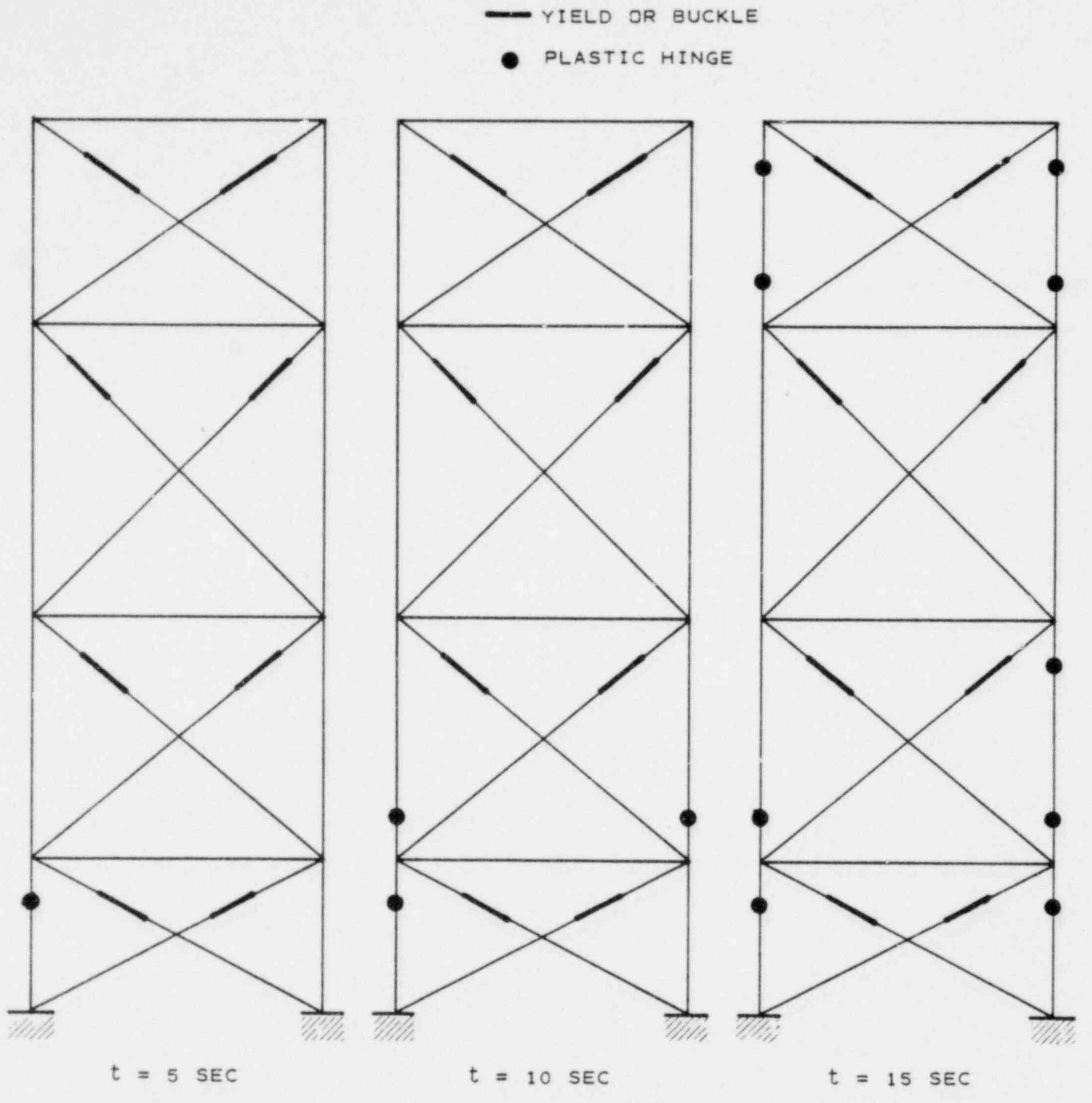

FIGURE 4.23
YIELDED MECHANISM OF STRUCTURE (REF. 4.13)

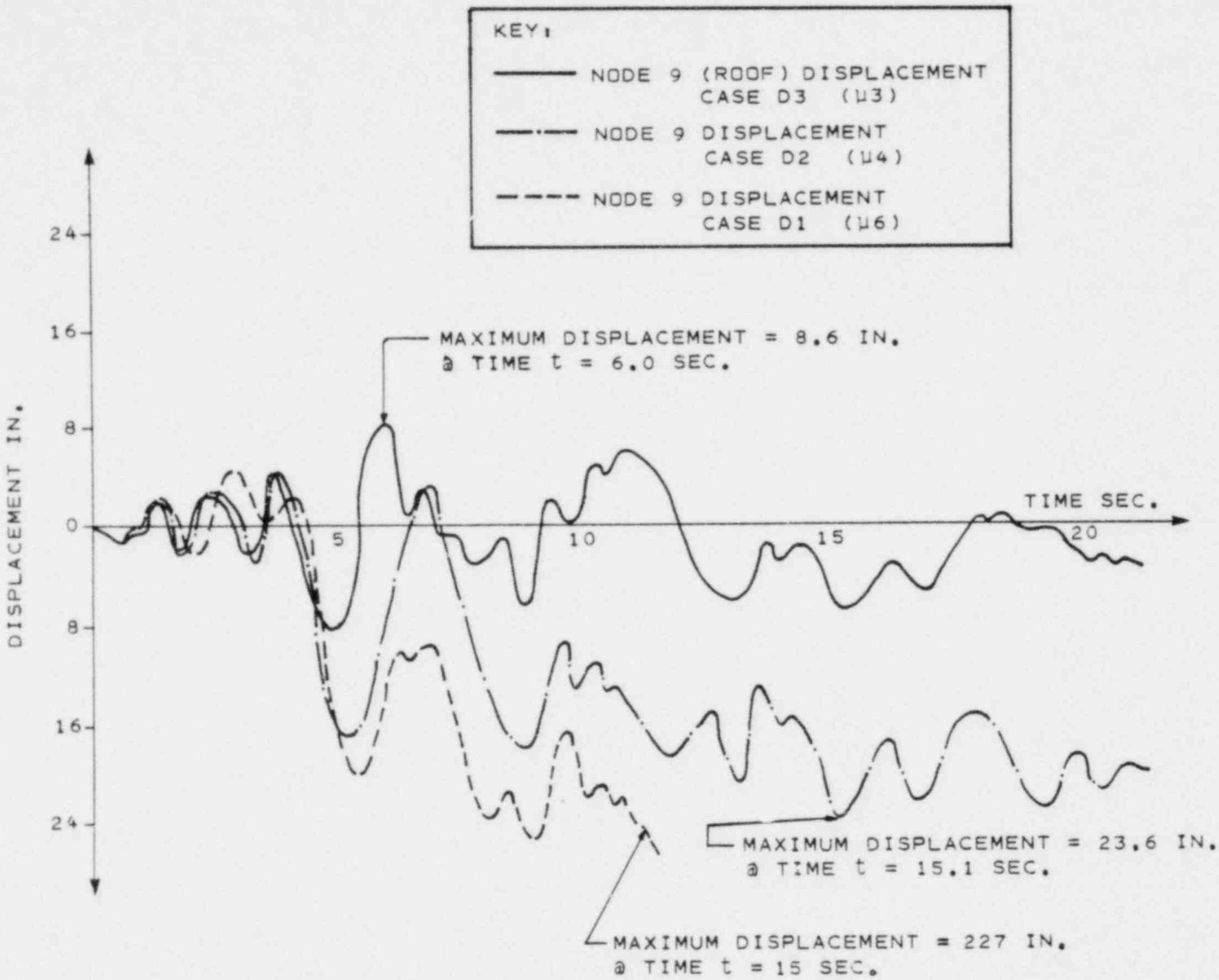

FIGURE 4.24

COMPARISON OF DISPLACEMENT TIME HISTORIES OF DIFFERENT DUCTILITY DESIGN (REF. 4.13)

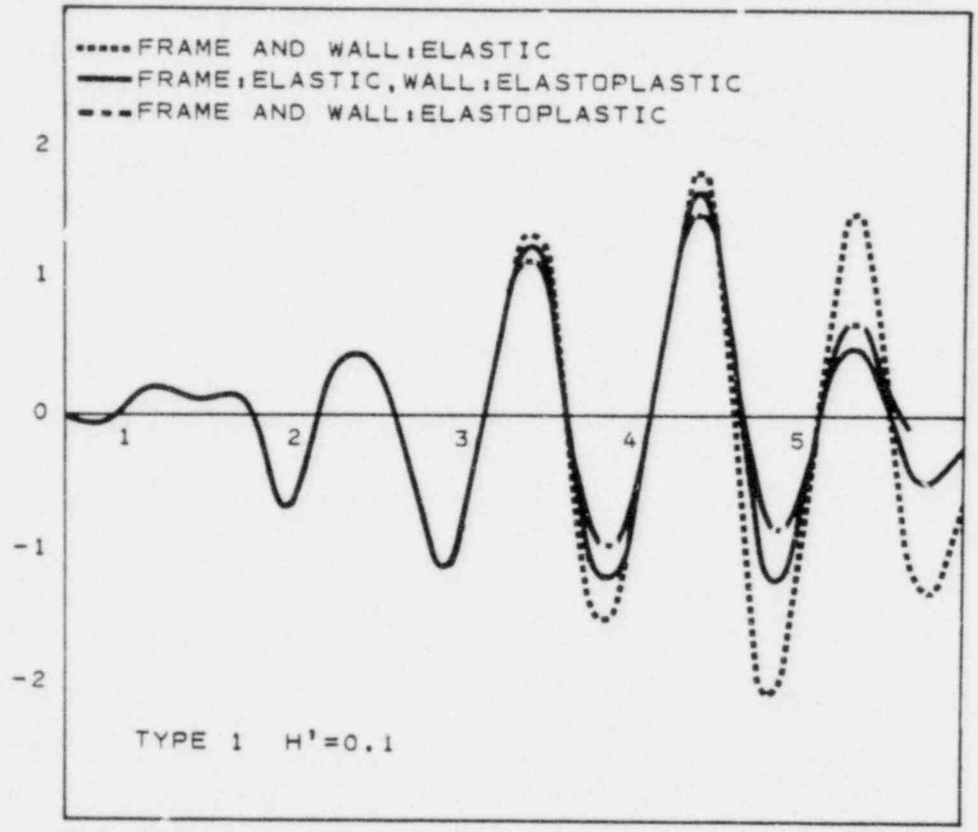

FIGURE 4.25
HORIZONTAL DISPLACMENT AT THE TOP OF MODEL (REF. 4.4)

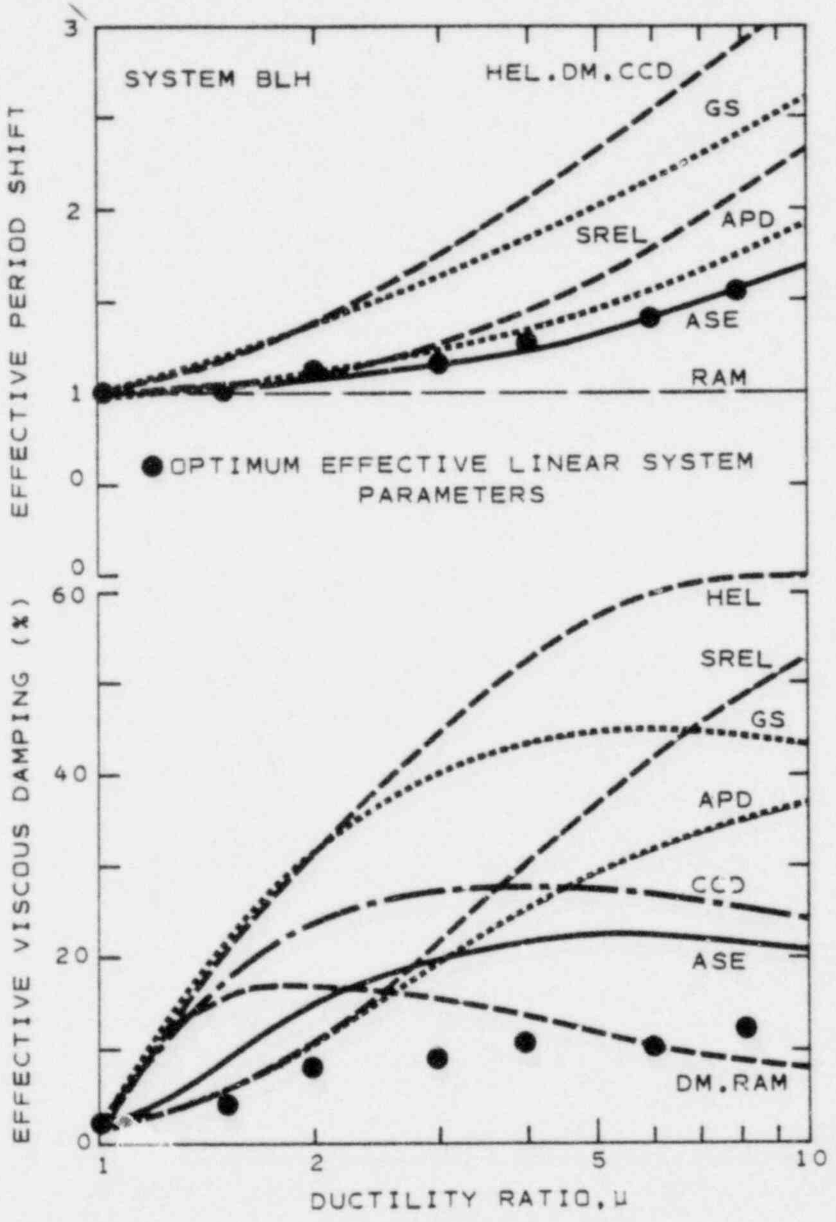

FIGURE 4.26
APPROXIMATE LINEAR SYSTEM PARAMETERS FOR BLH SYSTEM WITH α=5% AND ζ_0 =2%(REF. 4.15)

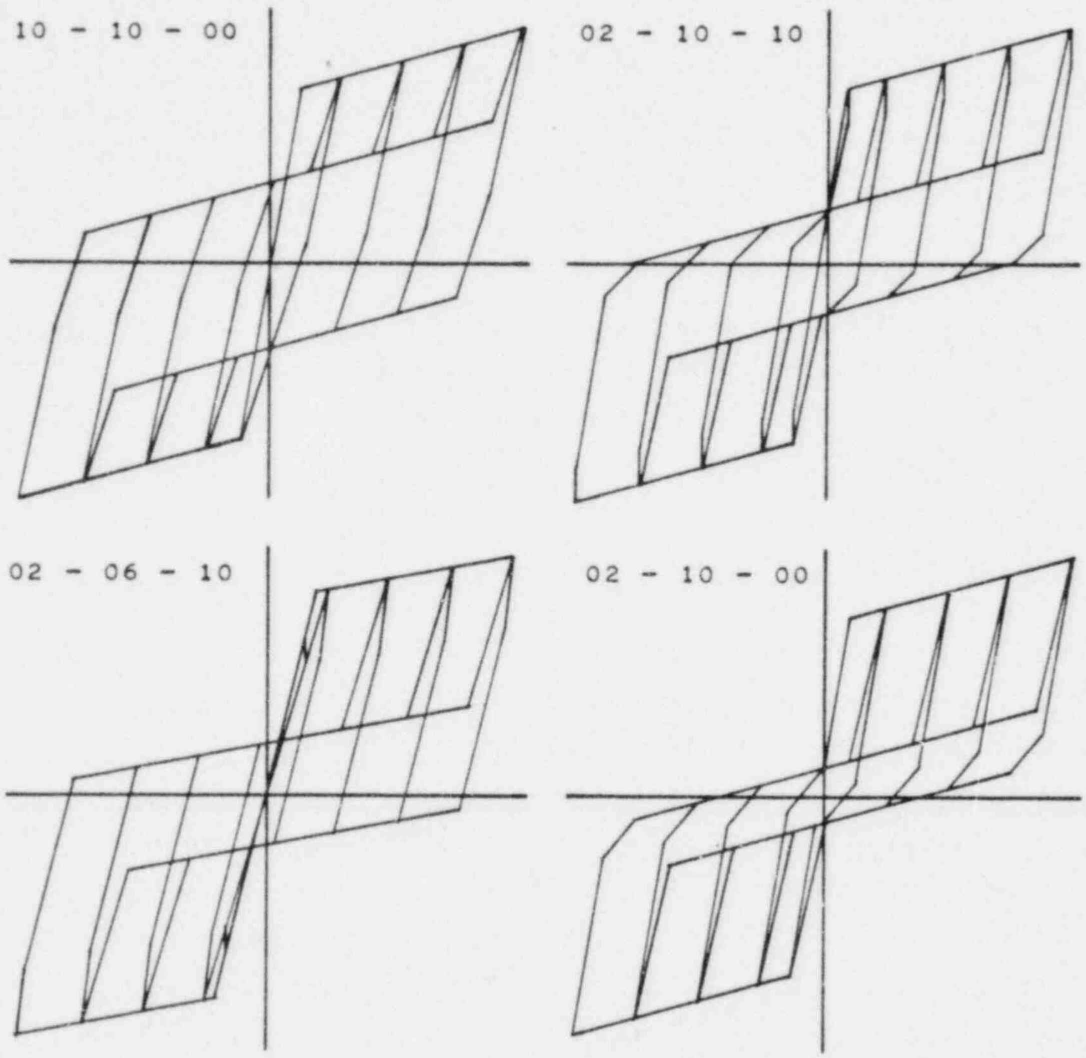

FIGURE 4.27

STIFFNESS DEGRADING SYSTEMS FOR NUMERICAL STUDY (REF, 4.15)

Chapter 5

Combination of Loads

5.1 Combination of Seismic and Nonseismic Loads

The development of a probabilistic computational methodology for seismic loadings on nuclear facilities must address the manner in which the multiplicity of load types are to be combined. The loads to be considered include service loads (dead load, operating live load, construction loads, soil and hydrostatic pressure, equipment reaction, operating pressure and temperature), severe environmental loads (operating basis earthquake, design wind and snow loads), abnormal loads (such as pressure and thermal loads generated by a postulated accident) and severe environmental loads (safe shutdown earthquake, tornado loads, hurricane loads, tsunami, missile loads).

The most direct approach would be to develop various combinations of input loading time histories prior to performing the response calculations. Such a procedure would require a knowledge of how the loads are phased and implies a probabilistic treatment of the individual load contributions to the composite input time history. Due to these technical uncertainties and in the interest of computational economy, this approach is not commonly used in current practice. Present procedures (Ref 5.1) involve the performance of analyses for each of the individual loads and to then add their effects by means of load combination factors. Load reduction factors are also employed to approximately account for the statistical effect of the unlikely occurrence of combined load effects. Such an approach, patterned after that routinely employed in building codes and design specifications, does not provide a level of probabilistic sophistication consistent with the SSMRP methodology. The assignment of load combination and reduction factors is largely based on the collective experience and judgement of the responsible code-writing group and, as such, does not consider the actual probability of occurrence of the total combined load effects and cannot therefore provide any consistency in terms of risk level. Such approaches generally provide conservative and often unduly conservative loads. However, it should be noted that the use of conventional load reduction factors, depending on the relative magnitudes of the individual load effects, may under- or overestimate a combined load effect established on a probabilistic basis (Ref 5.2). An additional source of concern is the fact that in current practice, nonlinear behavior, such as concrete cracking, under combined loads is treated by static analysis.

The recently developed ANSI/ANS-2.12 Standard (Ref 5.3) entitled "Guidelines for Combining Natural and External Man-Made Hazards at Power Reactor Sites" provides additional material on the quantification of combined load effects for nuclear power plant design. This Standard, while concerned only with natural and man-made external loads, is aimed at establishing a methodology for identifying proper combinations of loads for consideration in design. In this work, the concept of an acceptably low probability of occurrence is used to serve as a means of differentiating between load combinations which must be considered and those which need not be treated. The concepts employed in the development of this Standard have application to the generation of the more general combined load effects for SSMRP work. For example, the criteria for nonconsideration of particular loads and load combinations include the following: (a) Where acceptably small probability of occurrence exists, ie, if the probability of occurrence of the hazard is on the order of 10^{-7} per year; (b) Where the effect of the loads in the postulated combination are nonadditive, ie, they do not produce loads on the same part of the plant; (c) Where the effect on the plant due to the combined effect is determined to be less severe than the effect of another combination; and (d) Where the loads in the postulated combination are mutually exclusive, ie, they cannot occur simultaneously due to the physical laws of nature.

Attempts to refine the procedures for combining the large number of loads and load types in nuclear plant structures must necessarily deal with the statistical problem of estimating the peak combined effect of loads over the anticipated life of the facility. In the next section, a brief summary will be made of the approaches being taken by various researchers to address this problem from the standpoint of probability analysis.

5.2 Stochastic Determination of Maximum Combined Load Effects

Risk due to simultaneous occurrence of extreme loads can be evaluated from the mean occurrence rates, mean occurrence durations and intensity distributions of the individual loads. For such combinational analyses the macrotime behavior of load effects can be categorized into the following types; as shown in Figure 5.1: (Type a) Those loads changing at finite points in time but remain largely constant in between (eg, due to sustained live load, operational loads); and (Type b) Those loads occurring very infrequently and with short duration (eg, due to extraordinary live load, wind load) or those that are very rare and with extremely brief duration (eg, due to earthquake, tornadoes, blasts). The objective of these probabilistic analyses is to study the probability distribution of the maximum combined load effect, as shown in Figure 5.1(c). For studies such as the SSMRP, the probability of occurrence of the maximum combined load effect over the plant life is of considerable interest since the objective should be to design for load combinations which have occurrence probabilities consistent with those associated with single loads. Such calculations require the use of quite sophisticated techniques and to date no generic method has been developed for statistically combining loads. Some of the principal avenues of research in this regard are considered below.

As summarized in Reference 5.4, Turkstra (Ref 5.5) developed a procedure which has been adopted in the load factor design method for steel. The procedure is such that when one of the time-varying loads takes on a maximum value, the other loads are selected on a random basis. On a point-by-point basis, such an assumption is unconservative, however, bounds on the failure probability can be obtained by adding the probability for all possible combinations.

Wen (Refs 5.2 and 5.6) considered factors such as mean load occurrence rate, intensity variation, random duration of each occurrence and simultaneous occurrence of different loads. The probability distribution of the maximum combined effect over a given time interval was derived. The distribution parameters as a function of the lower moments and occurrence rates of individual loads were also obtained in closed form based on the theory of the statistics of extremes. The results obtained by modeling the loads as either Poisson square waves or a filtered Poisson process. The probability distribution and first two moments of the maximum of the combination of two or more loads effects over a given period of time were obtained as explicit functions of the above load parameters. Comparison of these results with Monte Carlo studies and with the combined loads provided by load and reduction factors in building codes indicated that depending on the relative magnitudes of the individual load effects, the reduction factor approach may provide conservative or unconservative combined load effects.

References 5.7 and 5.8 describe work by Cornell and others whereby the problem is approached by deriving expressions for the mean upcrossing rate for the sum of two time-varying loads modeled as Poisson square waves and for combinations of processes with intensity variations in each occurrence including triangular, rectangular and house-shaped wave pulses. Der Kiureghian (Refs [illegible] - 5.11) has derived an approximate method for calculating the first two moments of the extreme load effects. The problem of linear, independent stochastic processes for single and multiple cases was addressed by the method of load coincidences and expressions were derived by means of which the lifetime extreme values of combined load effects can be estimated in terms of the lower moments of the individual peak values. These results have been used to evaluate the load factors currently used in nuclear plant design with the result that some inconsistencies in current load factors have been demonstrated.

References (Chapter 5)

5.1 ASCE, Structural Analysis and Design of Nuclear Power Plant Structures, J D Stevenson, Ed, Draft, 1976.

5.2 Wen, Y K, "Statistical Combination of Extreme Loads," Journal of the Structural Division, ASCE, Vol 103, No. ST5, May 1977, pp 1079-1093.

5.3 American National Standards ANSI/ANS-2.12 - 1978, "Guidelines for Combining Natural and External Man-Made Hazards at Power Reactor Sites," New York, July 1978.

5.4 Committee on Safety of Nuclear Structures, "Safety of Nuclear Structures," ASCE Specialty Conference on Probabilistic Mechanics and Structural Reliability, Tucson, January 1979.

5.5 Turkstra, C J, "Theory of Structural Design Decisions," Solid Mechanics Study No. 2, University of Waterloo, Waterloo, Canada, 1972.

5.6 Wen, Y K, "Probability of Extreme Load Combinations," Transactions of the 4th International Symposium on Structural Mechanics in Reactor Technology, San Francisco, 1977, Paper 9/3.

5.7 Larrabee, R D and Cornell, C A, "A Combination Procedure for a Wide Class of Loading Processes," ASCE Specialty Conference on Probabilistic Mechanics and Structural Reliability, Tucson, January 1979, pp 76-80.

5.8 Madsen, H Kilcup, R and Cornell, C A, "Mean Upcrossing Rate for Sums of Pulse-Type Stochastic Load Processes," ASCE Specialty Conference on Probabilistic Mechanics and Structural Reliability, Tucson, January 1979, pp 54-58.

5.9 Der Kiureghian, A, "Probabilistic Load Combination," ASCE Specialty Conference on Probabilistic Mechanics and Structural Reliability, Tucson, January 1979, pp 59-64.

5.10 Der Kiureghian, A, "Reliability Analysis under Combinations of Stochastic Loads," ASCE Specialty Conference on Probabilistic Mechanics and Structural Reliability, Tucson, January 1979, pp 70-75.

5.11 Der Kiureghian, A, "Reliability Based Design under Multiple Load Combinations," Transactions of the 4th International Symposium on Structural Mechanics in Reactor Technology, San Francisco, 1977, Paper M 9/6.

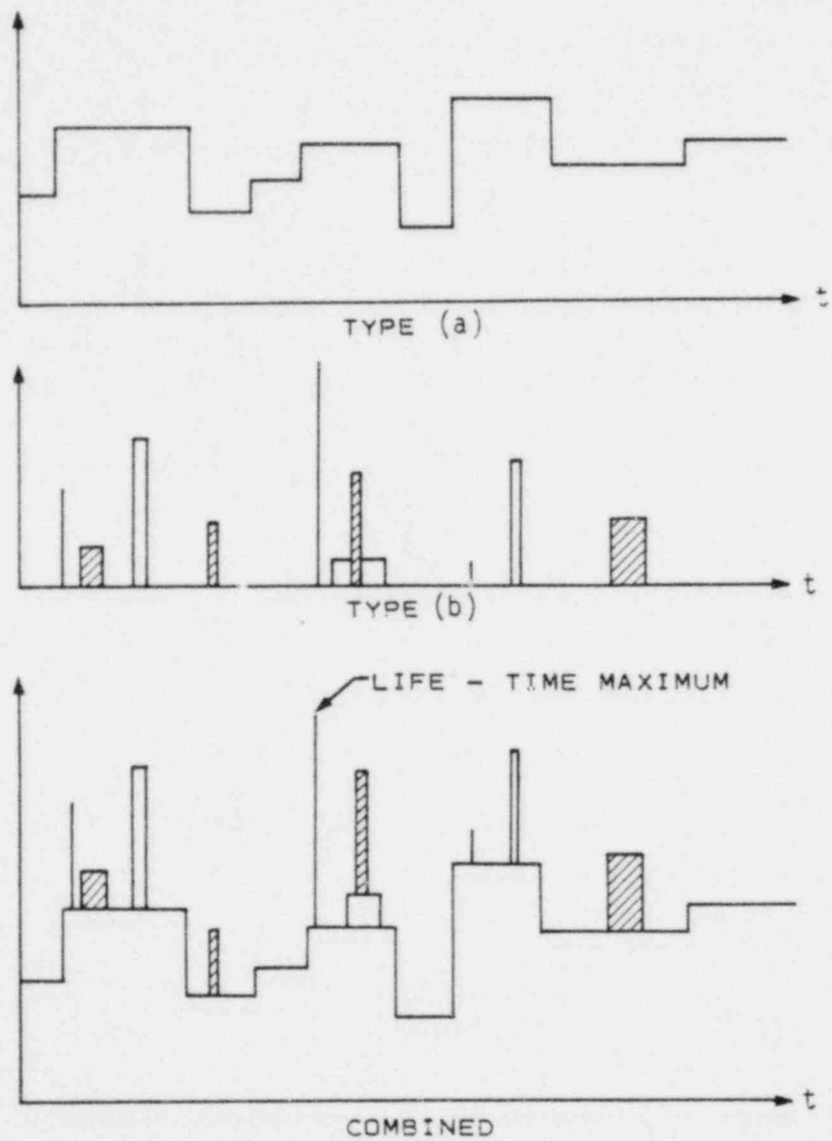

FIGURE 5.1
TEMPORAL VARIABILITY OF LOAD EFFECTS (REF. 5.2)

Chapter 6

Uncertainty in Dynamic Structural Analysis

6.1 General

Virtually every aspect o. analytical efforts to predict the actual in-service respor^e of nuclear power plant structures to a strong motion earthquake is affe ted by uncertainty considerations. Starting with the formulation of the mathematical models, the detailed modeling and preparation of input data and proceeding through the numerical computations and the comparison of calculated and measured response values, the process is subject to variability induced by uncertainty. In recognition of this, conservatism has been introduced into the prescribed analysis and design procedures. The net effect is that present-day seismic analysis and design methods, while generally quite conservative, cannot readily be associated with a quantitative measure of structural safety.

One of the principal objectives of the SSMRP is to develop a probabilistic methodology to explicitly account for the sources of uncertainty in seismic analyses and thereby eventually provide a refined estimate, with associated probability of occurrence, of the actual response of nuclear power plant structures.

The following sections will address the general topic of uncertainty, summarize available quantitative estimates of uncertainty in various aspects of seismic building analysis and finally consider the available methods for estimating structural system behavior from the individual component uncertainties.

6.2 Sources and Types of Uncertainty

Two inherently different types of uncertainty have been identified: (a) Random variability which is associated with statistical variations, eg, the natural heterogeneity in material properties, and (b) Modeling uncertainty which is a systematic type of variability related to the limited availability of information, inherent bias in certain models or predictions, consistent errors or deviations from reality in material and structural testing. A third potential type of variability can be associated with analysis and design errors, construction blunders, etc. In actuality, as will be illustrated below, there are few sources of variability which can be solely attributed to either random variability or modeling uncertainty.

The individual sources of uncertainty will be addressed in three broad categories; (1) Constitutive Properties - Primarily the elastic constants and strength values for steel, concrete and reinforcing bars but also the description of the stress-strain behavior over the entire range for use in nonlinear analyses; (2) Dynamic Structural Characteristics - Includes the mass, stiffness and damping characteristics as well as the calculated natural frequencies and mode shapes, and (3) Other Sources of Uncertainty including modeling techniques, analytical procedures, computer software reliability and effects such as the variation in field construction practices, errors in analysis, design and fabrication, and deterioration of members.

In Table 6.1, each of the individual sources is identified as to the type of uncertainty contributed as compared to "true" response of the structural system. For example, linear dynamic analysis represents a source of modeling uncertainty as compared to the more realistic estimate provided by nonlinear analysis. Nonlinear analysis, while ostensibly providing a more refined estimate, is itself subject to considerable additional uncertainty due to the computational complexity, including the demand upon the analysis to follow a complex physical process, as well as input data requirements which call for realistic constitutive relations for loading and unloading behavior in the inelastic region.

Material properties can certainly be identified as a source of random variability. In addition, however, the concrete quality control requirements lead to average concrete strengths consistently greater than the nominal values and similarly the steel industry practice of referencing a minimum yield point value leads to actual in-structure strength properties which are consistently higher than the nominal values. This type of variability is obviously a modeling or systematic type of uncertainty. The use of static versus dynamic material properties also introduces modeling uncertainty in the material properties for loading cases where the actual dynamic properties are significantly different from the static values. While conservative from a strength standpoint, the use of material constants different from those actually existent in service, will also contribute to observed differences between calculated and observed natural frequencies.

Another example of combined random variability and modeling uncertainty is the damping values which exhibit not only natural variability but also a systematic bias in present-day calculations since the prescribed values are felt to be decidedly less than those experienced in practice, especially at high response levels.

6.3 Quantitative Estimates of Uncertainty

6.3.1 Descriptive Parameters and Data Sources - While test data and pertinent information are available in certain areas it is difficult, if not impossible, to quantify many of the uncertainties affecting seismic analyses. Such difficult areas include the idealization of the structural system, the influence of assumptions underlying all analysis and failure prediction formulas, unknown variations in construction and fabrication, etc. Engineering judgement is and always will be necessary.

The various categories of data sources can be identified (a) Summaries of test data; (b) Limited parametric and sensitivity studies on particular topics; and (c) Subjective estimates by experienced engineers, eg, the estimates provided in References 6.8 and 6.27. While direct observation of component uncertainty is desirable, it is often not achievable in practice. In such cases, the relationship between true mean values and nominal values as well as a measure of the dispersion of values about the mean must be established on the basis of engineering experience and the engineer's feel for the completeness and adequacy of the particular analysis. In this regard, experienced overall judgement is as valuable as particular measurements of component variability.

Ideally each source of variability should be identified with a particular probability distribution function with the associated descriptive parameters. In actuality there is seldom sufficient data or other bases upon which to select the distribution function appropriate for each design parameter. Whereas the available observations can be used to estimate the parameters of a given distribution the number of observations are generally insufficient to establish the validity of the distribution for making predictions which rely upon the detailed characteristics of the distribution tails. In addition, other than for predicting the occurrence of extreme loads, there is seldom sufficient knowledge to select a distribution function on the basis of the physical relevance of the function to the particular parameter. In view of these limitations the following general practices have evolved: (a) The widespread use of the normal distribution function to describe uncertainties in analysis and design calculations, and (b) The development of engineering approaches (first order, second moment reliability methods) which rely on a knowledge of the first and second order (mean and variance) statistical properties only, rather than upon the probability distribution function as a whole. Similarly, analytical methods have been developed to generate probabilistic estimates of linear system performance based on a knowledge of the lower order moments of the contributing source of uncertainty.

6.3.2 Constitutive Properties and Dimensions - In this section, available information on the uncertainty in material constitutive properties and dimensions of concrete, reinforcing bars and structural steel is summarized. This data, as assembled in Table 6.1, considers data from a wide variety of sources and includes both objective and subjective estimates of the uncertainty. Table 6.1 provides the following information: An indication of the type of uncertainty identified with a particular source of uncertainty, ie, random variability (RV) and/or modeling uncertainty (MU); quantitative estimates of the uncertainty including an indication of the mean value, a measure of the dispersion of values about the mean (variance, σ^2,standard deviation, σ,or coefficient of variation, COV) and a recommended probability distribution.

Concrete Properties - A comprehensive review paper on the variability in concrete strength and stiffness-related properties has recently appeared in the literature (Ref 6.32). The paper presents estimates for the variability in properties for normal weight concrete and suggests appropriate distribution functions. Concrete strength variability is primarily attributable to variations in material properties and proportions of the concrete mix, variations in mixing, transporting, placing and curing methods, variation in testing procedures and variations between in-structure concrete and control specimens. The three main sources of this latter variation are the effect of volume, effect of rate of loading and the effect of concrete being in place rather than in cylinders.

Available test data and analyses (eg, Refs 6.1, 6.2, 6.9, 6.10 and 6.25) are considered in detail. The principal results from Ref 6.32 are summarized in Table 6.1. An expression is given for the mean in-place strength of concrete in terms of the design compressive strength. The relationship accounts for the fact that the strength of in-place concrete tends to be somewhat lower than the strength of the same concrete in cylinders. Overall, this reduction is generally offset by the requirement that the average cylinder strength must be greater than the specified strength in order to meet quality control requirements in design codes.

Dispersion estimates are provided in terms of the coefficient of variation for cylinder strength as a function of both the degree of quality control and the strength level. The dispersion in in-place concrete strength is given as a function of the dispersion estimate for cylinder strength. Evidence is also presented which indicates that the dispersion in concrete strength is unaffected by volume effects or rate of loading effects.

Various researchers have proposed alternate distributions to the standard assumption of a normal distribution for concrete strength, eg, Freudenthal's recommendation (Ref 6.42) of a lognormal distribution. It appears, however, that the evidence (Ref 6.44) most strongly supports the adoption of a normal distribution.

For concrete tensile strength an alternate to that presented in the ACI code (Ref 6.45) is developed and relationships are provided for the mean value and variance for both the splitting tensile strength of in-place concrete and the strength of in-place concrete in flexural tension (see Table 6.1). The normal distribution is considered appropriate for concrete tensile strength.

An expression is provided for the mean value and coefficient of variation for the concrete modulus of elasticity in compression and in tension. The expression is compared with the square root relationship from Ref 6.45.

Concrete Dimensions - Another recent paper by Mirza and MacGregor (Ref 6.30) provides an extensive treatment of the variabilities associated with the geometric properties of reinforced concrete member. They are related deviations from the prescribed value of cross-sectional shape and dimensions, the position of reinforcing bar ties and stirrups and imperfections related to the horizontality, verticality, alignment, grades and surfaces of the constructed members. The recommended distribution properties for slabs, beams and columns are shown in Tables 6.2, 6.3 and 6.4. The normal distribution is recommended for describing the statistical distribution of geometric imperfections in concrete members.

Reinforcing Bars - Reference 6.31, also by Mirza and MacGregor is a resent summary and analysis of avaliable data on the variability of properties of reinforcing bars. As indicated, the main source of yield strength variability for reinforcing bars is the variation of the strength of material itself, variations in the area of cross section of the bars, the effect of the rate of loading, the effect of bar diameter on properties of bars and the effect of the strain defined as the yield strain.

Table 6.1 shows the mean values and coefficient of variation for Grade 40 and Grade 60 bars. The development in Reference 6.31 indicates that a beta distribution is appropriate for reinforcing bar strength. The Mirza and MacGregor study provides an estimate of the mean ratio of measures to nominal bar area and the corresponding coefficient of variation. The effects of rate of loading, bar diameter and yield strain are considered in detail.

In terms of ultimate strength the summary results tabulated in Reference 6.31 indicate that the average ultimate strength of steel is about 55 percent more than the yield strength with both the distribution type (beta) and coefficient of variation remaining unchanged.

Results for the modulus of elasticity for reinforcing bars show a mean value of 29,200 ksi, coefficient of variation of 3.3 percent and a normal distribution.

Structural Steel - In the development of criteria for the Load and Resistance Factor Design method for steel buildings, Galambos and Ravindra (Ref 6.16) have provided a comprehensive summary with recommendations, for the statistical variation of the properties of structural steel. Data from a variety of sources was considered including mill test reports, the results of special research projects and experiments on structures and structural components. Estimated values are presented in Table 6.1 for the mean and coefficient of variation for the modulus of elasticity in tension, compression and shear, poisson's ratio, the yield stress in member flanges in webs, and in shear and the strain-hardening modulus. The strength and stiffness properties of structural steel can be treated as being normally distributed.

6.3.3 Dynamic Characteristics - The uncertainty related to the dynamic properties of a structure are most conveniently discussed in terms of (a) the relationship between calculated and measured natural frequencies, and by (b) the relationship between the nature of damping in actual structures and the damping values employed in dynamic analyses.

The calculated natural frequencies are dependent on the adequacy of the mass and stiffness structural modeling. Whereas, relatively speaking, the mass distribution in the structure can be modeled with reasonable accuracy, the stiffness response is a function of the complexity of the structure, the variability in material properties and dimensions and the modeling techniques employed. The accuracy of the mathematical determination of frequencies as compared to the actual structural frequency response is a function of the agreement of the model parameter with the as-built material properties, the choice of the mathematical formulation to describe the response phenomena including soil-structure interaction effects and, as will be discussed in a later section, the subjective process by which the engineer develops a mathematical model from the design drawings. If material or geometric nonlinearity are to be treated, further uncertainties are introduced in terms of the modeling of postyield strength and stiffness characteristics, large displacement P-delta effects and the contribution of nonstructural components in the nonlinear range.

A comprehensive address to the question of uncertainty in frequency response characteristics would entail detailed consideration of data on the accuracy of modeling, data on the variability of mass and stiffness and improved information on the underlying mechanisms relating alterations in input values to response quantities. As discussed in Reference 6.23, various types of studies have been undertaken to develop information in these areas, including, (a) detailed dynamic studies of buildings to evaluate the effects of one or several parameters, (b) the correlation of dynamic models with experimental work considering the influence of modeling assumptions, and (c) the collection and summarizing of natural periods for buildings versus structural properties.

The selection of damping coefficients for use in a particular analysis is an important determinant of the ability of the overall mathematical model to follow the actual energy-absorbing characteristics of the structure. The selection at present is highly dependent upon the consensus of engineering experience since little test data are available to support an accurate assessment of the true damping value on a case-by-case basis. Most tests correspond to small amplitude distortion or component tests and do not necessarily correspond to damping levels in actual structures at large distortions. Considerable attention on this topic is warranted since small changes in damping values have significant effects on calculated responses. In spite of the information which has been collected on the damping characteristics of individual components or structures, a fundamental understanding of damping mechanisms is lacking due to uncertainty regarding the amount of damping provided to the structure by the foundation and underlying soil, the effect of the duration of motion on time-dependent changes in damping, the effect of the previous vibrational history of the structure, the participation of nonstructural elements, the percent critical damping in higher modes and the change in damping at various amplitude levels.

In the remainder of this section available data on the uncertainty in natural frequency and damping values are summarized.

Data on Calculated Versus Measured Natural Periods of Structures - Reference 6.23 contains a comprehensive summary of natural period data for a wide range of structural types ranging from steel buildings with braced frames and moment-resisting frames, reinforced concrete buildings with shear walls and with moment-resisting frames and various types of composite construction. Data are reported for both large and small amplitude motions for various types of dynamic forcing functions. The data include pre, during and postearthquake measurements on the same structure. It should be pointed out that the contribution to the overall variation in measured values which might be assigned to soil-structure interaction effects is implicit in this data.

The difficulty of mathematically modeling the frequency characteristics of structures over the range of response levels is illustrated by the summary

(Figure 6.1) of measured natural periods prior to an earthquake versus the periods observed during an earthquake event. The loss in stiffness due to decreased participation of nonstructural elements, cracking of members or formation of plastic hinges causes a shift in period to larger values. Similarly, Figure 6.2 presents a comparison of pre versus postearthquake measurements for the same set of buildings and shows a general increase in period associated with a permanent loss in stiffness. These results illustrate the obvious need for nonlinear, as opposed to conventional linear, methods of analysis in order to effectively model the real behavior of structures. However, it must be recognized that while providing a more realistic, less conservative estimate of structural behavior, nonlinear analyses also introduce greater uncertainties in the modeling aspect.

Data collected from a variety of sources is shown in summary form in Table 6.1 and Figures 6.3, 6.4 and 6.5 for various structural types and for large and small amplitude vibrations. Mean values of the ratio of observed to computed period values, the coefficient of variation of the ratio values. In all cases, the gamma or lognormal distribution appear to be appropriate distribution functions for these statistical samples. Information of this type, hopefully with increased sample sizes, provide analysts with a statistical data base for studying the level of uncertainty in response calculations as related to structural type, response level, building height and other significant factors. For example, the mean ratio for small amplitude vibrations is 0.845 which indicates that conventional analyses consistently underestimate the actual stiffness available in structures. On the other hand, the mean ratio (1.15) associated with large amplitude vibrations includes the effects of alterations in the structural system which lead to structural performance which is more flexible in service than estimated by conventional calculations. The dispersion or variablility in natural period estimates is quite consistent for both levels of response and for all structural types and materials of construction.

Another source of valuable test data on actual structures is the available literature regarding on-site dynamic testing. For example, Reference 6.54 provides results on calculated vs measured natural frequencies for a nuclear power plant piping system, as shown in Table 6.7. The first two sets of modal frequencies show quite good agreement (within 7 percent) for independently performed calculations with different computer programs. In both cases, however, the measured results differed from the calculated results by up to 50 percent. A re-calculation, with one of the programs, taking into account the as-build condition (actual pipe diameter and wall thickness, revised hanger locations, insulation mass) reduced the difference from measured values to 35 percent. Possible sources of this significant deviation are suggested as modeling errors, the effect of transverse hanger stiffness, contact with other pipes and material uncertainties.

Data on Damping Values - Information on measured and recommended damping values from a variety of sources is summarized in Table 6.1 and Figures 6.6 through 6.17. References 6.4 and 6.28 provide subjective estimates of damping values which were used in probabilistic studies related to nuclear power plant structures. Figure 6.8, 6.9 and 6.10 present data gathered by Blume (Refs 6.47 and 6.48) which provide basic data on the uncertainty in damping values for actual structures. Reference 6.50 contains a summary of damping values for nuclear power plant structures and components as a function of the type and magnitude of excitation. These published and unpublished data were obtained from the recorded response of nuclear power plant structures and field tests. Also shown in Table 6.1 are some subjective estimates on damping uncertainty provided in Reference 6.27.

In addition, Reference 6.23 provides a summary of 244 damping values for 139 buildings, collected from 39 references. The results from this review are summarized in Table 6.1 and some histograms of data for selected cases are shown in Figures 6.11 through 6.17. These results for small and large vibrations of reinforced concrete, steel and composite buildings provide additional statistical data for studying the mechanism of damping. The considerable dispersion in measured damping values is indicated by the range of coefficient of variation values from 42 percent to 76 percent. Other general observations that can be made from these results are: (a) the mean value for each structural type increases from small to large amplitude motion; (b) steel buildings possess consistently less inherent damping than reinforced concrete structures; and (c) the sample distributions are consistently positively skewed and appear to be well represented by gamma and lognormal distributions.

It is interesting to compare these measurements with the values (Table 3.3) currently recommended for use in structural analyses of nuclear power plant structures, eg, References 6.36 and 6.49. In addition, Reference 6.52 contains updated recommendations (Table 6.5) by Newmark which give a range of damping estimates for the various categories of structures. The lower value is essentially a conservative lower bound value while the higher value is an average or above average value. Detailed comparisions are somewhat difficult due to the fact that the tests and the recommendations are not presented on the same basis and to the same degree of detail. For example, in order to attempt this comparison, it is necessary to assume that the small amplitude motion category in the test results corresponds to the recommended value for earthquakes at the OBE level and to the case of "working stress, no more than about 1/2 yield point". Similarly, the results for large amplitude motions are compared to the values recommended for SSE calculations and to the case of stresses "at or just below the yield point". In terms of structural types, the recommendations for steel structures are presented for both welded and bolted construction whereas the test results are given for the general category of steel structures.

For reinforced concrete structures, the average measured value of 4.26 percent at small amplitude compares favorably with the presently recommended OBE value of 4 percent and corresponds to the upper end of the working stress case for reinforced concrete with considerable cracking. The large amplitude value (6.63 percent) corresponds to the presently recommended SSE value but is at the lower end of the range recommended for reinforced concrete near yield (Ref 6.52).

For steel structures, the measured average value at low amplitude (1.68 percent) compares with the recommended OBE value of 2 percent for welded structures and is therefore at the lower end of the range recommended by Newmark (Ref 6.52). In all cases, the values recommended for bolted structures are considerably greater than the average measured value. As indicated above, since the number of bolted versus welded structures in the test sample is unknown, this may not be a fair comparison. At the higher stress levels, the average measured damping percentage (5.65 percent) is greater than the presently recommended SSE value for welded structures and is in the middle of the range recommended in Reference 6.52. The SSE values presently recommended for bolted structures (7 percent) and the proposed range of values (10 - 15 percent) are considerably greater than the measured average value for steel structures (5.65 percent).

As indicated previously, on-site dynamic testing programs provide some significant data on actual structural characteristics including damping values. Table 6.8, from Reference 6.54, is a compilation of experimental data on damping values for pressure vessel system components. These results indicate that applicable regulatory values are significantly lower, in virtually all cases, than measured damping values.

In order to derive maximum benefit from the comparison of such results, sufficient information must be available to relate all values to a common basis in terms of structural type, method of framing, connections, stress level, previous history of motion, load characteristics including method of application in tests, foundation type, soil effects, etc.

In summary these results, while helpful, provide little more than a starting point for the fundamental studies which are needed to develop realistic representations of the energy-absorbing characteristics of actual structures.

6.3.4 Other Sources of Uncertainty - The areas considered under this general heading include uncertainty directly attributable to the modeling techniques and options exercised by the engineering analyst, software uncertainty, uncertainty introduced by design and construction errors and field procedures.

As addressed in the previous sections, the uncertainty in modeling dynamic behavior involves the material properties and geometry of the structure, the mathematical formulation employed to describe the response phenomenon and - the present topic of interest - the subjective choices made by the engineer in developing the mathematical or computer model from a set of drawings. This contribution to the overall uncertainty is quite difficult to quantify since there is not just one set of "correct" input data corresponding to any given seismic analysis problem. The available input options and modeling techniques indicate that a wide range of "correct" solutions exist. However, depending upon the analyst's ability and upon the complexity of the structure being analyzed, the spread in these various solutions will be more or less spread about the as-measured response (which is itself subject to measurement uncertainties). Examples of the options available to the analyst include the choice of the numerical procedure for integration, the integration time step, modeling detail, the means of representing the mass distribution and stiffness characteristics and the manner in which the contribution of the nonstructural elements is included in the overall structural model. In recognition of the inability of mathematical analysis, by itself, to completely duplicate such complex physical behavior, procedures have evolved whereby low level, forced vibration tests on the actual structure and system identification techniques (Refs 6.22 and 6.53) are employed to upgrade the analytical model and enhance its ability to reproduce the dynamic characteristics of a given structural system.

There have been few attempts to quantify the contribution of modeling variability to overall uncertainty. One possible approach entails the performance of parametric studies to define the parameters which have a significant impact on the variation in output values. A logical extension of such an approach is the performance of systematic calculations in a probabilistic format such as the Monte Carlo study described in Reference 6.39. This analysis of of a BWR reactor building model employed a number of different types of input probability distributions to study the simultaneous effect of any uncertainties in the seismic analysis. The results indicate that the effect of parameter uncertainty is to reduce peak responses and to broaden the region over which this reduced maximum response occurs.

A different type of study into variability induced by structural modeling is described in Reference 6.18. In this study, a direct experiment was conducted with different groups of analysts. The groups were provided with the same basic design information regarding a structure and were asked to perform a dynamic analysis. This experiment was repeated for two different structural configurations (a shear wall box-type structure and a seven-story rigid frame steel structure). In the latter case, the dynamic properties were also obtained by using the parameter identification procedure in conjunction with the results of dynamic tests. The results of this study and other similar observations are presented in Figure 6.18 as a tentative probabilistic model for engineering judgement in structural modeling. Different situations ranging from the analysis of a simple structure by an experienced analyst to the analysis of a complex structural system by an inexperienced analyst, are presented. As indicated in Figure 6.18 and Table 6.1, the uncertainty introduced by judgement is indicated by coefficients of variation ranging from 2.5 percent to 30 percent. Some subjective estimates of modeling and other related uncertainties are provided in Table 6.1.

A factor which should be considered in terms of its influence on the overall reliability is the degree of correlation among the random parameters, eg, the correlation between frequency and damping, expressed in terms of a correlation coefficient which varies from zero for uncorrelated variables to ± 1 for variables which are fully correlated. In general, explicit data on the correlation of variables is lacking and engineering judgement must be employed if account is to be taken of any correlation. In general, however, zero correlation among the variables is usually assumed.

In recent years, increased attention has also been paid to the influence of software reliability. As both program complexity and reliance on computer-produced solutions have tended to develop simultaneously, a distinct need exists for tests for program verification and operational accuracy through comparison with independent analyses, closed-form solutions and test results.

In Reference 6.24, the subject of design errors and other forms of system degradation is studied and an approach is outlined for including such errors in probability estimates. An estimate of the possible number and influence of seismic-related design errors was obtained by examining the historical record of such errors for a specific reactor and assuming that, with inclusion of a factor to represent a learning curve, the record will be representative of other reactors.

Other contributing factors to the overall uncertainty involved in comparison of calculated and measured values include the quality of workmanship which is related to the amount and quality of checking of the design work and the quality of inspection during construction; variation in field practice (quality of the work force, placing and curing practices, etc; differences between test specimen results and in-structure material properties; and basic statistical uncertainty associated with making extrapolations and distributional assumptions based upon the unacceptably small sample sizes which are customarily encountered in the data related to variability in the structural analysis area.

6.4 Probabilistic Estimates of System Behavior

This section considers available methods for determining probabilistic estimates of overall structural system behavior based upon quantitative estimates of the contributing sources of uncertainty, as discussed previously. The SSMRP calls for a computationally efficient method which is compatible with the available data and sufficiently general in application.

Perhaps the most flexible method is Monte Carlo simulation which consists of numerical experiments in which a large number of trial structures are formed and subjected to varying loads. Loading and structural parameters are randomly chosen for each trial consistent with the individual frequency distributions. A distinct advantage of this method is its general applicability, eg, Monte Carlo trials can be performed on nonlinear structures subjected to dynamic loads. A drawback of the method is the large number of trials necessary to achieve high confidence in failure probability estimates. Extensions of the standard Monte Carlo method are available to reduce the total number of trials required. An example is the selective sampling technique, described in Reference 6.40, which yields the maximum amount of information in a chosen region of interest for a minimum number of simulations. Another possible means of reducing the amount of Monte Carlo calculations is the use of reanalysis techniques as described in References 6.26, 6.29 and 6.35. Such techniques involve the development of efficient computational algorithms to minimize the effort required for the reanalysis of structural systems subjected to variations in local geometry, dimensions or material properties. The method involves treatment of the modification only and avoids the complete reformulation of the problem and should, therefore, also be useful for performing sensitivity analyses of structures, ie, for determining the degree to which an individual model parameter influences the dynamic response of the structure.

Numerous applications of the Monte Carlo method appear in the literature (eg, Refs 6.3, 6.39 and 6.40). Reference 6.3 and associated studies have considered the influence of nonlinear moment-curvative relationships on the reliability of some simple structural systems. Depending upon the failure criterion employed, the results indicate not only a reduction in the mean failure load and a reduction in the variability in failure loads but also a transformation in the governing distribution function for the input variables to that corresponding to the output values. Other pertinent analyses include the following:

- A Monte Carlo study (Ref 6.4) of the probability of cracks in the shear wall of a BWR reactor building considering the variability in material properties, system damping, input seismic motion and the idealization of the physical structure to generate the mathematical model.

- A Monte Carlo analysis (Ref 6.13) of the effect of material and geometric variations on the dynamic response of a nuclear power plant turbine-generator pedestal.

- A study (Ref 6.28) of uncertainty in the generation of floor response spectra by analyzing a typical reactor building complex and assuming probability distributions for the various input values. The spectra derived by the Monte Carlo calculations were compared with the design floor response spectra developed by the peak broadening technique.

Since Monte Carlo simulation in either the time or frequency domain necessitates a considerable volume of calculations in order to achieve high confidence levels in the results, alternate methods of performing system reliability calculations come into consideration. Prominent among these are moment-estimating techniques (eg, Refs 6.21 and 6.40) which utilize probability theory to determine the first and second order statistical moments of the dynamic response parameters in terms of the statitical moments of the input structural parameters. In Reference 6.21, equations for the mean and second order statistics of the natural frequency and mode shapes are derived in terms of mean and second order statistics for the contributing parameters by utilizing a multifunction Taylor series expansion to express the natural frequencies in series form. Such approaches may suffer somewhat from a lack of general applicability, eg, its limitation to linear systems.

Examples of other approaches to predicting system performance, as employed on related topics, are the following:

- Study of the generation of floor response spectra for Category I applications by employing the method of generating system moments (Ref 6.5) and by the use of the extreme value theorem (Ref 6.6).

- An extended reliability study of seismic response of PWR containment (Ref 6.14).

- Analysis of the effect of the probabilistic distribution of soil-structure parameters (Ref 6.19) and the probability distribution of structural stiffness (Ref 6.17) on the probability distribution of natural frequencies.

REFERENCES (CHAPTER 6)

6.1 Allen, D E, "Probabilistic Study of Reinforced Concrete in Bending," Technical Paper No. 311, Division of Building Research, National Research Council of Canada, Ottawa, January 1970.

6.2 Ang, A H-S, and Cornell, C A, "Reliability Bases of Structural Safety and Design," Journal of the Structural Division, ASCE, Vol 100, ST9, Sept 1974, pp 1755-1769.

6.3 Borges, J F and Butler, D J, "Computer Experiments Concerning Random Nonlinear Structural Behavior," Final Report, On Concepts of Safety of Structures and Methods of Design, IABSE Symposium, London, 1969, pp 201-209.

6.4 Chelapati, C V and Wall, I B, "Probabilistic Assessment of Seismic Risk for Nuclear Power Plants," Preprints, 2nd International Conference on Structural Mechanics in Reactor Technology, Berlin, 1973, Vol 4, Paper K1/3, 16.

6.5 Chen, P C, "Floor Response Spectra of Buildings with Uncertain Structural Properties," Proceedings US National Conference on Earthquake Engineering, Ann Arbor, June 1975, pp 519-528.

6.6 Chen, P C and Chen, J H, "The Use of Extreme Value Theorem in Generating Floor Response Spectra," Specialty Conference on Probabilistic Mechanics and Structural Reliability, Tucson, January 1979, pp 35-38.

6.7 Costello, J F and Chu, K, "Failure Probabilities of Reinforced Concrete Beams," Journal of the Structural Divison, ASCE, Vol 95, ST10, Oct 1969, pp 2281-2305.

6.8 Dowdy, R W, "Structural Integrity Assessment for the Safeguard Ground Facilities Program - Non-EMP," Final Report, Department of the Army, Huntsville Divison, Corps of Engineers, March 1975.

6.9 Ellingwood, B R and Ang, A H-S, "Risk-Based Evaluation of Design Criteria," Journal of the Structural Division, ASCE, Vol 100, ST9, Sept 1974, pp 1771-1788.

6.10 Ellingwood, B, "Reliability Bases of Load and Resistance Factors for Reinforced Concrete Design," NBS Building Science Series 110, Washington, DC, 1978.

6.11 Ellingwood, B, "Reliability of Current Reinforced Concrete Designs," Journal of the Structural Division, ASCE, Vol 105, ST4, Apr 1979, pp 699-712.

6.12 Ellingwood, B, "Reliability Based Criteria for Reinforced Concrete Design," Journal of the Structural Division, ASCE, Vol 105, ST4, Apr 1979, pp 713-727.

6.13 Ellyin, F and Chandrasekhar, P, "Probabilistic Dynamic Response of Beams and Frames," Journal of the Engineering Mechanics Division, ASCE, Vol 103, EM3, June 1977, pp 411-421.

6.14 Fardis, M N, Cornell, C A and Meyer, J E, "Accident and Seismic Containment Reliability," Journal of the Structural Divison, ASCE, Vol 105, ST1, Jan 1979, pp 67-83.

6.15 Galambos, T V and Ravindra, M K, "Tentative Load and Resistance Factor Design Criteria for Steel Buildings," Strucutral Division Research Rept No. 18, Wash. Univ, St Louis, Mo, Sept 1973.

6.16 Galambos, T V and Ravindra, M K, "Properties of Steel for Use in FRFD," Journal of the Structural Division, ASCE, Vol 104, ST9, Sept 1978, pp 1459-1468.

6.17 Hadjian, A H and Hamilton, C W, "Probabilistic Frequency Variations of Concrete Structures," Preprints, 2nd International Conference on Structural Mechanics in Reactor Technology, Berlin, 1973, Vol 4, Paper K3/5, 12.

6.18 Hadjian A H, et al, "Variability in Engineering Aspects of Structural Modeling," 5th World Conference on Earthquake Engineering, International Assn for Earthquake Engineering, Rome, June 1973, pp 9-31 to 9-36.

6.19 Hamilton, C W and Hadjian, A H, "Probabilistic Frequency Variations of Structure-Soil Systems," Nuclear Engineering and Design, Vol 38, 1976, pp 303-322.

6.20 Hasselman, T K and Hart, Gary C, "Modal Analysis of Random Structural Systems, Journal of the Engineering Mechanics Division, ASCE, Vol 98, EM3, June 1972, pp 561-579.

6.21 Hart, Gary C, "Eigenvalue Uncertainty in Stressed Structures," Journal of the Engineering Mechanics Division, ASCE, Vol 99, No. EM3, June 1973, pp 481-493.

6.22 Hart, Gary C and Yao, James T P, "System Identification in Structural Dynamics," Journal of the Engineering Mechanics Division, ASCE, Vol 103, EM6, December 1977, pp 1089-1103.

6.23 Haviland, R, "A Study of the Uncertainities in the Fundamental Translational Periods and Damping Values for Real Buidlings," Report No. 5 on the "Evaluation of Seismic Safety of Buildings," Civil Engineering Dept, MIT, February 1976.

6.24 Hsieh, T M and Okrent, D, "On Design Errors and System Degradation in Seismic Safety," Transactions of the 4th International Conference on Structural Mechanics in Reactor Technology, Brussels, 1977, Vol K(b), Paper K9/4.

6.25 Julian, O G, "Synopsis of First Progress Report of Committee on Factors of Safety," Journal of the Structural Division, ASCE, Vol 83, ST4, July 1957, pp 1316-1-1316-22.

6.26 Kavlie, D and Powell, G H, "Efficient Reanalysis of Modified Structures," Journal of the Structural Divison, ASCE, Vol 97, ST1, January 1971, pp 377-392.

6.27 Kennedy, R P, "Overview of Uncertainites and Conservatism in the Seismic Design of Nuclear Facilities," ASCE National Convention, Boston, Mass., April 2-3, 1979.

6.28 Liu, L K, Child, C L and Nowotny, B, "The Effects of Parameter Variations on Floor Response Spectra," Specialty Conference on Structural Design of Nuclear Power Plant Facilities, Chicago, 1973.

6.29 Melosh, R J and Luik, R, "Multiple Configuration Analysis of Structures," Journal of the Structural Division, ASCE, Vol 94, ST11, November 1968, pp 2581-2596.

6.30 Mirza, S A and Mac Gregor, J G, "Variations in Dimensions of Reinforced Concrete Members," Journal of the Structural Divison, ASCE, Vol 105, ST4, April 1979, pp 751-766.

6.31 Mirza, S A and Mac Gregor, J G, "Variability of Mechanical Properties of Reinforcing Bars," Journal of the Structural Division, ASCE, Vol 105, ST5, May 1979, pp 921-937.

6.32 Mirza, S A, Hatzinikolas, M and Mac Gregor, J G, "Statistical Description of Strength of Concrete," Journal of the Structural Divison, ASCE, Vol 105, ST6, June 1979, pp 1021-1037.

6.33 Moses, F and Kinser, D E, "Analysis of Structural Reliability," Journal of the Structrual Division, ASCE, Vol 93, ST5, October 1967, pp 147-164.

6.34 Ravindra, M K and Galambos, T V, "Load and Resistance Factor Design for Steel," Journal of the Structural Division, ASCE, Vol 104, Sept 1978, pp 1337-1353.

6.35 Reese, R T and Kostem, C N, "A Method to Determine the Sensitivity of Mathematical Models in Deterministic Structural Dynamics," Fritz Engineering Laboratory Report No. 400.9, Lehigh University, February 1973.

6.36 Regulatory Guide No. 1.61, US Atomic Energy Commission, Government Printing Office, Washington, DC, 1973.

6.37 Sharpe, R L et al, "Behavior of Structural Systems under Dynamic Loads," Building Practices for Disaster Mitigation, Building Science Series 146, National Bureau of Standards, Feb 1973, pp 352-394.

6.38 Smith, P D, et al, "Seismic Safety Margins Research Program - Program Plan," UCID-17824, Lawrence Livermore Laboratory, Livemore, Calif, Aug 1978.

6.39 Tagart, S W and Torres, M R, "Seismic Analysis of Nuclear Components Considering Modeling Uncertainties," Preprints 5th World Conference on Earthquake Engineering, International Assn for Earthquake Engineering, Rome, June 1973, pp 2462-2464.

6.40 Warner, R F and Kabaila, A P, "Monte Carlo Study of Structural Safety," Journal of the Structural Division, ASCE, Vol 94, ST12, December 1968, pp 2847-2859.

6.41 Committe on Safety of Nuclear Structures, "Safety of Nuclear Structures," ASCE Specialty Conference on Probabilistic Mechanics and Structural Reliability, Tucson, January 1979.

6.42 Freudenthal, A M, "Safety and the Probability of Structural Failure," Transaction, ASCE, Vol 121, Paper No. 2843, 1956, pp 1337-75.

6.43 Mac Gregor, J G, "Safety and Limit States Design for Reinforced Concrete," Canadian Journal of Civil Engineering, Vol 3, No. 4, Dec 1976, pp 484-513.

6.44 Rüsch, H, Sell, R and Rackwitz, R, "Statistical Analysis of Concrete Strength," Deutscher Ausschuss für Stahlbeton, Heft 206, Berlin, 1969 (in German).

6.45 "Building Code Requirements for Reinforced Concrete (ACI 318-77)," ACI Standard 318-77, ACI Committee 318, American Concrete Institute, Detroit, 1977.

6.46 Collins, J D and Thomson, W T, "The Eigenvalue Problem for Structural Systems with Statistical Properties," American Institute of Aeronautic and Astronautics Journal, Vol 7, No. 4, Apr 1969, pp 642-648.

6.47 Blume, J A, "The Motion and Damping of Buildings Relative to Seismic Response Spectra, Vol 60, Bulletin of the Seismological Society of America, No. 1, Feb 1970, pp 231-259.

6.48 Scholl, R E, ed, "Effects Prediction Guidelines for Structures Subjected to Ground Motion," JAB-99-115, URS/John A Blume and Associates, Engineers, San Francisco, July 1975.

6.49 Newmark, N M, Blume, J A, and Kapur, K K, "Design Response Spectra for Nuclear Power Plants," ASCE Structural Engineering Meeting, San Francisco, April 1973.

6.50 Morrone, A, "Damping Values of Nuclear Power Plant Components," Nuclear Engineering and Design, Vol 26, 1974 (condensed from Westinghouse Report WCAP-7921, November 1972).

6.51 Shooman, M L, "Software Reliability; Management and Models," Proceedings, 1975 Annual Reliability and Maintainability Symposium, Washington, DC, June 1975, pp 485-491.

6.52 Newmark, N M, "Inelastic Design of Nuclear Reactor Structures and Its Implications on Design of Critical Equipment," Transactions of the 4th International Symposium on Structural Mechanics in Reactor Technology, San Francisco, 1977, Vol K(a), Paper K 4/1.

6.53 Gersch, W, Nielsen, N and Akaike, H, "Maximum Likelihood Estimation of Structural Parameters from Random Vibration Data," Journal of Sound and Vibration 31(3), 1973, pp 295-308. Also, Gersch, W, "On the Achievable Accuracy of Structural System Parameter Estimates," Journal of Sound and Vibration, 34(1), 1974, pp 63-79.

6.54 Ibanez, P, "Review of Analytical and Experimental Techniques for Improving Structural Dynamic Models," Welding Research Council, Bulletin 249, June 1979.

TABLE 6.1

SUMMARY OF ESTIMATED UNCERTAINTIES

Source of Uncertainty	Type	Uncertainty Estimate	Reference
<u>CONSTITUTIVE PROPERTIES</u>			
<u>CONCRETE</u>			
COMPRESSIVE STRENGTH	RV^1, MU^2	• MEAN, IN-PLACE STRENGTH $\bar{f}_{str} = 0.675\ f'_c + 1100 \leq 1.15 f'_c$ f'_c = DESIGN COMPRESSIVE STRENGTH	6.32
		• DISPERSION CYLINDER STRENGTH FOR $f'_c < 4000$ psi cov = 10% EXCELLENT QC cov = 15% AVERAGE QC cov = 20% POOR QC FOR $f'_c > 4000$ psi σ = 400 psi EXCELLENT QC σ = 600 psi AVERAGE QC σ = 800 psi POOR QC	6.32
		IN-PLACE STRENGTH $V^2_{str} = V^2_{cyl} + 0.0084$ WHERE V = cov • DISTRIBUTION FUNCTION-NORMAL FOR BOTH CYLINDER STRENGTH AND IN-PLACE STRENGTH	6.32
TENSILE STRENGTH	RV, MU	SPLITTING TENSILE STRENGTH (IN-PLACE) • MEAN $\bar{f}_r = 6.4 \bar{f}_{35}^{1/2} \left[0.96(1+0.11)(\log R)\right]$ $\bar{f}_{35}$ = STRENGTH AT R=35psi/sec R= LOADING RATE • DISPERSION $V_R^2 = \frac{V^2_{cyl}}{4} + 0.0190 \geq V^2_{str}$	6.32

RV DENOTES RANDOM VARIABLE

MU DENOTES MODELING UNCERTAINITY

TABLE 6.1 (CONT'D)

SUMMARY OF ESTIMATED UNCERTAINTIES

Source of Uncertainty	Type	Uncertainty Estimate	Reference
		FLEXURAL TENSION STRENGTH (IN-PLACE) • MEAN $\overline{f}_R = 8.3\overline{f}^{\frac{1}{2}}_{35}\left[0.96(1+0.11)(\log R)\right]$ • DISPERSION $V_R^2 = \frac{V^2_{cyl}}{4} + 0.0421 \geq V^2_{str}$ • DISTRIBUTION FUNCTION- NORMAL FOR BOTH SPLITTING TENSILE STRENGTH AND FLEXURAL TENSION	6.32
MODULUS OF ELASTICITY	RV,MU	MODULUS IN COMPRESSION AND TENSION • MEAN- $\overline{E} = 60400\ \overline{f}^{\frac{1}{2}}_{str35}\ (1.16-.08\log t)$ t= LOADING DURATION (SEC) • DISPERSION $V^2 = V^2_{cyl/4} + 0.0085$ • DISTRIBUTION FUNCTION: NORMAL	6.32
CONCRETE MEMBER DIMENSION	RV,MU	SEE TABLES 2,3 AND 4	6.30
<u>CONCRETE REINFORCING BARS</u>			
YIELD STRENGTH	RV,MU	• GRADE 40 BARS MEAN f_y = 48.8 ksi cov= 10.7% • GRADE 60 BARS MEAN f_y = 71 ksi cov = 9.3% • DISTRIBUTION FUNCTION- BETA DISTRIBUTION	6.31

TABLE 6.1 (CONT'D)

SUMMARY OF ESTIMATED UNCERTAINTIES

Source of Uncertainty	Type	Uncertainty Estimate	Reference
AREA	RV,MU	MEASURED TO NOMINAL AREA LOWER LIMIT 0.94 MEAN VALUE = 0.99 cov = 2.4% NORMAL DISTRIBUTION	6.31
ULTIMATE STRENGTH	RV,MU	ULTIMATE STRENGTH = 1.55 f_y cov = SAME AS FOR YIELD STRENGTH BETA DISTRIBUTION	6.31
MODULUS OF ELASTICITY	RV,MU	MEAN VALUE = 29200 ksi cov = 3.3% NORMAL DISTRIBUTION	6.31
STRUCTURAL STEEL			
YIELD STRESS	RV,MU	• FLANGES MEAN = 1.05 F_y F_y = SPECIFIED TENSILE YIELD STRESS cov = 10% • WEBS MEAN = 1.10 F_y cov = 11% • SHEAR MEAN = 0.64 F_y cov = 10% DISTRIBUTION FUNCTION: NORMAL	6.16
POISSON'S RATIO	RV,MU	MEAN = 0.30 cov = 3%	6.16
MODULUS OF ELASTICITY	RV,MU	• TENSION,COMPRESSION MEAN = 29000 ksi cov = 6%	6.16

TABLE 6.1 (CONT'D)

SUMMARY OF ESTIMATED UNCERTAINTIES

Source of Uncertainty	Type	Uncertainty Estimate	Reference
		• SHEAR MEAN = 11200 ksi cov = 6% • STRAIN-HARDENING MODULUS MEAN = 600 ksi cov = 25% DISTRIBUTION FUNCTION: NORMAL	
DYNAMIC CHARACTERISTICS			
NATURAL PERIOD	RV,MU	ALL BUILDING TYPES (STEEL,RC & COMPOSITE) • RATIO OF OBSERVED/COMPUTED PERIOD SMALL AMPLITUDE VIBRATIONS MEAN RATIO = 0.845 cov = 31.1% LARGE AMPLITDE VIBRATIONS MEAN RATIO = 1.15 cov = 30% DISTRIBUTION FUNCTION (BOTH CASES) LOG NORMAL, GAMMA	6.23
DAMPING	RV,MU	• REINFORCED CONCRETE BUILDINGS SMALL VIBRATIONS (AMPLITUDE) MEAN = 4.26% cov = 76% LARGE VIBRATIONS (AMPLITUDE) MEAN = 6.63% cov = 64%	6.23
		• STEEL BUILDINGS SMALL AMPLITUDE VIBRATIONS MEAN = 1.68% cov = 65% LARGE AMPLITUDE VIBRATIONS MEAN = 5.65% cov = 45% DISTRIBUTION FUNCTION (BOTH CASES) LOG-NORMAL, GAMMA	6.23
		• COMPOSITE BUILDINGS SMALL AMPLITUDE VIBRATIONS MEAN = 2.72% cov = 42%	6.23

TABLE 6.1 (CONT'D)

SUMMARY OF ESTIMATED UNCERTAINTIES

Source of Uncertainty	Type	Uncertainty Estimate	Reference
DAMPING (CONTINUED)	RV,MU	LARGE AMPLITUDE VIBRATIONS MEAN = 3.23% cov = 54% DISTRIBUTION FUNCTION LOG-NORMAL, GAMMA	
	RV,MU	REACTOR BUILDING COMPLEX (SUBJECTIVE ESTIMATE) • CONCRETE MEAN = 5% RANGE= 3% to 15% DISTRIBUTION: UNIFORM • STEEL MEAN = 2%, RANGE 0.05% - 4%	6.28
	RV,MU	• REINFORCED-CONCRETE CONTAINMENT (SUBJECTIVE ESTIMATE) MEAN = 5% RANGE = 2% to 10% DISTRIBUTION: FIGURE 6.6	6.4
	RV,MU	• REINFORCED CONCRETE BU[illegible]G MEAN = 5.4% RANGE = 1% to 11%	6.47
		• VARIOUS BUILDINGS, LOW AMPLITUDE MEAN = 3.1% RANGE = 0% to 13%	6.48
		• HIGH RISE BUILDINGS SHEAR WALL TYPE, MEAN = 2.34% FRAME TYPE, MEAN = 3.48%	6.48
		CONSERVATISM IN NOMINAL VS ACTUAL DAMPING VALUES = 20-40% cov = 20%	6.27
<u>STRUCTURAL MODELING</u>			
MODELING	RV,MU	• SIMPLE STRUCTURE EXPERIENCED ENGR: cov =2.5% INEXPERIENCED ENGR: cov = 5% • COMPLEX STRUCTURE EXPERIENCED ENGR: cov = 10% INEXPERIENCED ENGR:cov = 30%	6.18
	RV,MU	SUBJECTIVE ESTIMATE cov= 15%	6.27
	RV,MU	SUBJECTIVE ESTIMATE RANGE OF UNCERTAINTY = ± 20%	6.8

TABLE 6.1 (CONT'D)

SUMMARY OF ESTIMATED UNCERTAINTIES

Source of Uncertainty	Type	Uncertainty Estimate	Reference
MASS PROPERTIES	RV,MU	SUBJECTIVE ESTIMATE RANGE OF UNCERTAINTY = ±10%	6.8
NUMERICAL ACCURACY	MU	SUBJECTIVE ESTIMATE RANGE OF UNCERTAINTY = ±5%	6.8

TABLE 6.2

Recommended Distribution Properties of Slab Dimensions, in inches

Dimension description (1)	In-Situ Slabs Nominal range (2)	Mean deviation from nominal (3)	Standard deviation (4)	Precast Slabs Nominal range (5)	Mean deviation from nominal (6)	Standard deviation (7)
Thickness	4-9	+1/32	15/32	6-9	0	3/16
Effective depth concrete cover						
Top reinforcement	4-8	-3/4	5/8	4-8	0	3/32
		+25/32	25/32		0	7/32
Bottom reinforcement	4-8	-5/16	5/8	4-8	0	3/32
		+11/32	13/32		0	7/32

Note: All distributions are assumed to be normal. For concrete cover, the lower tail should be truncated at zero. 1 in. = 25.4 mm.

TABLE 6.3

Recommended Distribution Properties of Beam Dimensions, in inches

Dimension description (1)	In-Situ Slabs Nominal range (2)	Mean deviation from nominal (3)	Standard deviation (4)	Precast Slabs Nominal range (5)	Mean deviation from nominal (6)	Standard deviation (7)
Width						
Rib	11-12	+3/32	3/16	14	0	3/16
Flange	—	—	—	19-24	+5/32	1/4
Overall Depth	18-27	-1/8	1/4	21-39	+1/8	5/32
Concrete cover, effective depth						
Top reinforcement	1-1/2	+1/8	5/8	2-2 1/2	0	5/16
		-1/4	11/16		+1/8	11/32
Bottom reinforcement	3/4-1	+1/16	7/16	3/4	0	5/16
		-3/16	1/2		+1/8	11/32
Beam spacing and span	—	0	11/16		0	11/32

Note: All distributions assumed to be normal. For concrete cover of main reinforcement, a normal distribution with the lower tail truncated at one stirrup diameter should be used. 1 in. = 25.4 mm.

TABLE 6.4

Recommended Distribution Properties of Column Dimensions, in inches

Dimension description (1)	In-Situ Columms Nominal range (in inches) (2)	Mean deviation from nominal (in inches) (3)	Standard deviation (in inches) (4)	Precast Columns Nominal (in inches) (5)	Mean deviation from nominal (in inches) (6)	Standard deviation (in inches) (7)
Rectangular column: width, thickness	11-30	+1/16	1/4	7-16	+1/32	1/8
Circular column: diameter	11-13	0	3/16	11-13	0	3/32

Note: All distributions assumed to be normal. 1 in. = 25.4 mm.

TABLE 6.5

RECOMMENDED DAMPING VALUES

STRESS LEVEL COMBINED	TYPE AND CONDITION OF STRUCTURE	PERCENTAGE CRITICAL DAMPING
Working stress, no more than about ½ yield point	a. Vital piping	1 to 2
	b. Welded steel, prestressed concrete, well reinforced concrete (only slight cracking)	2 to 3
	c. Reinforced concrete with considerable cracking	3 to 5
	d. Bolted and/or riveted steel, wood structures with nailed or bolted joints	5 to 7
At or just below yield point	a. Vital piping	2 to 3
	b. Welded steel, prestressed concrete (without complete loss in prestress)	5 to 7
	c. Prestressed concrete with no prestress left	7 to 10
	d. Reinforced concrete	7 to 10
	e. Bolted and/or riveted steel, wood structures, with bolted joints	10 to 15
	f. Wood structures with nailed joints	15 to 20

TABLE 6.6

RECOMMENDED VERSUS MEASURED DAMPING VALUES

STRESS LEVEL	STRUCTURAL TYPE	PERCENTAGE- CRITICAL DAMPING: RECOMMENDED VALUE REF.6.49 & R.G. 1.61	PERCENTAGE- CRITICAL DAMPING: RECOMMENDED RANGE REF.6.52	PERCENTAGE- CRITICAL DAMPING: MEASURED AVERAGE VALUE REF. 6.23
SPECIFIED LEVEL VARIES, I.E.: 'WORKING STRESS" IN REF. 6.52; "OBE" IN REF. 6.49 AND R.G. .61.; AND "SMALL PLITUDE VIBRATION" IN REF. 6.23	Welded Steel	2	2-3	
	Bolted Steel	4	5-7	
	Steel			1.68
	Reinforced Concrete	4		4.26
	R.C.(Slight Cracking)		2-3	
	R.C.(Considerable Cracking)		3-5	
SPECIFIED LEVEL VARIES, I.E.: T OR JUST BELOW ELD" IN REF. 6.52; SSE" IN REF. 6.49 ND R.G. 1.61;AND LARGE AMPLITUDE VIBRATION" IN REF. 6.23	Welded Steel	4	5-7	
	Bolted Steel	7	10-15	
	Steel			5.65
	Reinforced Concrete	7	7-10	6.63

TABLE 6.7
THEORETICAL VERSUS EXPERIMENTAL RESONANT FREQUENCIES OF A NUCLEAR PLANT PIPING SYSTEM

MODE NUMBER	SAP-IV a priori	PIPESD a priori	MEASURED	SAP-IV a posteriori STIFFNESS AND MASS CHANGE
1	1.40	1.31	2.16	1.53
2	1.82	1.75	2.58	1.90
3	2.23	2.24	2.77	2.43
4	2.73	2.81	3.25	2.92
5	2.94	2.91	3.50	3.34

TABLE 6.8

MEASURED VERSUS REGULATORY DAMPING VALUES
FOR PRESSURE VESSEL SYSTEMS

NUCLEAR POWER PLANT	COMPONENT	RESPONSE LEVEL (g)	MEASURED DAMPING (% OF CRITICAL)	APPLICABLE REGULATORY VALUE REF. 6.49 (OBE)
EXPERIMENTAL GAS COOLED REACTOR	STEAM GENERATOR	0.001 1.0	1.0 2.0-3.0	2.0
	STEAM LINE	0.1	2.0-3.0	1.0
ENRICO FERMI I	INTERMEDIATE HEAT EXCHANGER	0.001	10.0	2.0
	SECONDARY SODIUM PUMP	0.010	3.0	
	SODIUM/WATER STEAM GENERATOR	0.010	10.0	
SAN ONOFORE	PRESSURIZER	0.001 0.10	1.5-2.0 1.5-2.0	2.0
	PRIMARY COOLANT LOOP	0.01 0.10	1.5 2.0-4.0	
	REACTOR VESSEL	0.0001	1.5	
INDIAN POINT II	STEAM GENERATOR	0.010	2.2-5.0	2.0
	CROSSOVER LEG	0.001	5.0	2.0
	PUMP	0.001	1.0-1.3	2.0
TSURUGA	6" TO 16" PIPE-LINE	LOW LEVEL	3.2-8.6	2.0
	0.75" TO 2.5" PIPELINE	LOW LEVEL	0.2-3.4 (AVG. 1.4)	1.0
UCLA LABORATORY	6" DIA PIPE	1.00	4.0	1.0

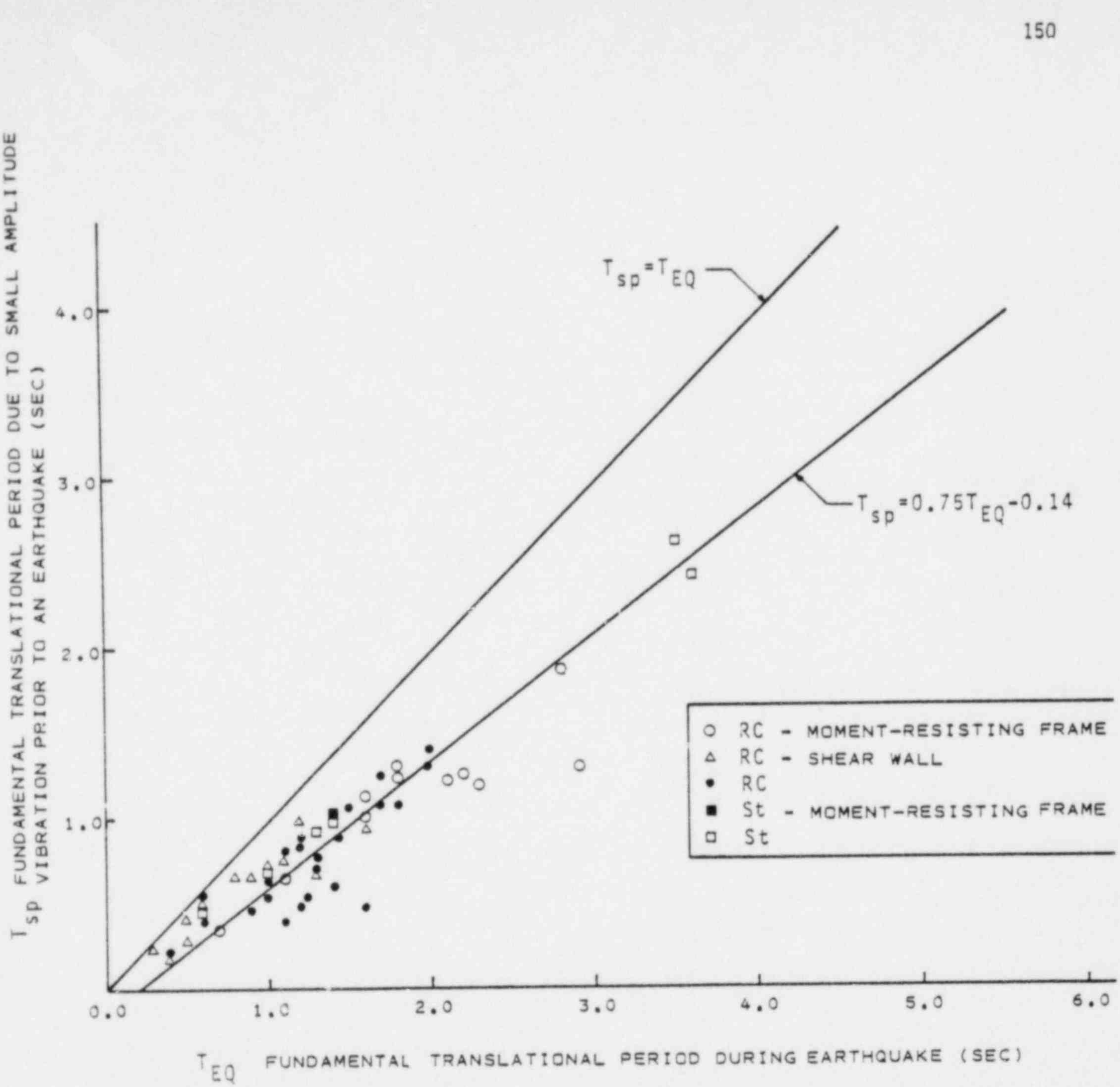

FIGURE 6.1

PRE- VS. DURING EARTHQUAKE PERIOD DETERMINATIONS FOR BUILDINGS SUBJECTED TO THE SAN FERNANDO EARTHQUAKE

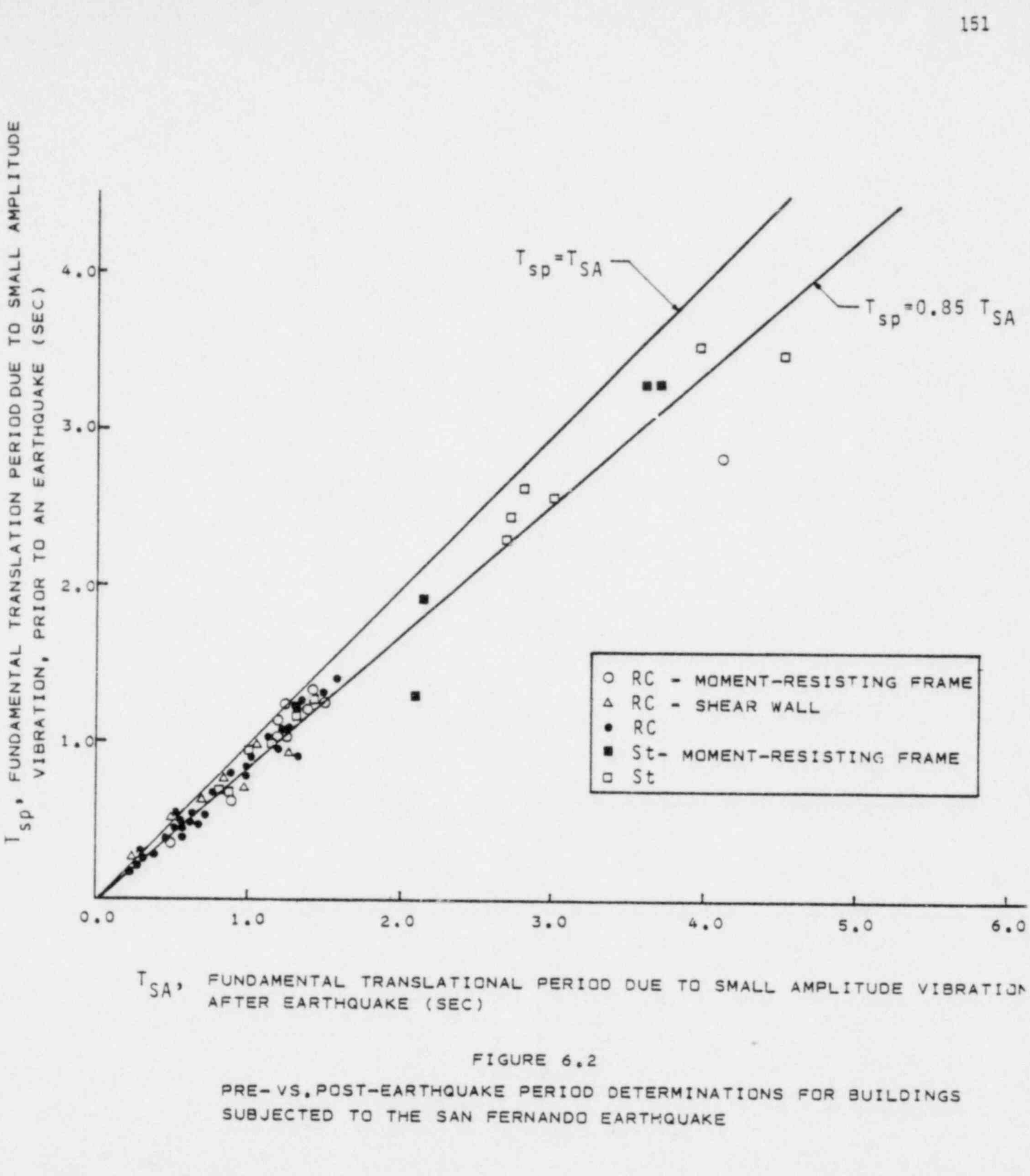

FIGURE 6.2

PRE- VS. POST-EARTHQUAKE PERIOD DETERMINATIONS FOR BUILDINGS SUBJECTED TO THE SAN FERNANDO EARTHQUAKE

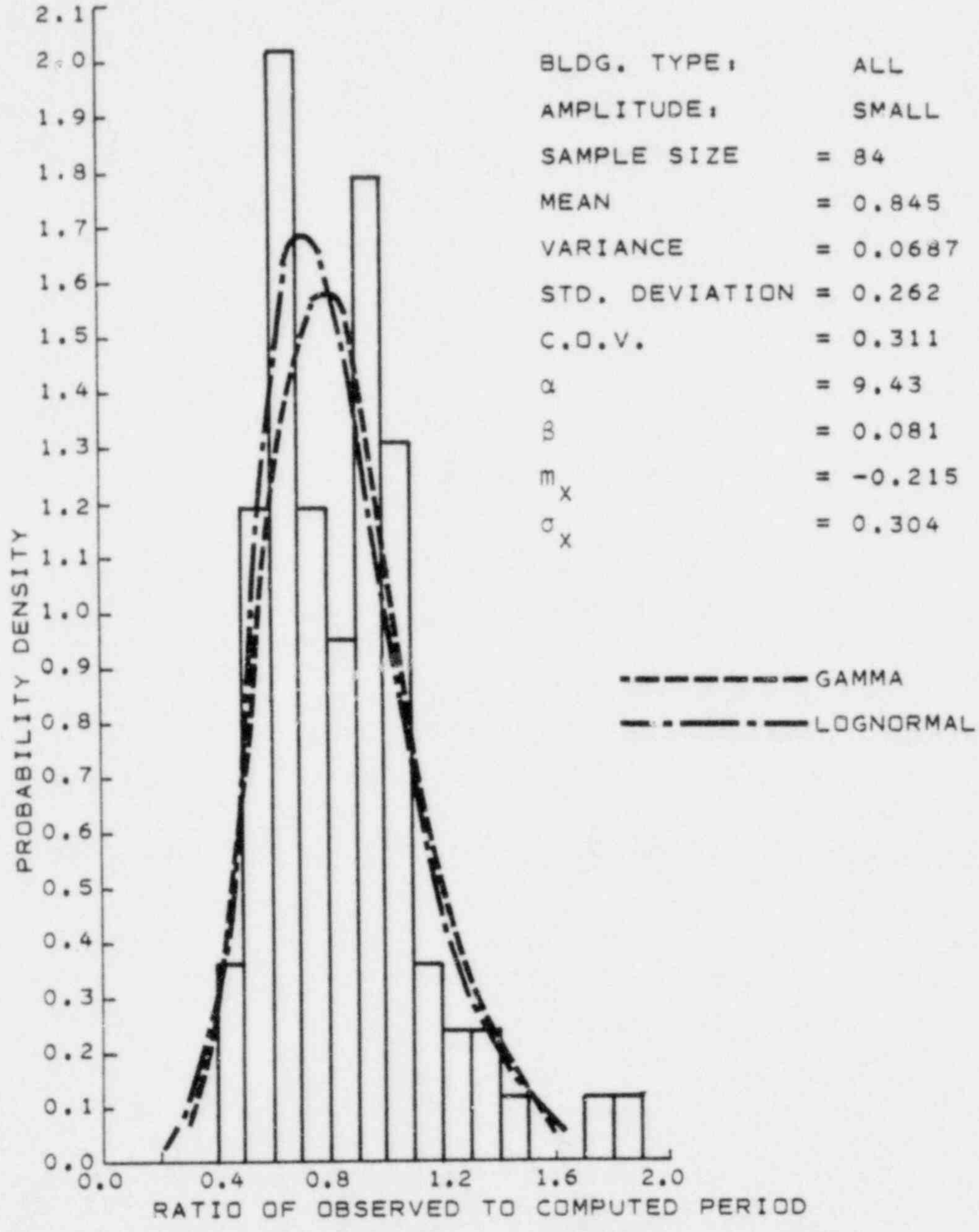

FIGURE 6.3
HISTOGRAM OF RATIOS OF OBSERVED-TO-COMPUTED PERIOD DETERMINATIONS FOR SMALL AMPLITUDE VIBRATIONS OF ALL BUILDING TYPES

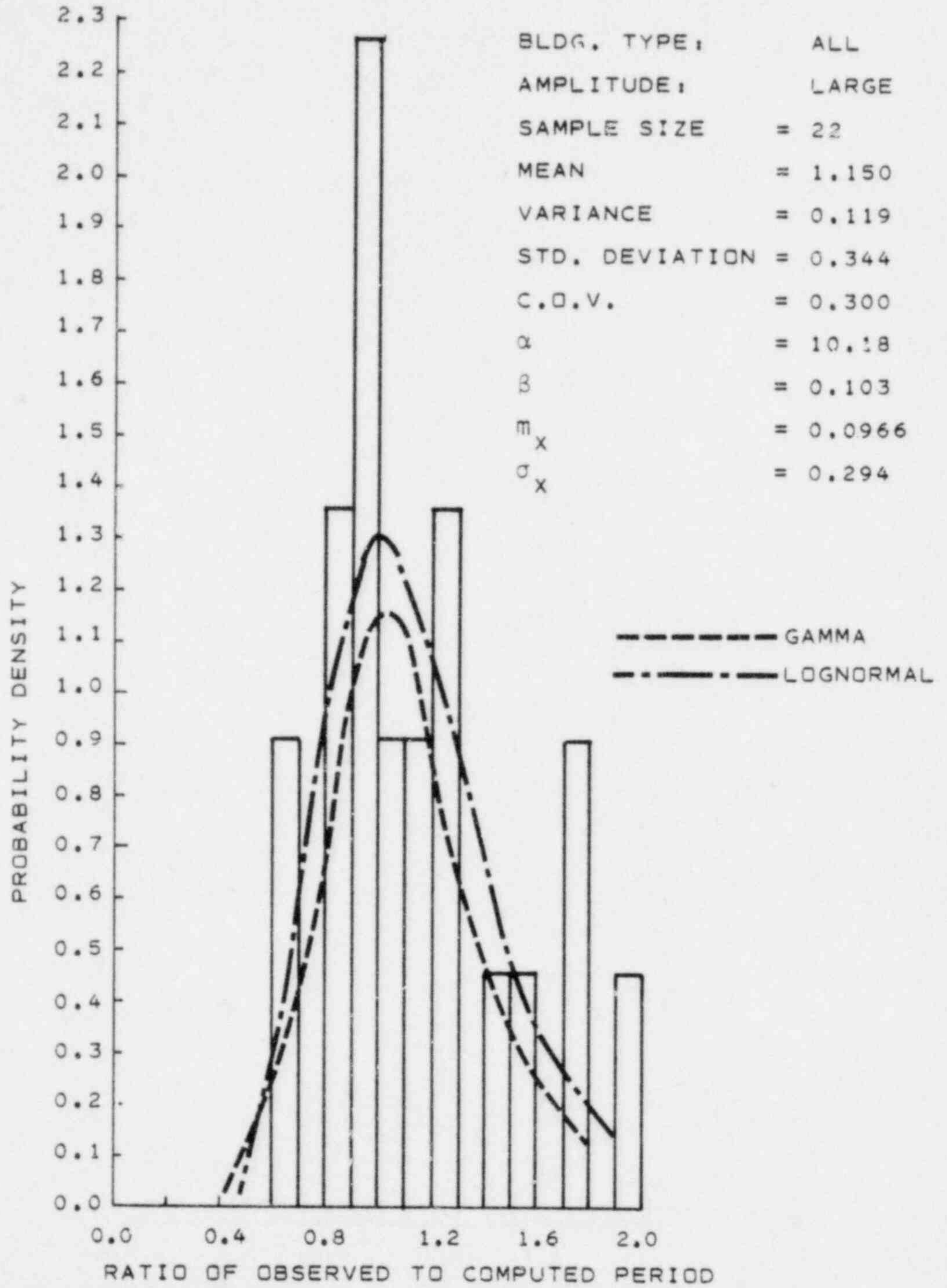

FIGURE 6.4
HISTOGRAM OF RATIOS OF OBSERVED-TO-COMPUTED PERIOD DETERMINATIONS FOR LARGE AMPLITUDE VIBRATIONS OF ALL BUILDINGS TYPES

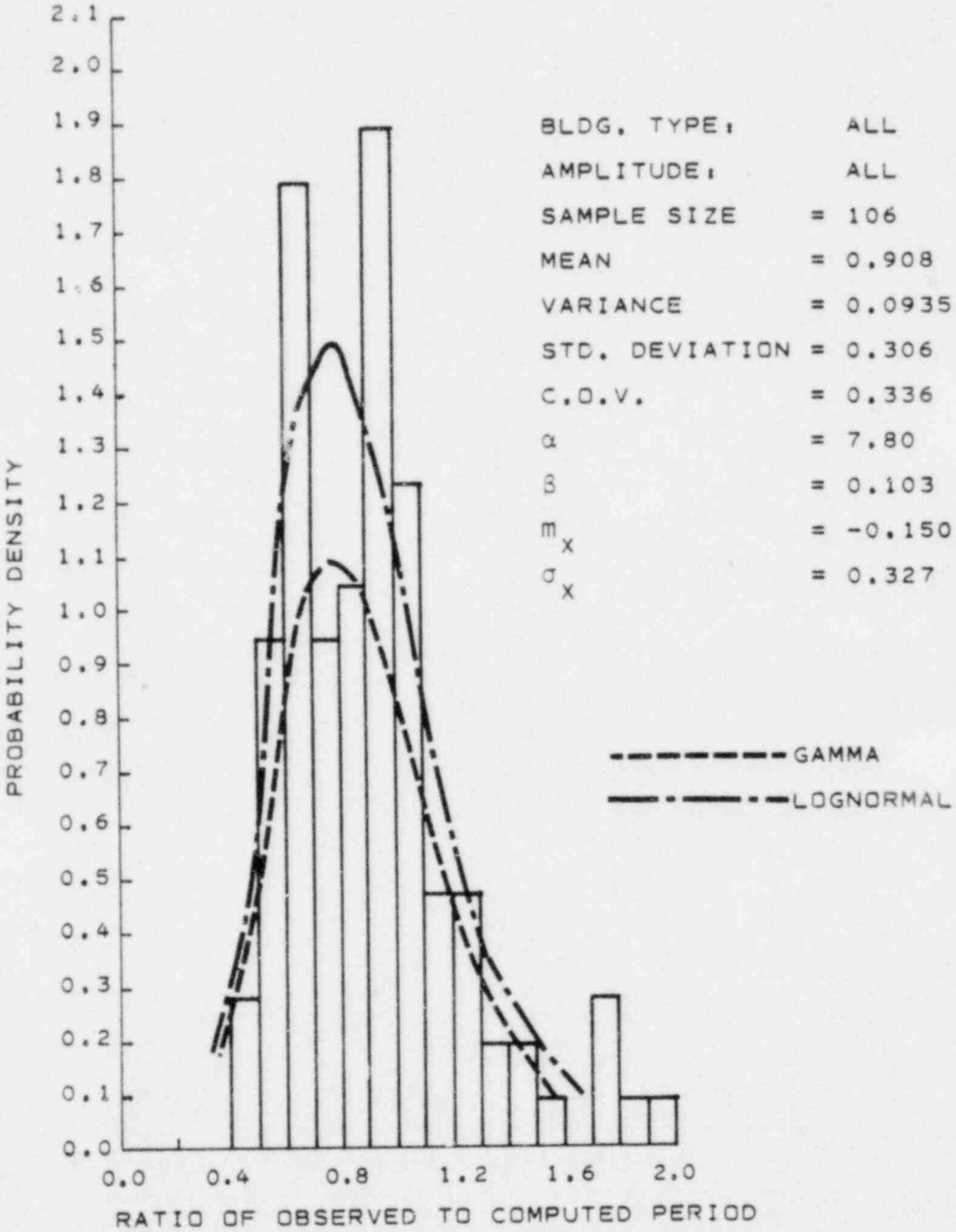

FIGURE 6.5

HISTOGRAM OF RATIOS OF OBSERVED-TO-COMPUTED PERIOD DETERMINATIONS FOR SMALL AND LARGE AMPLITUDE VIBRATIONS OF ALL BUILDING TYPES

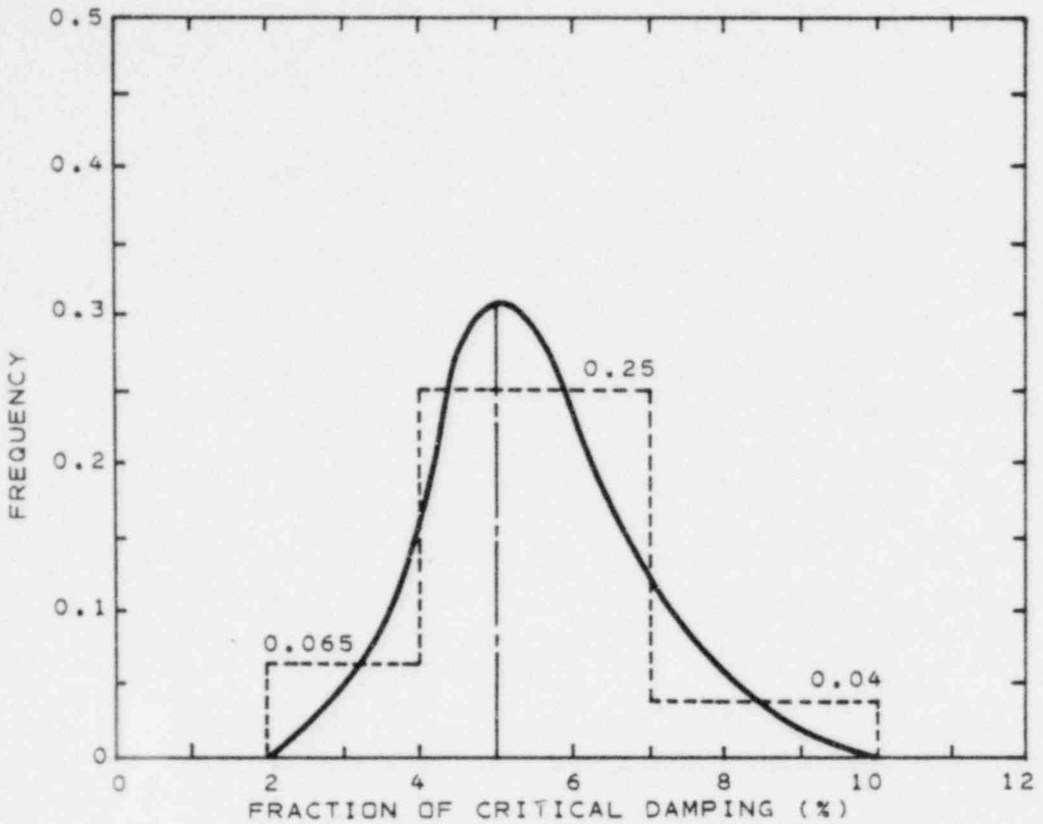

FIGURE 6.6
SUBJECTIVE PROBABILITY DISTRIBUTION FOR DAMPING
REINFORCED CONCRETE STRUCTURES (REF. 6.4)

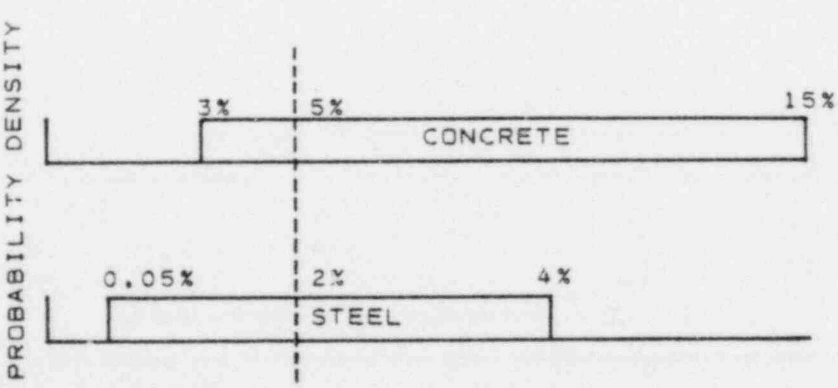

FIGURE 6.7
SUBJECTIVE PROBABILITY DISTRIBUTION FOR DAMPING
REACTOR BUILDING COMPLEX (REF. 6.28)

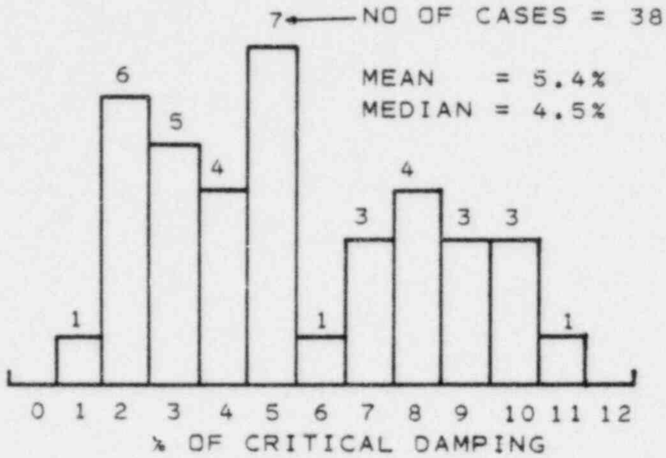

FIGURE 6.8

HISTOGRAM OF 32 DAMPING DETERMINATIONS EXPERIMENTALLY OBTAINED DURING UNDERGROUND NUCLEAR EVENTS, REINFORCED CONCRETE BUILDINGS (REF. 6.47)

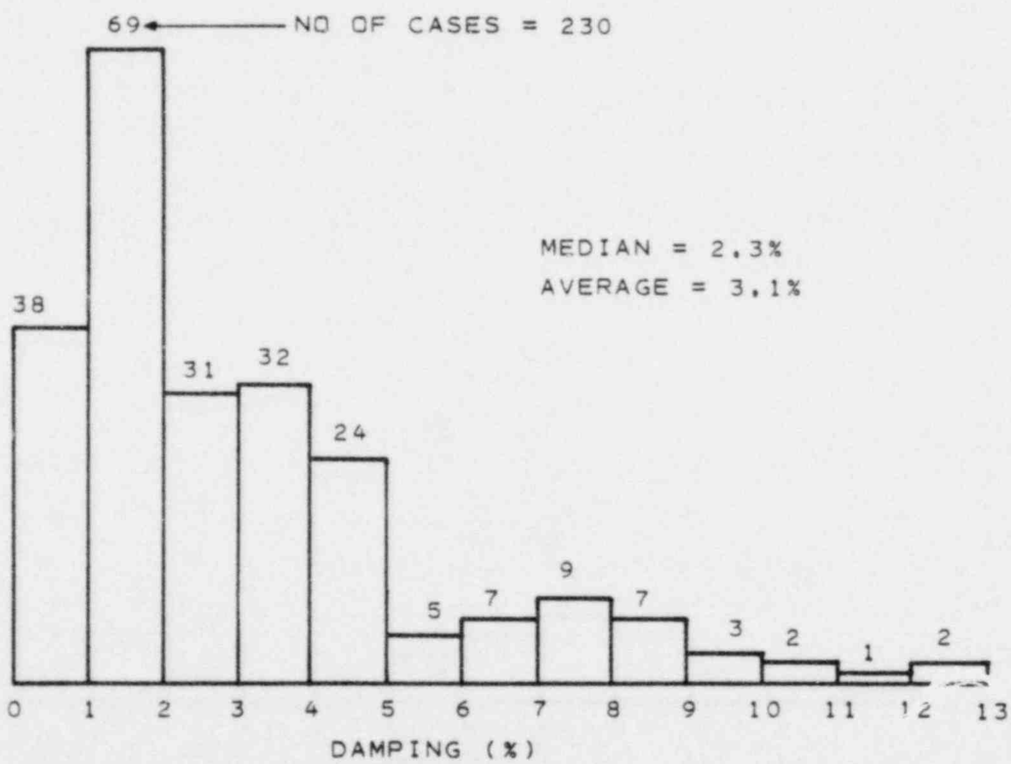

FIGURE 6.9

HISTOGRAM OF 230 DAMPING DETERMINATIONS ,VARIOUS STRUCTURAL TYPES, LOW AMPLITUDE MOTIONS (REF. 6.48)

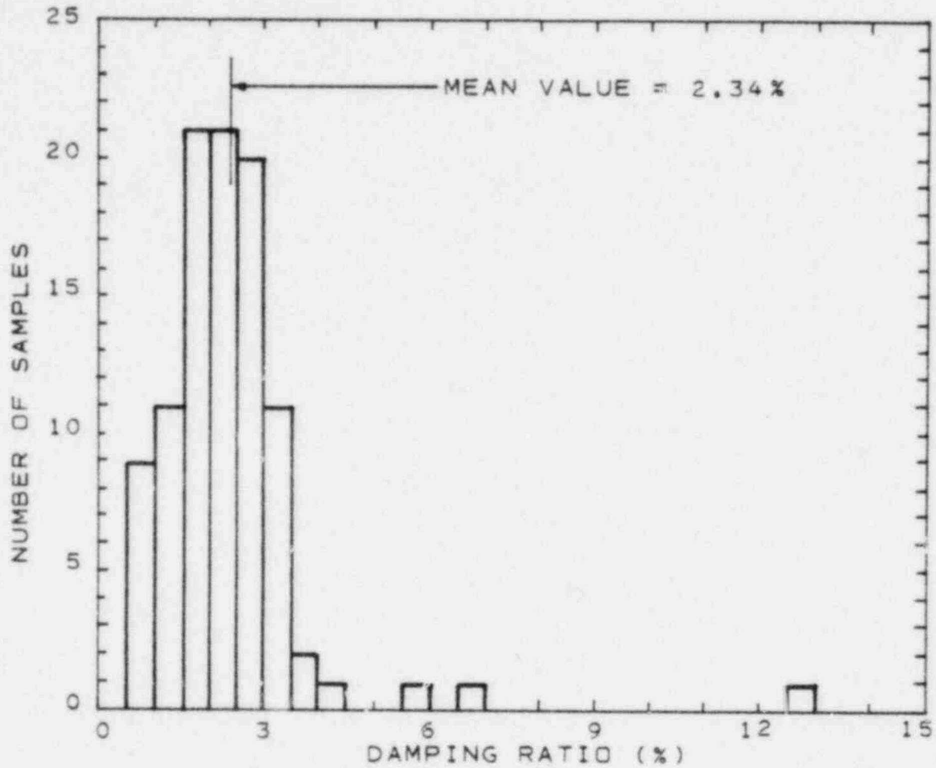

SHEAR WALL STRUCTURES = 99 SAMPLES

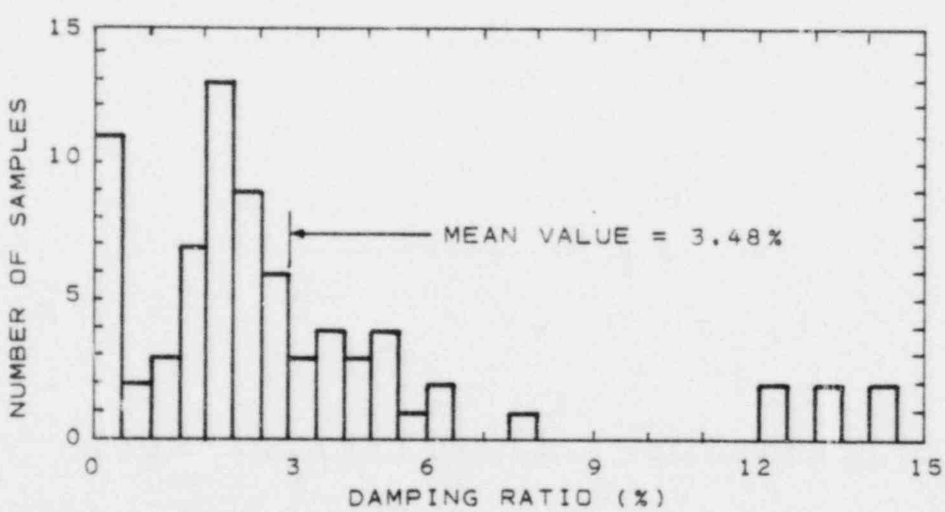

FRAME STRUCTURES = 76 SAMPLES

FIGURE 6.10

HISTOGRAM OF EXPERIMENTALLY OBTAINED DAMPING VALUES FROM LAS VEGAS HIGH-RISE BUILDINGS (REF.6.48)

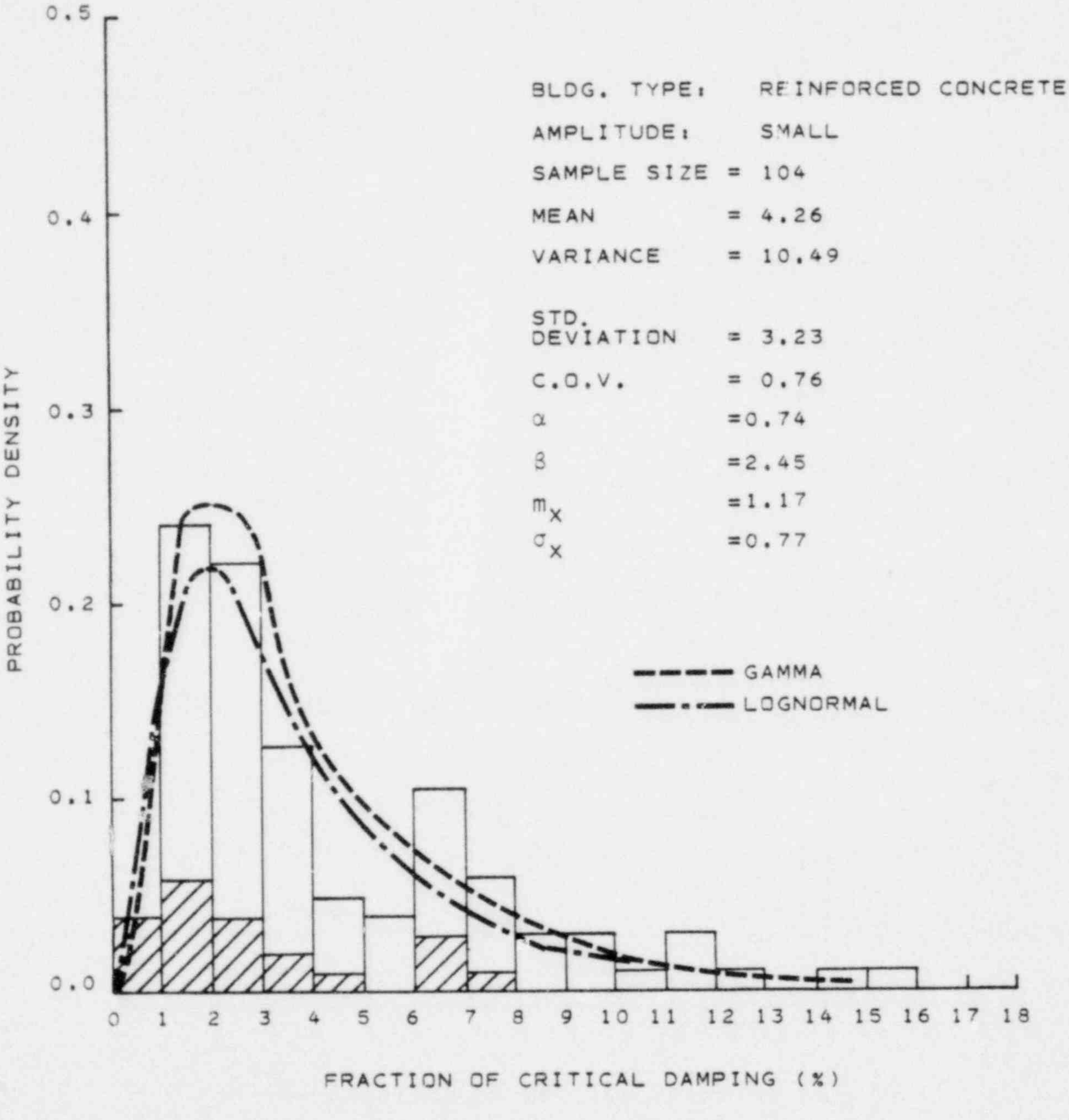

FIGURE 6.11
HISTOGRAM OF DAMPING DETERMINATIONS
FOR SMALL AMPLITUDE VIBRATIONS OF
REINFORCED CONCRETE BUILDINGS

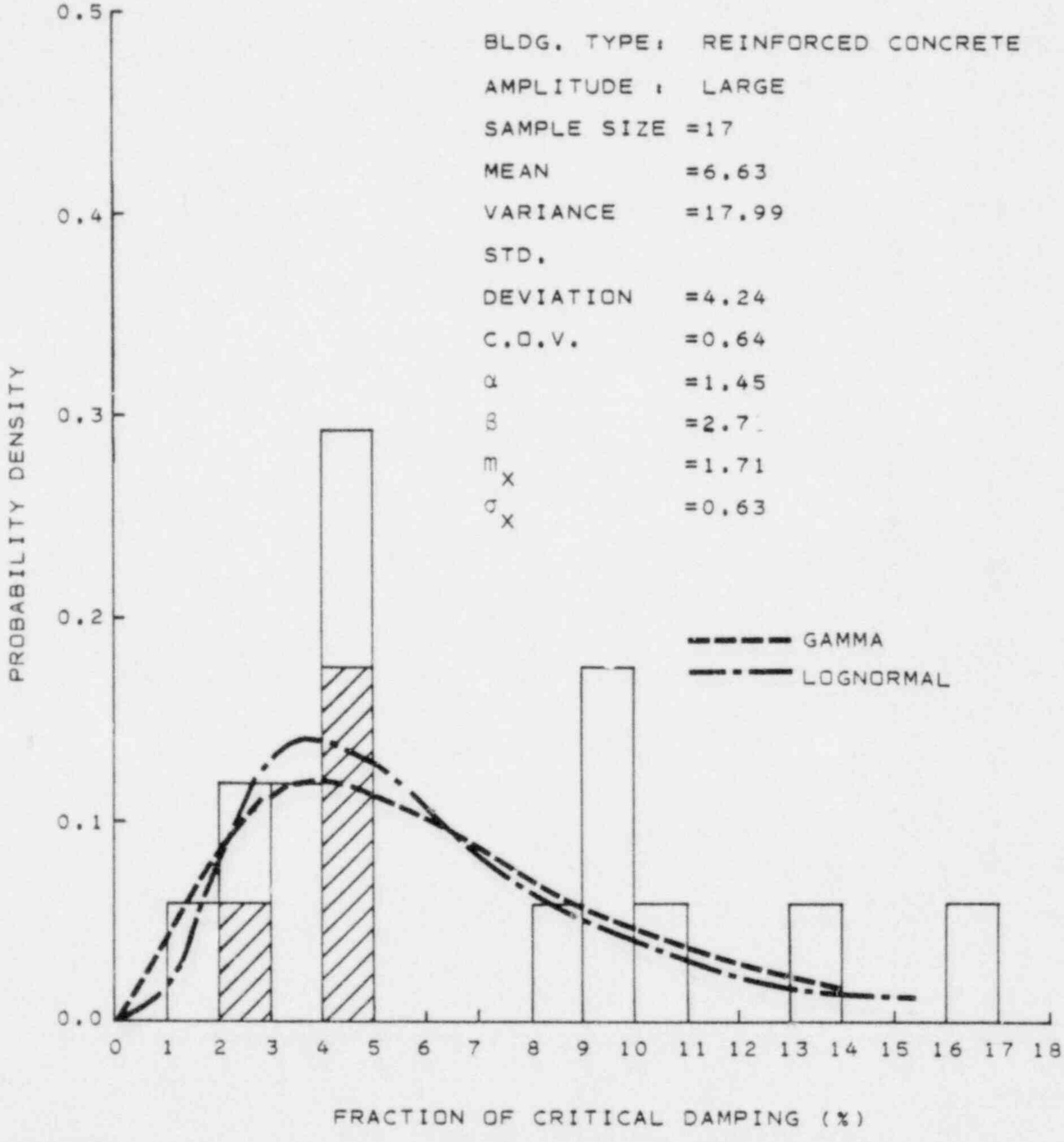

FIGURE 6.12

HISTOGRAM OF DAMPING DETERMINATIONS FOR LARGE AMPLITUDE VIBRATIONS OF REINFORCED CONCRETE BUILDINGS

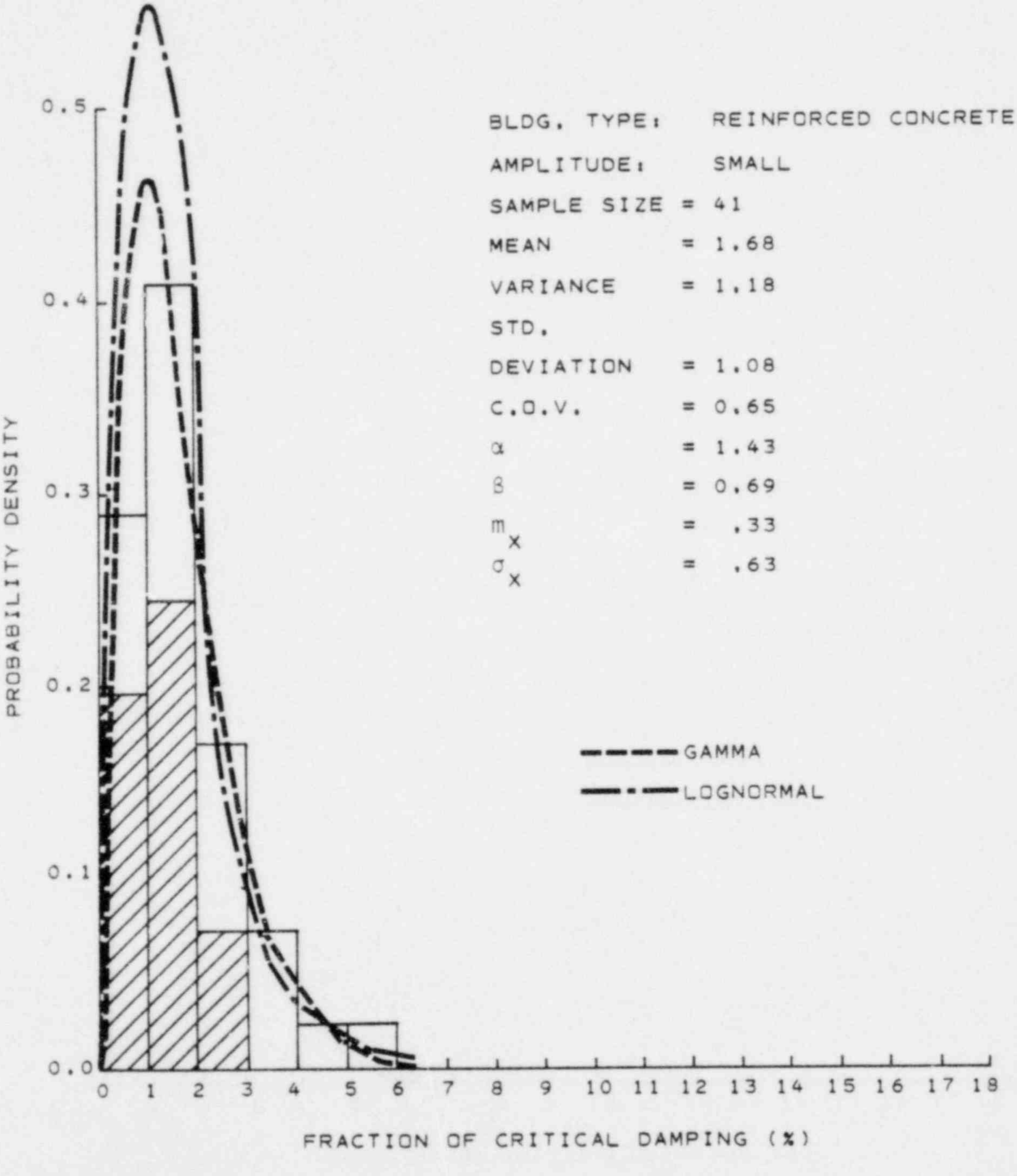

FIGURE 6.13

HISTOGRAM OF DAMPING DETERMINATIONS FOR SMALL AMPLITUDE VIBRATIONS OF STEEL BUILDINGS

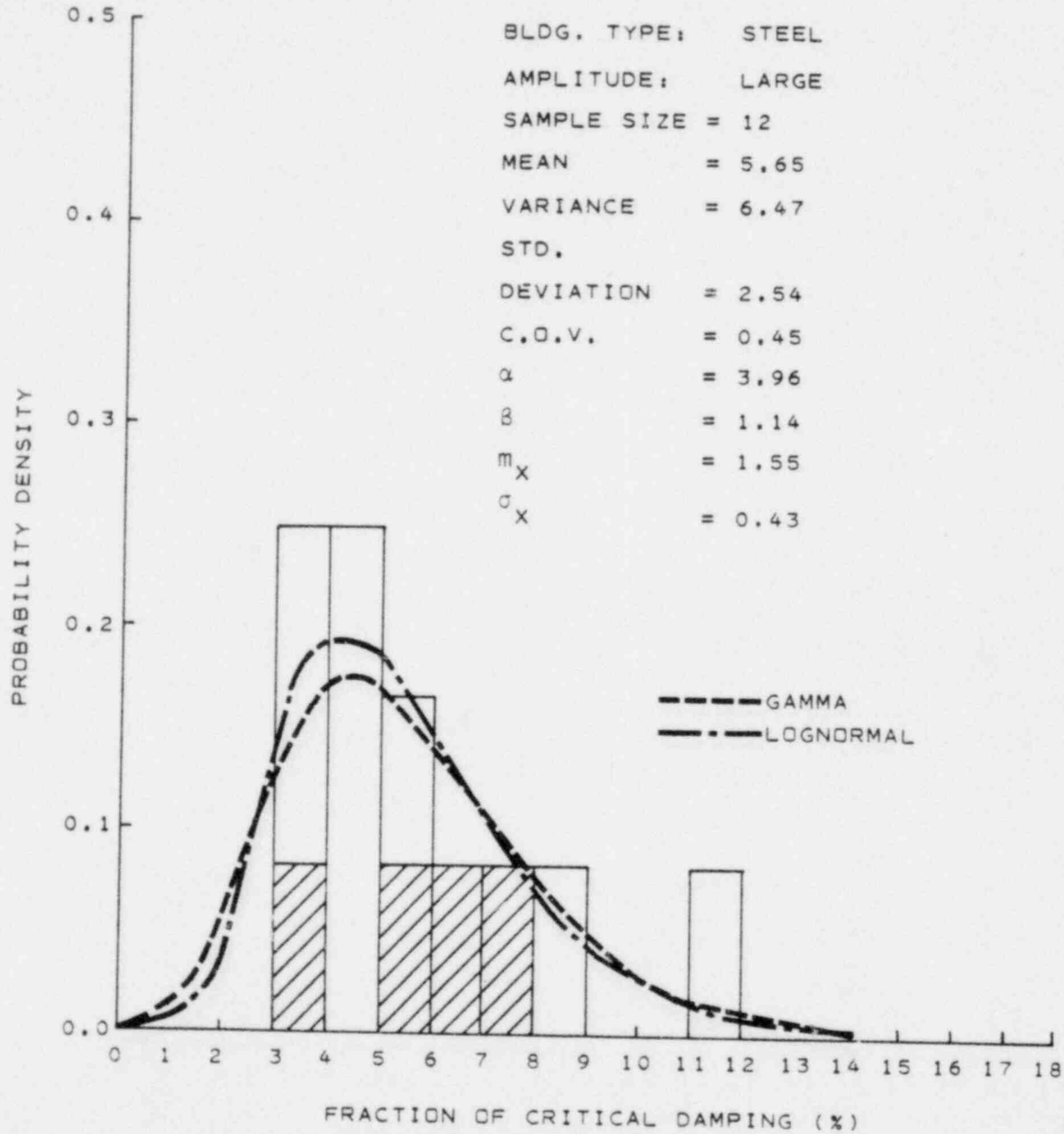

FIGURE 6.14

HISTOGRAM OF DAMPING DETERMINATIONS FOR LARGE AMPLITUDE VIBRATIONS OF STEEL BUILDINGS

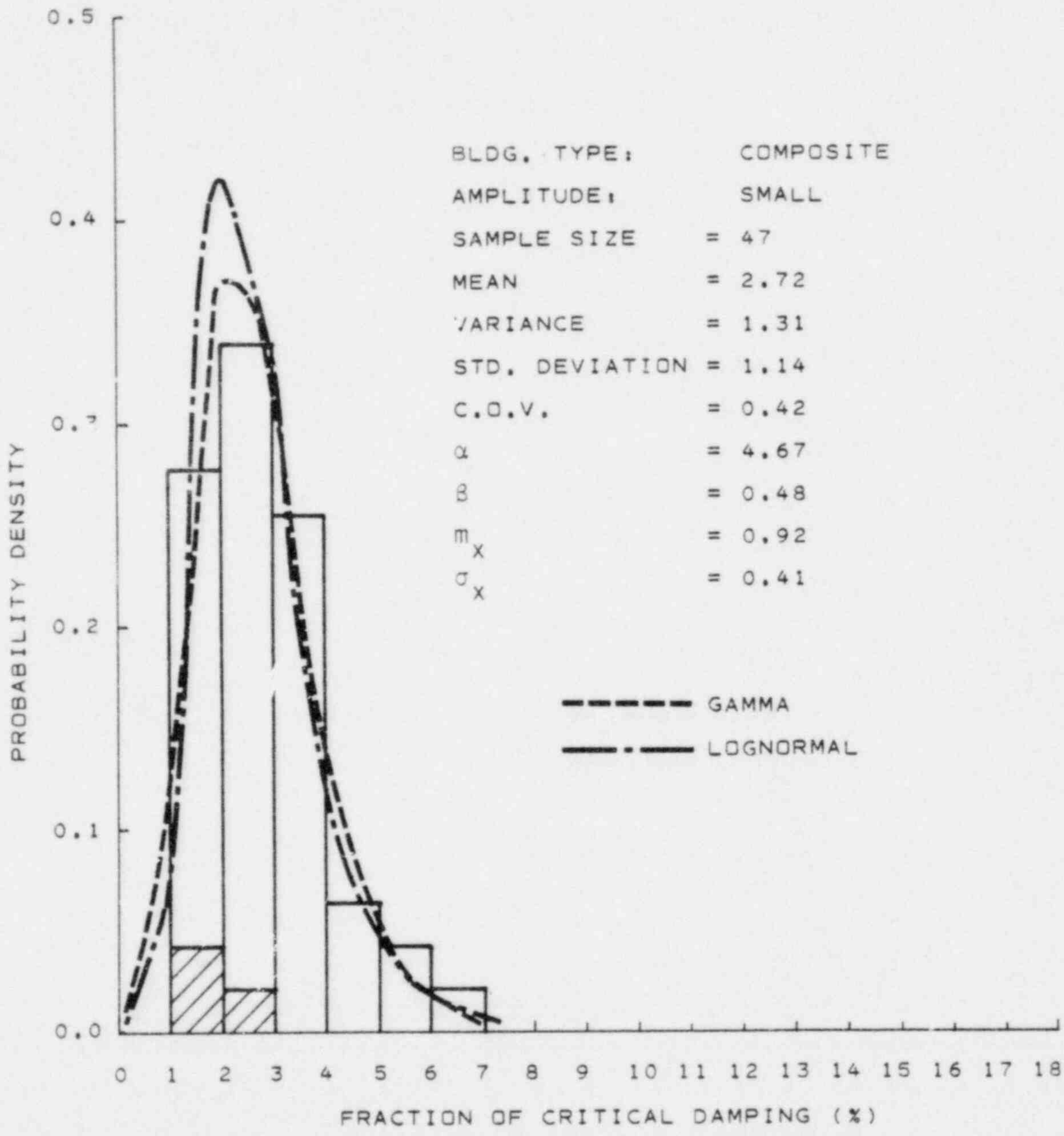

FIGURE 6.15

HISTOGRAM OF DAMPING DETERMINATIONS FOR SMALL AMPLITUDE VIBRATIONS OF COMPOSITE BUILDINGS

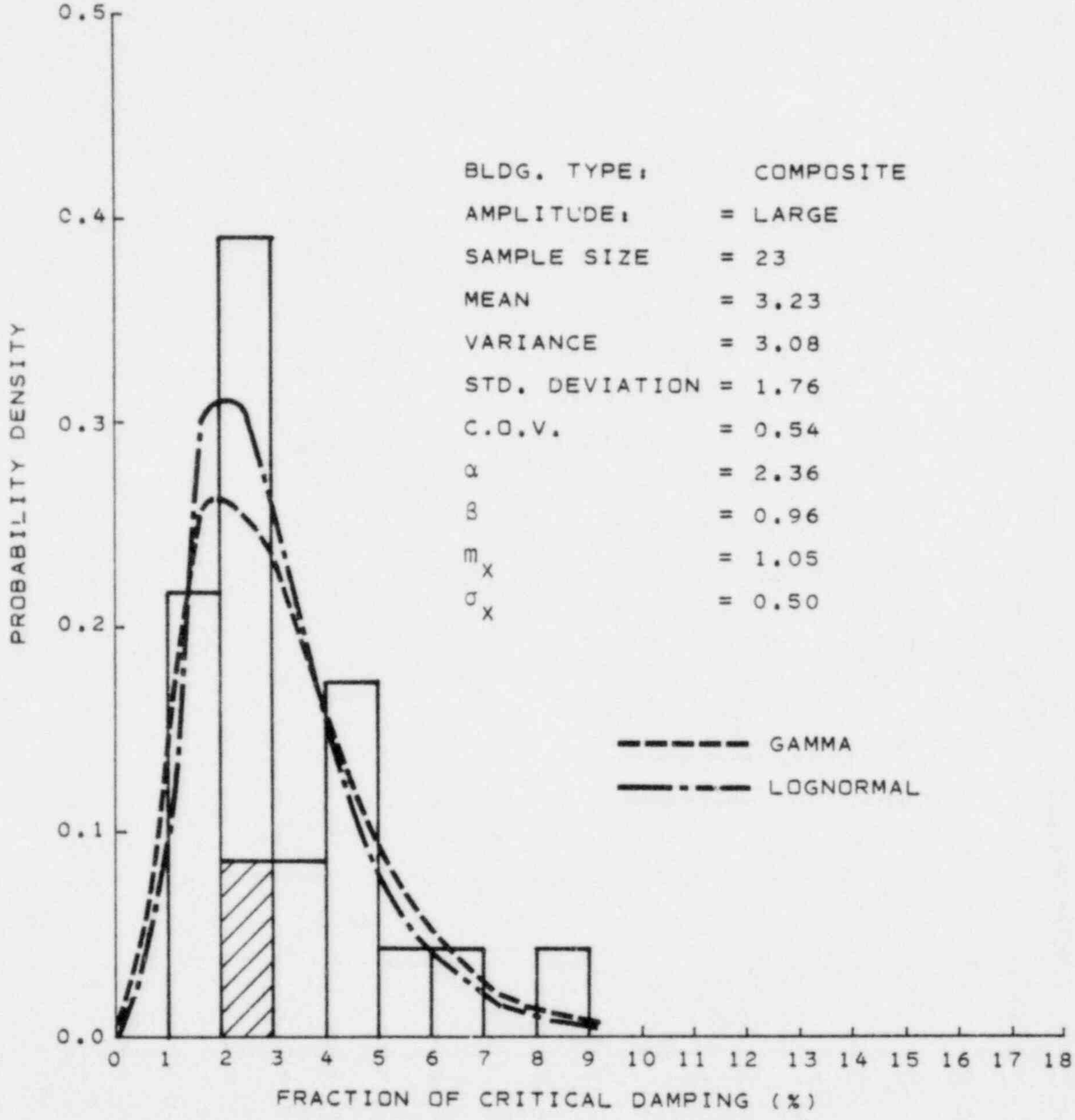

FIGURE 6.16

HISTOGRAM OF DAMPING DETERMINATIONS FOR LARGE AMPLITUDE VIBRATIONS OF COMPOSITE BUILDINGS

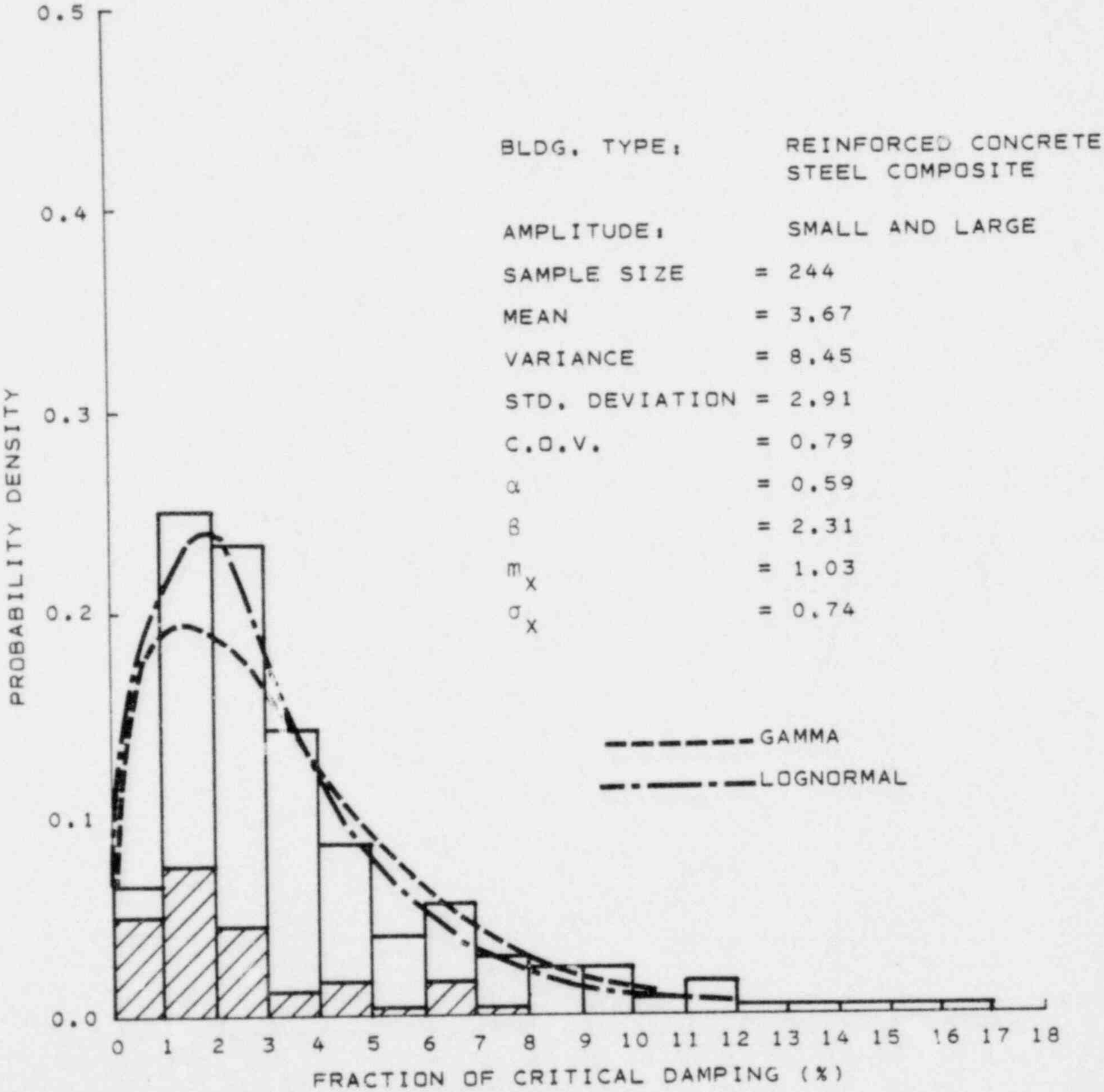

FIGURE 6.17

HISTOGRAM OF DAMPING DETERMINATIONS FOR SMALL AND LARGE AMPLITUDE VIBRATIONS OF REINFORCED CONCRETE, STEEL AND COMPOSITE BUILDINGS

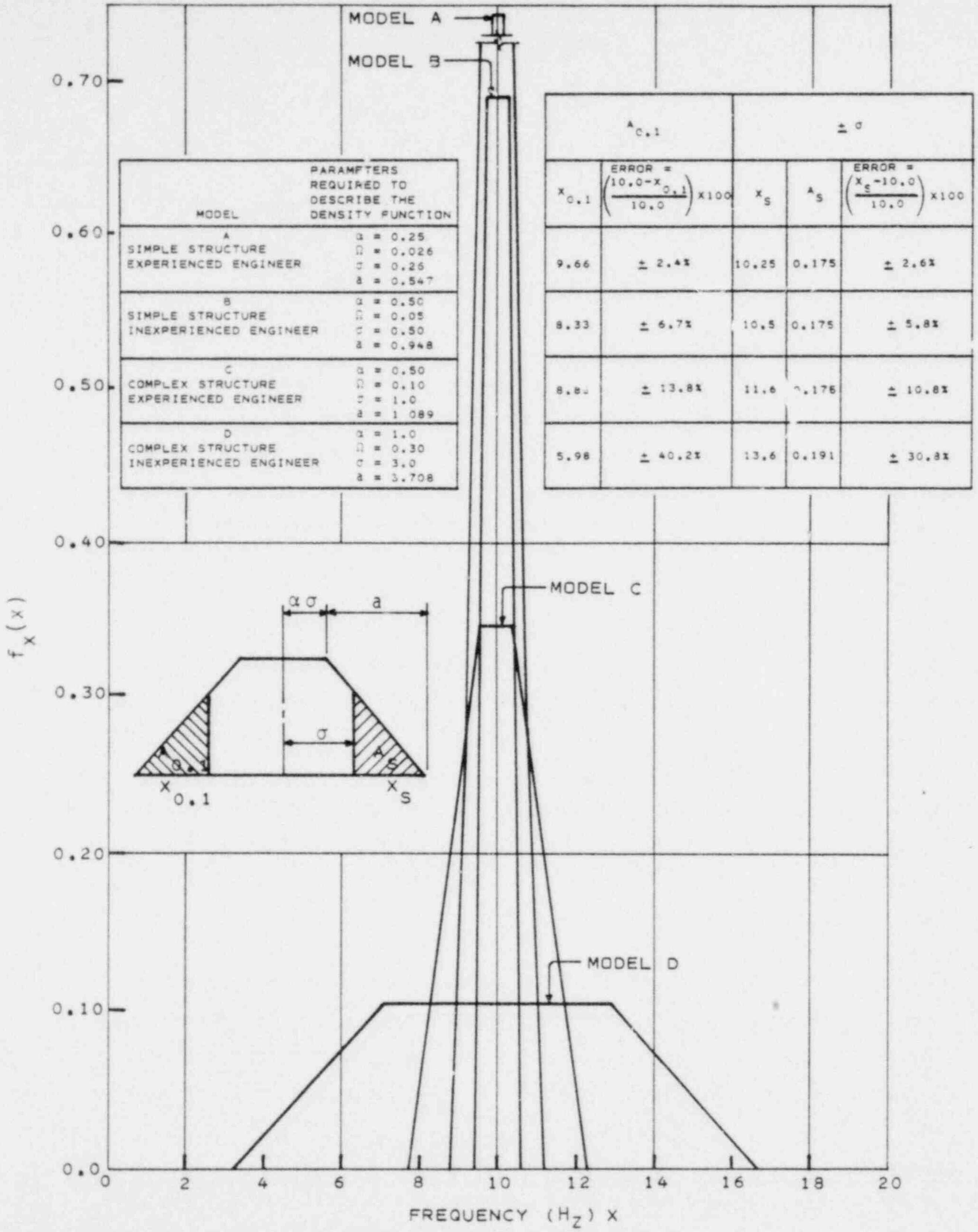

MODEL	PARAMETERS REQUIRED TO DESCRIBE THE DENSITY FUNCTION
A SIMPLE STRUCTURE EXPERIENCED ENGINEER	α = 0.25 Ω = 0.026 σ = 0.26 a = 0.547
B SIMPLE STRUCTURE INEXPERIENCED ENGINEER	α = 0.50 Ω = 0.05 σ = 0.50 a = 0.948
C COMPLEX STRUCTURE EXPERIENCED ENGINEER	α = 0.50 Ω = 0.10 σ = 1.0 a = 1.089
D COMPLEX STRUCTURE INEXPERIENCED ENGINEER	α = 1.0 Ω = 0.30 σ = 3.0 a = 3.708

$A_{0.1}$		$\pm\sigma$		
$x_{0.1}$	ERROR = $\left(\frac{10.0-x_{0.1}}{10.0}\right)\times 100$	x_S	A_S	ERROR = $\left(\frac{x_S-10.0}{10.0}\right)\times 100$
9.66	± 2.4%	10.25	0.175	± 2.6%
8.33	± 6.7%	10.5	0.175	± 5.8%
8.8[illegible]	± 13.8%	11.6	0.176	± 10.8%
5.98	± 40.2%	13.6	0.191	± 30.8%

FIGURE 6.18

TENTATIVELY RECOMMENDED PROBABILISTIC MODEL FOR ENGINEERING JUDGMENT IN STRUCTURAL MODELING

Chapter 7
Summary and Recommendations

In the following paragraphs, the main subjects addressed in this report are summarized together with some particular indications regarding the needs of the SSMRP:

Structural Modeling

The methods of discretization are described and comparison between the finite element approach and the lumped-beam approach is given for selected structures. In general, the lumped-mass beam approach is acceptable if the beam characteristics are developed based upon certain accepted guidelines developed as a result of usage in engineering practice.

The basic approaches for determining the sectional properties of superstructure models are described. Engineering experience is a significant factor in properly selecting model parameters considering both economy and accuracy.

Decoupling of equipment and subsystems from the structural system is discussed. The criteria currently employed are primarily for single degree-of-freedom systems. For multiple degree-of-freedom systems, single criteria should be developed.

The topic of structural modeling for hydrodynamic effects has been addressed. For tank-type structures, earlier development by Housner is usually followed. For structures with other geometric shapes, such as the BWR structure, various approaches are under development.

Structural Analysis

Methods for determining structural response are described in detail for both linear and nonlinear systems. Various ways of treating the damping factors are also presented. Due to the fact that certain methods are more efficient for particular types of problems, no strict recommendation regarding the choice of analysis method is appropriate.

For linear structures, it is usually advantageous to perform a modal superposition analysis, that is, to solve the eigenvalue problem, and then perform the integration of the set of decoupled differential equations. The modal integration scheme is also convenient for the case where a few of the equations remain coupled when the damping matrix does not satisfy the orthogonality condition. The utilization of direct integration for linear structures is generally confined to those situations where the loading either has a specially short duration or is such that it can be anticipated that the response will be associated with modes of very high order.

For nonlinear problems, direct integration is the most powerful approach. However, even in this area, other methods, such as modal analysis can also be employed to efficiently solve certain types of problems.

Nonlinear Behavior of Materials and Structures

The topic of nonlinearity in seismic analysis is considered for various systems. In general, lumped plasticity, distributed plasticity and stiffness degradation are the major phenomena due to material nonlinearity. In order to determine realistic estimates of structural behavior under high levels of seismic loading, nonlinear analysis is necessary. Various methods are summarized for establishing equivalent linear systems as a means of determing the seismic response of nonlinear single degree-of-freedom system. Such methods have value as practical design tools for behavior which can be represented by a simple system. In addition, these equivalent linear approaches have significant potential for contributing to the development of guidelines and procedures for inelastic analysis and design of complicated systems.

Research and development is being pursued in the area of multi-degree-of-freedom systems and nonstationary processes. The development of a generalized, efficient procedure for the performance of nonlinear analysis at high seismic loads is a particular area where significant developments are necessary.

Combination of Loads

The methodology employed in current practice for combining load effects is discussed and its shortcomings are addressed. For the SSMRP, it is obvious that the approach to load combination should be based upon a methodology developed from detailed consideration of the stochastic character of the individual and combined load effects.

Uncertainties in Structural Dynamic Analysis

A general discussion of the basic sources of uncertainty in dynamic structural analysis is presented. Quantitative estimates of the uncertainties are collected, from a variety of data sources, for possible use in subsequent phases of the SSMRP. In addition, various possible approaches for combining estimates of individual sources of uncertainty into an overall estimate of structural system performance are described.

In order to develop an effective computational procedure for the SSMRP calculations, it will obviously be necessary to concentrate on the most critical sources of uncertainty. Final identification of the most significant sources and groupings of the various sources into an appropriate small number of groups is an important SSMRP task. Such studies will necessarily include the performance of sensitivity analyses to develop a quantitative basis for decisions which will have a direct impact on the validity of the overall results.

At the present time, it is possible to identify, in a preliminary and relative manner, those parameters whose contribution to the overall uncertainty will most likely be significant.

The dynamic structural characteristics including the mass, stiffness and damping characteristics are probably the most significant category of uncertainty factors. Within this category, the damping properties must be considered the most sensitive source of uncertainty especially for calculations to high response levels where the treatment of energy absorption is particularly significant. This general category (dynamic characteristics) can also be considered to include the important uncertainty source of structural modeling which includes the analyst's decisions regarding the creation of the mathematical model as influenced by the structural complexity and the analyst's experience.

The second category in order of possible contribution is considered to be the analytical methods including the choice of analysis method, computer code, numerical integration schemes, etc. It should be noted, however, that considering the present state of the art, the relative contribution of this source to the overall uncertainty is relatively more significant for nonlinear as opposed to linear problems.

The constitutive property category may be considered as, relatively speaking, the last in order of the contributing types of uncertainty. However, here also, the relative contribution is felt to be increased for nonlinear analyses.

NRC FORM 335 (7-77) U.S. NUCLEAR REGULATORY COMMISSION

BIBLIOGRAPHIC DATA SHEET

1. REPORT NUMBER (Assigned by DDC) NUREG/CR-1423, Vol. I	
4. TITLE AND SUBTITLE (Add Volume No., if appropriate) "Structural Building Response Review" Project IV Structural Building Response of the Seismic Safety Margins Research Program (Phase I)	2. (Leave blank)
	3. RECIPIENT'S ACCESSION NO.
7. AUTHOR(S) Ebasco Services Incorporated John J. Healey, Spencer T. Wu, Mikel Murga	5. DATE REPORT COMPLETED MONTH February YEAR 80
9. PERFORMING ORGANIZATION NAME AND MAILING ADDRESS (Include Zip Code) Lawrence Livermore Laboratory P.O. BOX 808 Livermore, California 94550	DATE REPORT ISSUED MONTH May YEAR 80
	6. (Leave blank)
	8. (Leave blank)
12. SPONSORING ORGANIZATION NAME AND MAILING ADDRESS (Include Zip Code) U. S. Nuclear Regulatory Commission Division of Reactor Safety Research Office of Nuclear Regulatory Research Washington, DC 20554	10. PROJECT/TASK/WORK UNIT NO.
	11. CONTRACT NO. FIN No. A0130
13. TYPE OF REPORT Technical	PERIOD COVERED (Inclusive dates)
15. SUPPLEMENTARY NOTES	14. (Leave blank)

16. ABSTRACT (200 words or less) The body of this report is organized in six chapters: Chapter 2 treats the subject of structural modeling including methods of discretization, basic modeling approaches, decoupling and other important modeling topics; Chapter 3 covers the various methods of linear and nonlinear structural dynamic analysis, numerical methods, damping, etc; Chapter 4 contains a discussion of the nonlinearity as it relates to nuclear plant structures and presents a discussion of basic analytical considerations and computational algorithms for treating nonlinearity; Chapter 5 treats the subject of combining seismic and nonseismic load effects with particular reference to the state-of-the-art in this area as related to the probabilistic methodology. This material was not fully elaborated on in this report since the SSMRP has a special project to address this topic; Chapter 6 presents a summary of the various sources of uncertainty in seismic dynamic analysis together with a discussion of the sources of data available to quantitatively define these uncertainties; Chapter 7 provides a summary of the principal observations and recommendations of the study.

17. KEY WORDS AND DOCUMENT ANALYSIS 17a. DESCRIPTORS

17b. IDENTIFIERS/OPEN-ENDED TERMS

18. AVAILABILITY STATEMENT	19. SECURITY CLASS (This report) Unclassified	21. NO. OF PAGES 169
	20. SECURITY CLASS (This page)	22. PRICE $

NRC FORM 335 (7-77)

UNITED STATES
NUCLEAR REGULATORY COMMISSION
WASHINGTON, D. C. 20555

OFFICIAL BUSINESS
PENALTY FOR PRIVATE USE, $300

POSTAGE AND FEES PAID
U.S. NUCLEAR REGULATORY
COMMISSION

U.S. MAIL